

Electronic Thesis and Dissertation Repository

12-7-2016 12:00 AM

The Role of Scapular Morphology in Reverse Shoulder Arthroplasty

Ashish Gupta, *The University of Western Ontario*

Supervisor: Dr Louis M Ferreira, *The University of Western Ontario*

Joint Supervisor: Dr George Athwal, *The University of Western Ontario*

A thesis submitted in partial fulfillment of the requirements for the Master of Science degree in Surgery

© Ashish Gupta 2016

Follow this and additional works at: <https://ir.lib.uwo.ca/etd>



Part of the [Biomechanics and Biotransport Commons](#), [Biomedical Devices and Instrumentation Commons](#), and the [Orthopedics Commons](#)

Recommended Citation

Gupta, Ashish, "The Role of Scapular Morphology in Reverse Shoulder Arthroplasty" (2016). *Electronic Thesis and Dissertation Repository*. 4357.

<https://ir.lib.uwo.ca/etd/4357>

This Dissertation/Thesis is brought to you for free and open access by Scholarship@Western. It has been accepted for inclusion in Electronic Thesis and Dissertation Repository by an authorized administrator of Scholarship@Western. For more information, please contact wlsadmin@uwo.ca.

Abstract

Baseplate fixation in a reverse shoulder arthroplasty depends on adequate bone stock. In cases of severe glenoid bone loss and revision shoulder arthroplasty, deficiency of the glenoid vault compels the surgeon to attain screw fixation in the three columns of the scapula. The relationship of these columns demonstrated that the coracoid is closer to the lateral scapular pillar in females than in males. Significant gender dimorphism exists between the orientations of the three columns. The gender dimorphism is further evaluated by anthropometric measurements of the scapular body and the glenoid. The clinical significance lies in the ability to reconstruct the glenoid to its premorbid anatomy, thereby being able to predict the glenoid dimensions from scapular body dimensions.

Adequate positioning of the glenoid baseplate requires it to be positioned orthogonal to the scapular plane. Typically, calculation of the scapular plane relies on the glenoid being intact. As such, the scapular plane cannot be recreated if the glenoid has an abnormal morphology. This mandates the utilization of alternate planes that are independent of glenoid reference points. A relationship between the various planes independent of the glenoid reference points and the current scapular plane dependent upon the normal glenoid anatomy has been established.

Keywords

Reverse Shoulder Arthroplasty, Baseplate position, Screw Position, Glenoid bone loss, shoulder, revision, Scapular plane, ISB axis, 3 columns of scapula, gender dimorphism

Co-Authorship Statement

Chapter 1: Dr Ashish Gupta - sole author

Chapter 2: Dr Ashish Gupta – study design, data collection, statistical analysis,

wrote manuscript

Nikolas Knowles – study design, data collection

Dr Louis Ferreira – study design, reviewed manuscript

Dr George Athwal – study design, reviewed manuscript

Chapter 3: Dr Ashish Gupta – study design, data collection, statistical analysis,

wrote manuscript

Nikolas Knowles – study design, data collection

Dr Louis Ferreira – study design, reviewed manuscript

Dr George Athwal – study design, reviewed manuscript

Chapter 4: Dr Ashish Gupta – study design, data collection, statistical analysis,

wrote manuscript

Nikolas Knowles – study design, data collection

Dr Louis Ferreira – study design, reviewed manuscript

Dr George Athwal – study design, reviewed manuscript

Chapter 5: Dr Ashish Gupta - sole author

Acknowledgment

For Jai and Aayan

Acknowledgments

I would like to thank my supervisor Dr Louis Ferreira. If not for your guidance, insight and unwavering support this thesis would not have reached fruition. I thank you for your patience and technical expertise for guiding me and keeping me on track. You have been my trouble shooter, resource manager, steadfast supporter and mate. I thank you.

Dr George S Athwal you have been a role model for my career. I have learned so much from you. Your clinical prowess, passion for innovation and inquisitive mind gave me the direction and encouragement to complete this thesis. Your guidance both clinical and in life has metamorphosed our relationship. I came as a student and I leave as a good friend. Thank you for all your support and faith in my ability.

To Nikolas Knowles this thesis would not have been possible if was not for your help and support. You have one of the sharpest minds I have ever met and your enthusiasm and passion for shoulder research is electrifying. I thank you for all your technical support and guidance. You shall forever be my Mimics guru.

I shall like to thank Janice Sutherland for always being there and helping out. Janice thank you for being so efficient and organized; the program would not run without you in the driving seat. Dr Abdel Lawendy thank you for spearheading the Masters of surgery program. This will forever transform lives of young academic surgeons.

To my parents and parents in law. The completion of this thesis has been a team event. I thank you for entertaining many of my crazy ideas in life and patiently supporting them all. You are the four pillars of strength in my life. Aastha, Prateek, Anuj and Malavika thanks for your constructive criticism; always keeping me focused.

Finally, to my amazing wife, Gina. Your support, love, dedication and faith in me helps me make my dreams come true. I will never forget the sacrifices you have made so that I could complete my fellowships and this thesis. Thank you for everything and most of all thank you for Jai and Aayan.

Table of Contents

| | |
|--|----------|
| Abstract..... | ii |
| Co-Authorship Statement..... | iii |
| Acknowledgements..... | v |
| Table of Contents | vi |
| List of Tables | x |
| List of Figures | xi |
| List of Appendices | xv |
| | |
| CHAPTER 1 – INTRODUCTION | 1 |
| 1.1 ANATOMY OF THE SCAPULA | 2 |
| 1.1.1 Anatomy of the Glenohumeral Joint | 6 |
| 1.2 BONE FORMATION AND DEVELOPMENT | 9 |
| 1.2.1 Development of the Scapula | 10 |
| 1.2.2 Development of the Glenoid | 12 |
| 1.2.3 Development of the Scapular Body | 15 |
| 1.3 BIOMECHANICS | 17 |
| 1.3.1 Normal Shoulder Joint Biomechanics | 18 |
| 1.4 GLENO- HUMERAL JOINT OSTEOARTHRITIS | 20 |
| 1.5 REVERSE SHOULDER ARTHROPLASTY | 23 |

| | |
|--|-----------|
| 1.5.1 Components of a Reverse Shoulder Arthroplasty | 24 |
| 1.5.2 Biomechanics of a Reverse Shoulder Arthroplasty | 25 |
| 1.5.3 Current Baseplate Designs | 25 |
| 1.6 GLENOID BONE LOSS AND REVERSE SHOULDER | |
| ARTHROPLASTY | 29 |
| 1.6.1 Glenoid Bone Loss in Current Reverse Shoulder Arthroplasty | |
| Designs | 29 |
| 1.6.2 Management of Bone Loss Using Current Designs | 30 |
| 1.7 SCOPE OF THE PROBLEM | 31 |
| 1.8 PROJECT OBJECTIVES AND HYPOTHESIS | 32 |
| 1.9 THESIS OVERVIEW | 34 |
| 1.10 REFERENCES | 35 |
| CHAPTER 2 - COMPARISON OF THREE SCAPULAR CO-ORDINATE | |
| SYSTEMS IN THE CONTEXT OF GLENOID FIXATION IN SHOULDER | |
| ARTHROPLASTY | 39 |
| 2.1 INTRODUCTION | 40 |
| 2.2 MATERIALS AND METHODS | 41 |
| 2.3 RESULTS | 47 |
| 2.4 DISCUSSION | 49 |
| 2.5 CONCLUSION | 52 |
| 2.6 REFERENCES | 52 |

CHAPTER 3 – MORPHOLOGIC ANALYSIS OF THE SCAPULAR BODY

AND THE GLENOID..... 55

3.1 INTRODUCTION 56

3.2 MATERIALS AND METHODS 57

3.3 RESULTS 62

3.4 DISCUSSION67

3.5 CONCLUSION 70

3.6 REFERENCES 70

**CHAPTER 4- MORPHOLOGIC ANALYSIS OF THE THREE COLUMNS
OF THE SCAPULA: SURGICAL IMPLICATIONS IN REVERSE**

SHOULDER ARTHROPLASTY..... 72

4.1 INTRODUCTION 73

4.2 MATERIALS AND METHODS 74

4.3 RESULTS 80

4.4 DISCUSSION81

4.5 CONCLUSION 84

4.6 REFERENCES 85

| | |
|---|------------|
| CHAPTER 5- GENERAL DISCUSSION AND CONCLUSION | 89 |
| 5.1 SUMMARY | 90 |
| 5.2 STRENGTH AND LIMITATIONS | 92 |
| 5.3 CURRENT AND FUTURE DIRECTIONS | 93 |
| 5.4 CONCLUSION | 95 |
| | |
| <i>APPENDIX A – SCAPULAR CO-ORDINATE SYSTEM DATA</i> | |
| ANALYSIS | 96 |
| | |
| <i>APPENDIX B – SCAPULAR ANTHROPOMETRIC MEASUREMENTS</i> | |
| AND DATA ANALYSIS..... | 100 |
| | |
| <i>APPENDIX C – SCAPULAR CO-ORDINATE SYSTEM DATA</i> | |
| ANALYSIS | 113 |
| APPENDIX D COPYRIGHT RELEASES | 116 |
| CURRICULUM VITAE | 123 |

LIST OF TABLES

| | |
|---|----|
| Table 2.1-Relationship To The Scapular Axis Of The NEW ISB And Old ISB Axis ... | 47 |
| Table 3.1 Glenoid And Scapular Dimensions | 63 |
| Table 4.1: Relationship between the 3 Columns and SI- Glenoid Axis | 80 |
| Table 4.2 Relationship between the 3 Columns of the Scapula..... | 80 |
| Table A-1 Relationship between the Scapular Plane and the New ISB and Old ISB Axis (Degrees) | 96 |

LIST OF FIGURES

| | |
|---|----|
| Figure 1.1 Dorsal Surface Of The Scapula..... | 3 |
| Figure 1.2 Measurement Of Glenoid Version And AP And SI Dimensions | 7 |
| Figure1.3 Development Of The Scapula..... | 10 |
| Figure 1.4 The Perinatal Scapula | 11 |
| Figure 1.5 Development Of The Glenoid | 13 |
| Figure 1. 6 Development Of The Lower Glenoid | 14 |
| Figure 1. 7 Times Of Appearance (A) And Fusion (F) Of Scapular Ossification Centers | 15 |
| Figure 1.8(A)The Deltoid Is Tensioned And The Rotator Cuff Stabilizes The Center Of Rotation (Balanced Force Couple) | 18 |
| Figure 1.8(B) In A Rotator Cuff Deficient Shoulder (Unbalanced Force Couple) | 18 |
| Figure 1. 9 Reverse Shoulder Arthroplasty (RSA) | 24 |
| Figure 1. 10 Current Circular Baseplate Design | 26 |
| Figure1.11 The 3 Columns Of The Scapula With Glenoid Subtraction | 28 |
| Figure 2. 1 Scapular Co- Ordinate Systems A) New ISB, B) Old ISB, C) Scapular Plane | 42 |
| Figure 2. 2 A) Superior Axial View | 43 |
| Figure 2.2 B) Scapular Y View | 43 |
| Figure 2.2 C) Posterior View Demonstrating These Points | 44 |

Figure 2. 3 Calculation Of The Glenoid Center Point And Si Glenoid Axis 45

Figure 2. 4: A. Old ISB Plane (A), New ISB Plane (B), And Scapular Plane (C)..... 46

Figure 2.5 The New ISB Is The Most Posterior Axis. The Old ISB Is The Most Anterior Axis. The Mean For Male And Females Combined Is $17.0 \pm 2.0^\circ$ 48

Figure 3.1 Coronal View Of The Scapula And The Sagittal Y View Demonstrating The Superior Scapular Point- SSP, Inferior Scapular Point ISP And The Medial Scapular Point MSP..... 58

Figure 3. 2A Glenoid Enface View..... 60

FIGURE 3.2 B Center Point Of Glenoid Is Calculated..... 60

Figure 3. 3 Posterior View (Coronal View) of the Scapula 61

Figure 3.4 Box Plot Demonstrates The Sexual Dimorphism In The Scapular Body Dimensions And Glenoid Dimensions Between Gender..... 64

Figure 3.5 Box Plot Demonstrates The Sexual Dimorphism In The Scapular Body Dimensions And Glenoid Dimensions Between Gender..... 64

Figure 3.6 Scatter Plot Demonstrating The Correlation Between Estimation Of Glenoid Height By Apparent Scapular Height (AC) $R^2 = 0.54$ 65

Figure 3.7 Scatter Plot Demonstrating The Correlation Between Estimation Of Glenoid Height By Apparent Scapular Height (AC) $R^2 = 0.54$ 65

Figure 3.8 Scatter Plot Demonstrating Poor Correlation Between Estimation Of Glenoid Height By Apparent Scapular Height (AC) Amongst Sexes 66

Figure 3.9 Scatter Plot Demonstrating The Poor Correlation Between Estimation Of Glenoid Width By Apparent Scapular Height (AC) R^2 0.10 And 0.23 For Females And Males Respectively 66

Figure 3.10 Scatter Plot Demonstrating The Poor Correlation Between Estimation Of Glenoid Width By True Scapular Height (AC) $R^2 = 0.05$ And 0.26 For Females And Males Respectively 67

| | |
|--|-----|
| Figure 4. 1 Superior Axial View, Scapular Y View And Inferior Para-Axial View | 75 |
| Figure 4. 2 Calculation Of The Glenoid Center Point And Establishment Of The Superior Inferior SI Glenoid Axis..... | 76 |
| Figure 4.3 The Images Demonstrate The 3 Standardized Views | 77 |
| Figure 4. 4 Orthogonal Plane Developed Parallel To The Glenoid Face And Perpendicular To The Scapular Plane Using Med CAD Algorithm | 79 |
| FigureB.1Glenoid Height measurement in Females and Males | 100 |
| FigureB.2A Glenoid Measurements in Females and Males..... | 101 |
| Figure B.2 B En Face view of the Glenoid | 101 |
| Figure B.3 Anthropometric measurements of the Scapula and Glenoid | 102 |
| Figure B.4 Pearson Correlation Coefficients demonstrating Good correlation between the various measurements when male and female data is combined | 104 |
| Figure B.5 Tests of Normality to assess distribution of the data | 105 |
| Figure B.6 Spearman’s Rho Correlation Coefficients (for Non Parametric Data) demonstrating Good correlation between the various measurements when male and female data is combined | 106 |
| Figure B.7 Scatter Plot Demonstrating Poor Correlation Between Apparent Scapular Height (AC Length) and Glenoid Height in Females | 107 |
| Figure B.8 Scatter Plot Demonstrating Poor Correlation Between Apparent Scapular Height (AC Length) and Glenoid Height in Males | 107 |
| Figure B.9 Regression Equation Glenoid Height | 108 |
| Figure B.10Regression Equation Glenoid Height | 109 |
| Figure B.11 Regression Equation Glenoid | 110 |
| Figure B-12 Regression Equation Glenoid Width | 111 |

Figure B-13 Regression Equation Glenoid Height 112

Figure C.1 Demonstrating Results of t- Test For the Acromion – Coracoid Angle and the Coracoid- Inferior Pillar Angle between Males and Females..... 113

Figure C.2 Demonstrating Results of T Test For the Acromion Spine – Coracoid Angle and the Acromion Spine - Inferior Pillar Angle between Males and Females 113

Figure C.3 Demonstrating Results of T Test For the Acromion Spine – Inferior Pillar Angle and the Coracoid- Inferior Pillar Angle between Males and Females 114

Figure C.4 Demonstrates the Acromion Spine - Coracoid Angle Measurement for Females (0) and Males (1) 115

Figure C.5 Demonstrates the Coracoid – Inferior Pillar Angle Measurement for Females (0) and Males (1) 115

Figure C.6 Demonstrates the Acromion Spine – Inferior Pillar Angle Measurement for Females (0) and Males (1) 115

LIST OF APPENDICES

| | |
|--|-----|
| <i>APPENDIX A</i> – SCAPULAR CO-ORDINATE SYSTEM DATA ANALYSIS | 96 |
| <i>APPENDIX B</i> – SCAPULAR ANTHROPOMETRIC MEASUREMENTS AND DATA ANALYSIS | 100 |
| <i>APPENDIX C</i> – SCAPULAR CO-ORDINATE SYSTEM DATA ANALYSIS..... | 113 |
| APPENDIX D COPYRIGHT RELEASES | 114 |

Chapter 1- Introduction

***Overview:** Shoulder arthroplasty has become the gold standard to treat end stage arthritis in the elderly. The clinical results and longevity of the procedure hinge upon appropriate patient selection, implant design and recreating normal shoulder anatomy; with the aim of restoring pre-morbid joint biomechanics. This requires a detailed knowledge of anatomy, biomechanics and pathology of various arthritic patterns affecting the shoulder. In this chapter, the anatomy of the normal shoulder joint is reviewed. The development of the scapula is described and special emphasis is paid to the development of the glenoid. In the second part of this chapter, the various morphologic patterns of glenohumeral joint arthritis are discussed. Additionally, the challenges of baseplate fixation in the setting of glenoid bone deficiencies are discussed. Finally, the overall purpose and scope of the thesis are explained.*

THE SHOULDER GIRDLE

The gleno-humeral joint (GHJ), anecdotally referred to as the shoulder joint, is the articulation between the humeral head and the glenoid, and is the most mobile joint of the human body. It is a synovial joint with a ball and socket type of articulation. The articular surface is lined by hyaline cartilage. The only osseous link to the axial skeleton is through the clavicle. Both the sterno-clavicular joint and acromio-clavicular joint have developed with appositional articulations - ie. both are fibro cartilaginous joints with interposed fibro cartilaginous discs. Further, the scapula is one of the only bones in the body, which is mainly connected to the axial skeleton by predominantly muscular attachments. This affords the shoulder a large range of motion.

1.1 ANATOMY OF THE SCAPULA¹

The scapula is a flat triangular bone located at the dorsolateral aspect of the thorax. It articulates with the shoulder at the gleno-humeral joint (GHJ) and the axial skeleton via the clavicle at the acromio-clavicular joint (ACJ). It is suspended through muscle attachments connected to the vertebral column, thorax and base of the skull. It has a concave anterior surface due to the barrel shaped nature of the thorax, and a convex posterior surface. It has three borders, commonly referred to as the medial or vertebral border, the lateral border and the superior border. It has two bony projections: the acromion with its spine and the coracoid.

The anterior surface is concave and is called the subscapular fossa. It is concave both medio-laterally and supero-inferiorly. Most of the curvature arises due to the superior one third of the medial border, which corresponds to the third rib, and the curved lateral border/pillar, which provides a strong mechanical strut against buckling due to the

strong muscular forces across a weak thin bone. It has numerous ridges, which give origin to the musculotendinous units of the subscapularis muscle. The large tendon of the subscapularis muscle passes under the coracoid process and inserts onto the lesser tuberosity of the humerus. The entire medial vertebral border on the ventral surface provides attachment to the serratus anterior muscle.

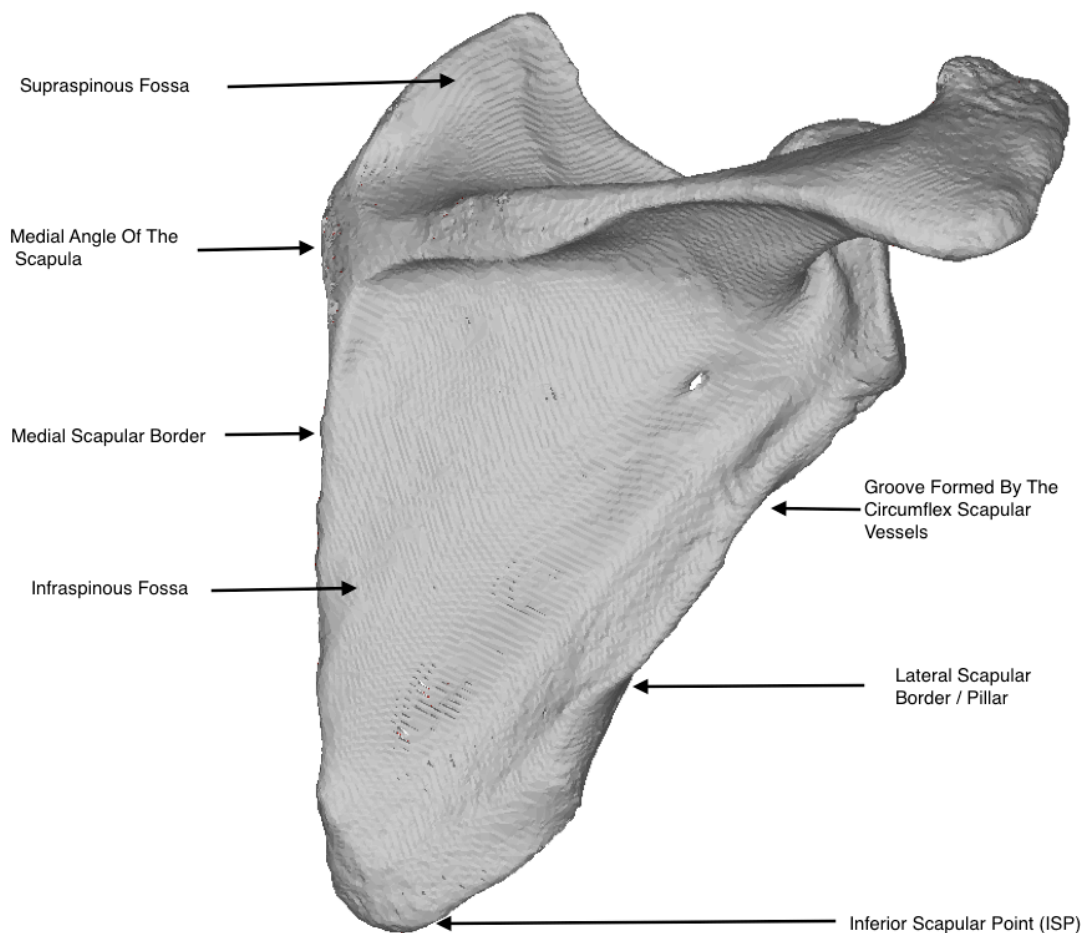


Figure 1.1 Dorsal Surface Of The Scapula

On the dorsal surface of the scapula (Figure 1.1), the scapular spine divides the convex surface into two fossae - the supraspinous fossa and an infraspinous fossa. They are contiguous laterally where they meet at the spinoglenoid notch just medial to the scapular neck. The supraspinous fossa is entirely occupied by the supraspinatus muscle. The bulk of this muscle gives the fossa its shape. The supraspinatus muscle forms a

narrow tendon which passes under the arch of the acromion and inserts onto the greater tuberosity of the humerus.² The suprascapular nerve and artery pass into the supraspinous fossa through the suprascapular notch (via a small fibro osseous tunnel) located posterior to the base of the coracoid. Numerous variations of this notch anatomy have been described.³ The suprascapular artery is the main nutrient vessel to the scapula. It enters the bone through a nutrient foramen located on the lateral aspect of the supraspinous fossa. The suprascapular nerve provides the motor nerve supply to the supraspinatus muscle and through its infra glenoid branch provides the nerve supply to the infraspinatus muscle. It gives out numerous sensory branches, which provide sensation around the shoulder joint.

The infraspinous fossa is the larger of the two dorsal fossae. The majority of its convex surface gives origin to the infraspinatus muscle. The teres minor muscle originates from the lateral border of the scapula. Both these muscles form broad tendons that insert onto the greater tuberosity of the humeral head.²

The lateral border of the scapula is formed of dense cortical bone and extends from the glenoid to the inferior angle of the scapula. The junction of this lateral border or lateral pillar to the glenoid is delineated by the infraglenoid tubercle, which is formed by the insertion of the long head of the triceps muscle. Further caudally, the border gives origin to the teres minor muscle, teres major and part of the latissimus dorsi muscle, respectively. Most caudally, the lateral border meets the medial border of the scapula to form the inferior angle of the scapula. This is a prominent part of the scapula and is easy to palpate. The circumflex scapular artery turns from anterior to posterior hugging the scapula in its course and forms a groove on the lateral border of the scapula. This is roughly located midway along the length of the lateral border. This constant landmark has been used for measurements in the study of the three columns of the scapula (Chapter 4).

The medial border of the scapula lies adjacent to thoracic vertebrae 2-7. It has a shorter superior segment and a longer inferior segment. The two segments meet at the medial

angle. The spine of the scapula intersects the medial angle to form a triangular ridge formed by the attachment of the rhomboid minor. This is the most prominent part of the medial border of the scapula and is easily palpated. The medial border has several muscular attachments, including muscles stemming from the base of the skull, the vertebral column, and from the thorax. These muscles assist in elevating and retracting the scapula.

The superior border of the scapula is the sharpest and shortest of the three borders. It slopes laterally towards the base of the coracoid process and terminates at the posterior boundary of the suprascapular notch. It is completely covered by muscles. The junction of the medial border and the superior border form the superior angle of the scapula. This is completely covered by the trapezius muscle and is not palpable.

The spine of the scapula passes between the superior one third and lower two thirds demarcating the supraspinous and infraspinous fossae. It is a strong dense structure made up of cortico-cancellous bone. It runs from the medial vertebral border of the scapula to the neck of the glenoid, forming the keel of the scapula. Analogous to that of a ship, it provides structural integrity to this broad weak bone. It also gives attachment to the trapezius and deltoid muscles and helps suspend the scapula.

The lateral free extension of the spine is referred to as the acromial process. Its name originated from the Greek word *acros* meaning top, thus it is anecdotally referred to as the top of the shoulder. It is a quadrilateral structure with its posterior surface forming a distinct angle (Angular Acromialis). The acromion overlies the humeral head and the rotator cuff muscles. It is connected to the coracoid by the thick coracoacromial ligament. This complex of bone and ligament forms an arc above the humeral head and rotator cuff.⁴

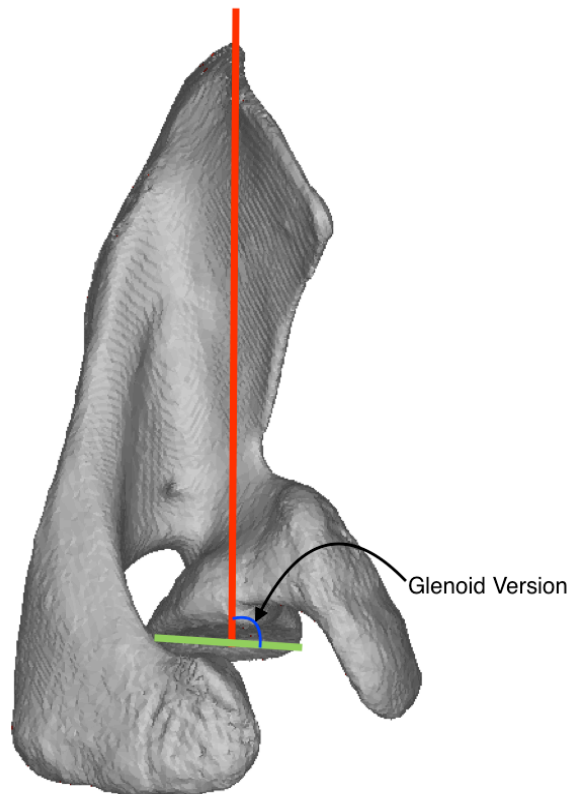
The coracoid process originates from the supero-medial surface of the glenoid. The root of the coracoid is marked by a small tubercle called supraglenoid tubercle laterally and

by the suprascapular notch medially. The coracoid passes vertically from its root and bends sharply at the coracoid tubercle to become almost horizontal. Its distal tip gives the origin to the short head of the biceps and the coracobrachialis muscles (conjoint tendon) and the body provides insertion to the pectoralis minor; the forces exerted by these muscles alter the shape of the tip of the coracoid.⁴⁻⁶ The rough superior surface of the coracoid attaches to the clavicle by means of strong ligaments (conoid and the trapezoid ligaments) and helps suspend the scapula from the clavicle.

1.1.1 ANATOMY OF THE GLENOHUMERAL JOINT

The glenoid is the lateral extension of the scapula. It has a neck bounded by the supraglenoid fossa medially and the glenoid fossa laterally. The size and shape of the neck greatly varies amongst individuals.⁷ The glenoid is composed of a dense cortical rim which gives attachment to a large almost circumferential cartilaginous labrum. This fibro-cartilaginous structure increases the depth of the glenoid cavity for articulation with the humeral head. The capsule of the shoulder joint attaches from the glenoid neck to the humeral head.

The glenoid fossa forms the socket of the GHJ. It is a pear shaped structure in the majority of adults; however in 30% of adults, it may be elliptical.⁸ The length of the glenoid is measured along the long axis of the glenoid from the supraglenoid tubercle to the inferior cortical rim of the glenoid. The maximum width of the glenoid is measured as the horizontal distance between its anterior and posterior cortical rim. It is the largest anteroposterior measurement perpendicular to its longitudinal axis. The size of the glenoid varies between men and women with the overall mean width 28 mm for men and 24 mm for women. The mean height of the glenoid has been reported as 38 mm and 33 mm for men and women, respectively.⁹ The ratio of the antero posterior measurement from the superior half of the glenoid to the lower half has been reported as 1:1.08.¹⁰ The superior inferior radius of curvature of the glenoid is on an average 2.3 mm greater than the superior inferior radius of curvature of the humeral head.¹⁰



Glenoid version is measured as the angle between the scapular plane and the anteroposterior axis of the glenoid

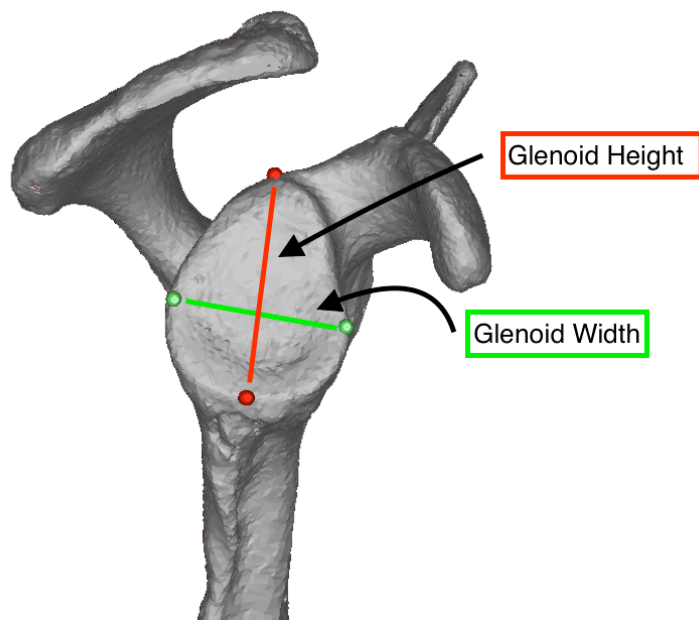


Figure 1.2 Measurement Of Glenoid Version And AP And SI Dimensions

The orientation of the glenoid articular surface is described in terms of version and inclination (Figure 1.2). Glenoid version is measured by the angle between the glenoid fossa and a perpendicular line known as the scapular axis. It is defined by a line from the center of the glenoid fossa to the medial angle of the scapula. This is measured in the axial plane. It is termed as retroversion if the glenoid faces posteriorly and anteversion if the glenoid faces anteriorly. The glenoid version in normal healthy adults varies from anteversion of 2° to retroversion of 6° depending upon the method of measurement. Further, the concave articular surface is noted to have a spiral twist with the cephalad part being more retroverted than the caudal part. This differential version may be as much as 11° .¹¹⁻¹⁴ Glenoid inclination is the angle between the glenoid fossa to the horizontal in the coronal plane. Normal inclination varies between -2° to $+6^{\circ}$ (negative value indicating a downward facing glenoid).¹⁵

The humeral head articulates with the glenoid. The humeral head is spherical in the center whilst is elliptical at its periphery. Head size ranges from 37 mm to 57 mm in adults, though the vast majority of humeral heads have a mean diameter from 46-52 mm. The mean radius of curvature for men is 23-28 mm whilst in females the mean is between 19-22 mm.¹⁰ The mean inclination angle measured from the shaft axis is 130° and the mean retroversion measured from the trans-epicondylar axis is 18° . However, both values show high variance, with head inclination varying from 120° - 135° and retroversion varying from -7° to 48° . In addition, the humeral articular surface has a posterior mean offset of 2.6 (1 to 6mm) and medial (mean offset 7 mm (3-11 mm) offset relative to the long axis of the humeral shaft.¹⁵

1.2 BONE FORMATION AND DEVELOPMENT

Intramembranous Ossification is defined as direct mineralisation of a highly vascular connective tissue membrane.⁴ In foetal life, a mesenchymal membrane causes appositional growth; this later changes to a periosteal layer which remains actively osteogenic throughout life. To simplify the mechanism, growth occurs in layers whereby the surface (periosteum) keeps adding new layers of bone which mature and later remodels to reach its adult form. Most of the flat bones in the body such as the skull, the bones of the face, mandible, clavicle and the body of the scapula display growth by this means.

Enchondral Ossification, as the name suggests, is development of bone within a cartilage core (anlage). In this mechanism of bone development, bone forming cells migrate into a developed cartilage and replace the cartilage over time with bone. This kind of process is described to define the growth of long bones of the upper and lower limbs. In the simplest of terms, two cartilage anlage develop at opposing ends of the long bone and enchondral ossification occurs to form a long bone in foetal life. During years of growth as a child, each end of the long bone grows by development of a growth plate (physeal plate or physis) and the central diaphysis is formed by the transformation of the cancellous metaphyseal bone to dense cortical diaphyseal bone.

When osteogenesis surpasses chondrogenesis, the process of physeal fusion commences. The control and initiation of union is under the influence of hormones. Growth ceases earlier in females than in males. It is well known that estrogen favours bone maturation whilst testosterone is chondrogenic.

Primary Ossification Center- The connective tissue precursor of future bone generally commences osteogenesis in a constant locus. This osteogenic precursor will expand in

size until the whole locus is replaced by bone. These primary ossification centres are generally found in embryonic/foetal life.

Secondary Ossification Center- The primary ossification center is usually not sufficient to form bone in the whole cartilaginous anlage. In such a scenario, secondary ossification (epiphyseal) centres develop and grow rapidly by means of the physeal growth plate.

1.2.1 DEVELOPMENT OF THE SCAPULA⁴

The scapula arises in the neck and descends to the 5th costal cartilage by day 52 of embryonic growth. The principal primary center of ossification of the scapula arises in the ventral surface in the vicinity of the neck of the scapula towards the end of the 2nd month of foetal life. Bidirectional expansion of the ossification leads to the formation of two enchondral radiating cones - a medial vertebral and lateral glenoidal with its ends undergoing epiphyseal formation. The growth of the medial vertebral cone is accelerated compared to the lateral glenoid cone, resulting in a much larger medial border (Figure 1.3). The space between the two cones is filled by inter membranous ossification, which forms the blade of the scapula (explaining its flat morphology).

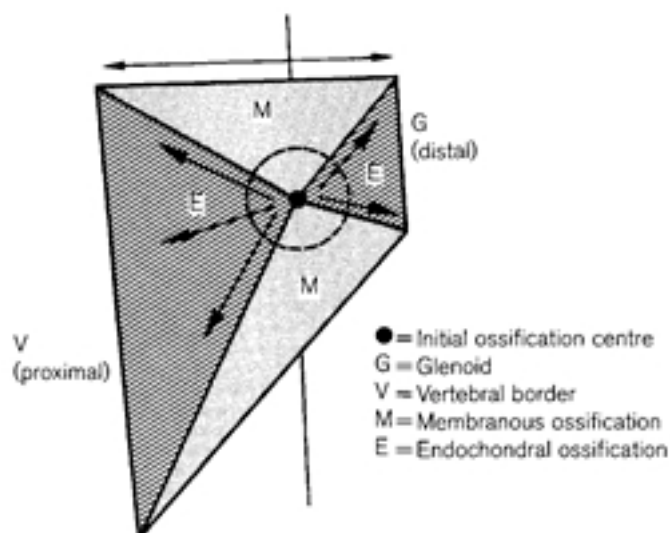


Figure1.3 Development Of The Scapula. © Permission from © Developmental Juvenile Osteology, Louise Scheuer, Sue Black, 2000 Elsevier

At birth, the acromion, coracoid, glenoid articular surface, medial border and inferior angle are cartilaginous. The supraspinous and infraspinous fossae are very flat. The spinous process ends in a bulbous lateral extension with a dorsal epiphyseal surface (later develops as the acromion process). The glenoid is oval and concave with articular surface extending onto the superior and ventral surfaces to articulate with the coracoid process. A ventral notch (formed by the passage of subscapularis tendon) delineates the coracoid from the glenoid (Figure 1.4)

The Body of Scapula

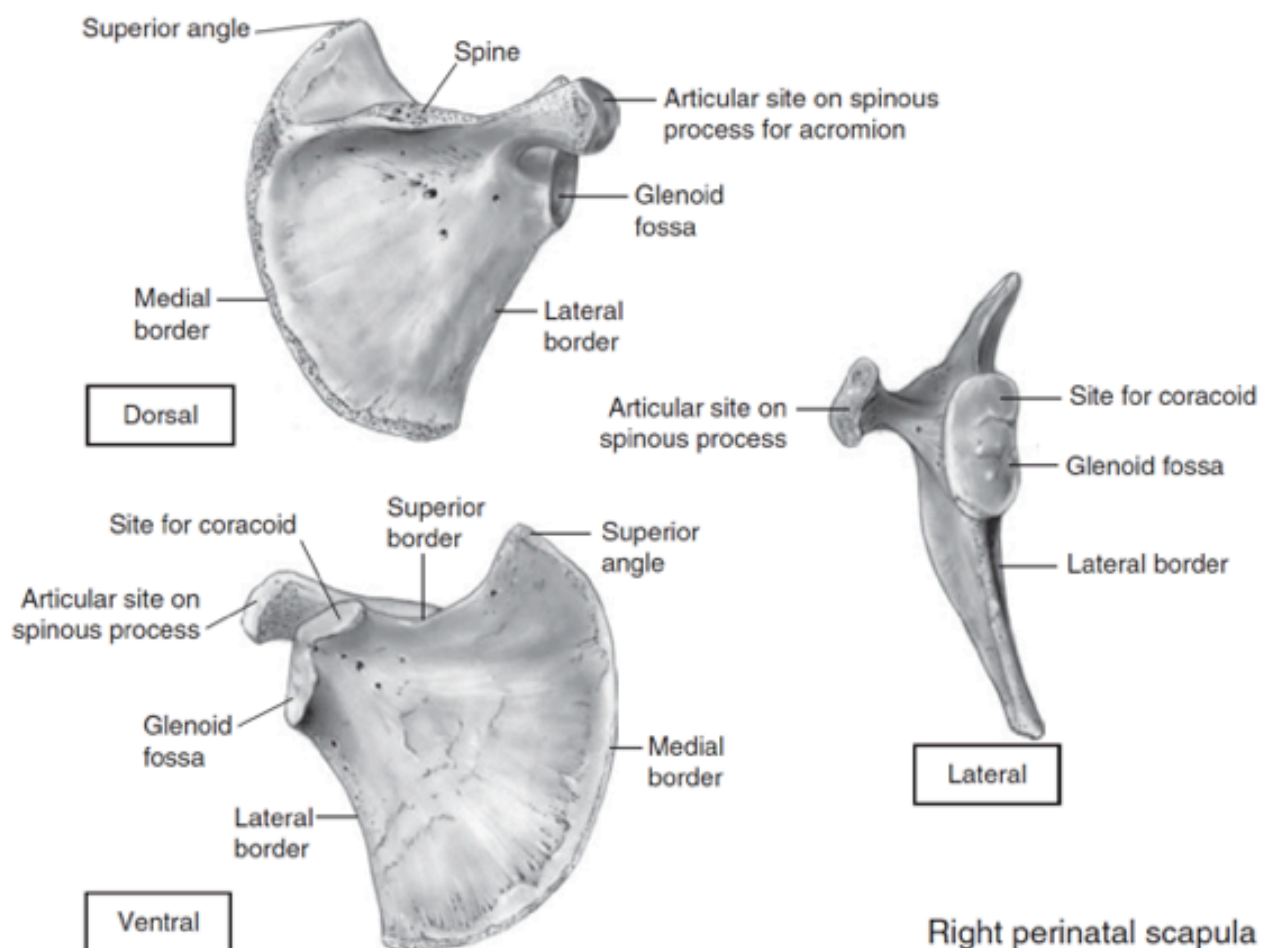


FIGURE 1.4 PERINATAL SCAPULA © Permission from © Developmental Juvenile Osteology.
Louise Scheuer, Sue Black, 2000 Elsevier

The center of ossification for the coracoid develops from the 1st to 2nd year of life. The hook shaped coracoid is recognised as a separate structure. The broad base has a large surface for articulation with the scapula and a smaller postero lateral surface for the sub coracoid center.

The coracoid usually fuses to the scapula around 14-15 years. Fusion commences dorsally and the ventral sub coracoid center, next to the scapula is the last region to fuse.

The scapula has seven secondary ossification centres. Three for the coracoid, one for the inferior glenoid, one for the acromion, one for the inferior angle and one (or more small ones) for the medial border of the scapula.

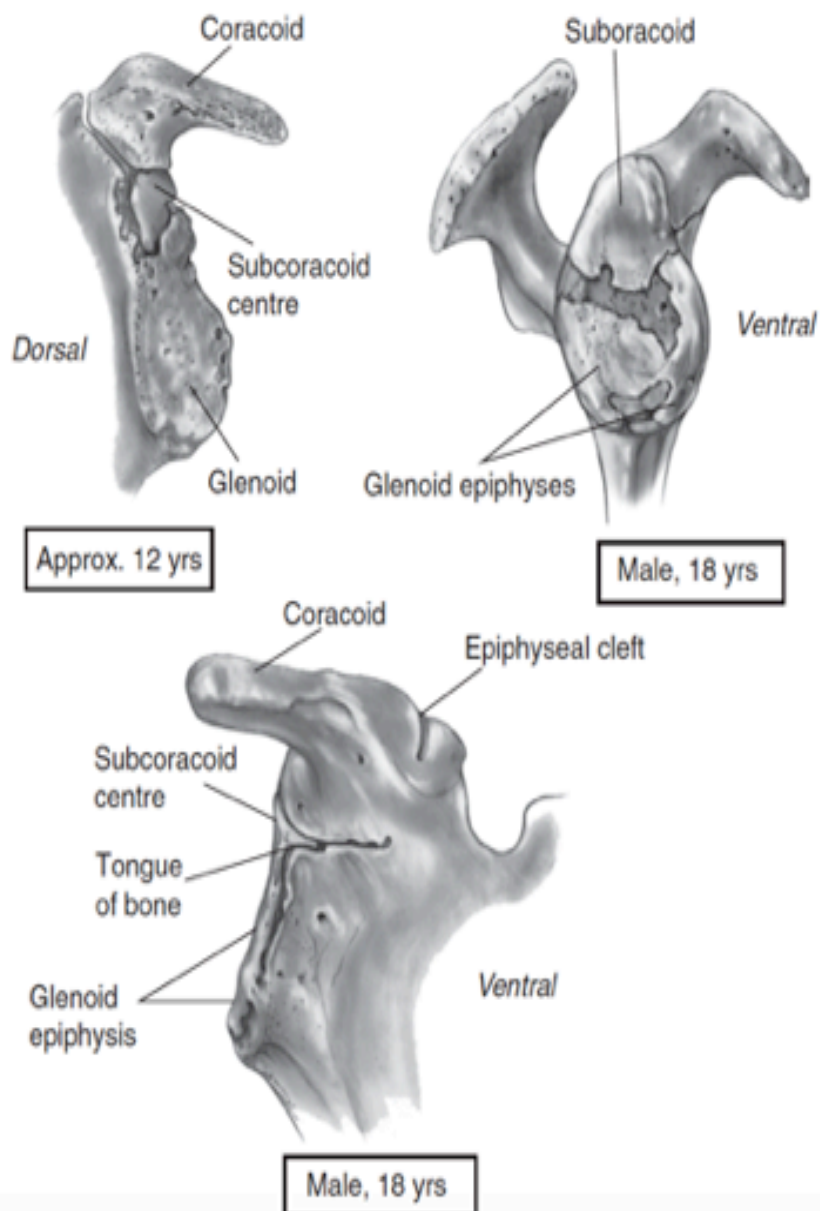
To understand the development of the scapula, it is vital to look at the development of the scapula and glenoid individually.

1.2.2 DEVELOPMENT OF THE GLENOID

The superior and the inferior part of the glenoid develop independent of each other. The 2 ossification centres fuse between 17-18 years to form the adult glenoid (Figure 1.5)

The **Subcoracoid Center** (*forms the base of the coracoid and the upper 1/3 of the glenoid*) is the 1st secondary ossification center to appear (8-10 years of age). It appears on the superior surface of the glenoid, dorsal to the base of the coracoid. Its double epiphyseal surfaces allow differential union (this epiphyseal plate culminates to form a tubercle upon fusion, which is referred to as the supraglenoid tubercle in the adult). The superior part of this epiphyseal growth plate unites first with the base of the coracoid. The inferior part of this ossification center continues to grow and forms the top 1/3 of the glenoid. By the age of 16-17 year's, complete fusion of the sub coracoid, coracoid and scapular centres occurs, demarcated by a ventral indentation on the upper glenoid rim (Figure 1.6).

The Subcoracoid Center and Glenoid Epiphyses



Development of the right subcoracoid and glenoid epiphyses

FIGURE 1.5 - DEVELOPMENT OF THE GLENOID © Permission from
 © Developmental Juvenile Osteology, Louise Scheuer, Sue Black, 2000 Elsevier

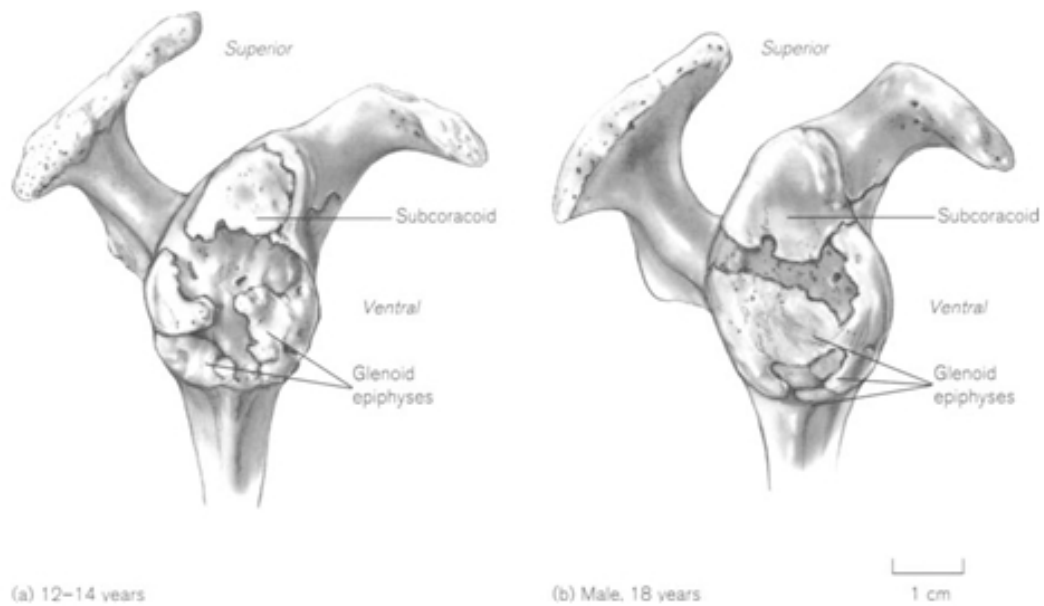


FIGURE 1.6 DEVELOPMENT OF THE LOWER GLENOID © Permission from © Developmental Juvenile Osteology, Louise Scheuer, Sue Black, 2000 Elsevier

1.2.2.1 Glenoid Center (*forms the inferior circular part of glenoid*)

The inferior aspect of the glenoid develops from islands of secondary ossification located around the periphery of the glenoid. Each island grows with tongue like projections and ultimately fuses with down growths from the sub coracoid center to form the adult glenoid (Figure 1.6). Fusion occurs around 17-18 years of age (Figure 1.7). Delayed fusion or arrested development of this center results in glenoid dysplasia.

1.2.2.2 Development of the Coracoid

Secondary centres develop at *the angle of the coracoid, apex of the coracoid and accessory trapezoid islands*. These epiphyses fuse amongst one another and then to the sub coracoid epiphyseal plate to form the mature adult coracoid. Fusion is usually complete by 20 years of age.

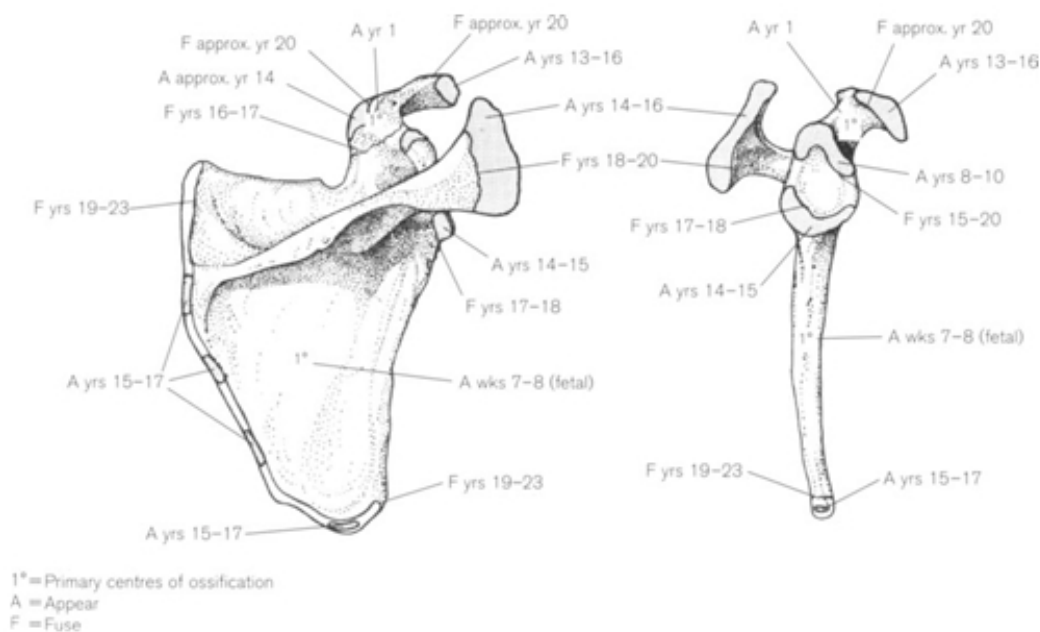


Figure 1. 7 Times Of Appearance (A) And Fusion (F) Of Scapular Ossification Centers© Permission from © Developmental Juvenile Osteology, Louise Scheuer, Sue Black, 2000 Elsevier

1.2.3 DEVELOPMENT OF THE SCAPULAR BODY

The majority of the scapular body develops from the primary center of ossification during foetal life. Further growth of this region is by intramembranous ossification and depends upon the development of the surrounding muscles. Both the supraspinous and infraspinous fossae are initially very flat. As the muscle bulk increases these fossae take their adult shape.

1.2.3.1 Medial Border Epiphysis (*forms medial/ vertebral border*) is formed by the coalescence of a number of small islands on the medial border of the scapula. Fusion is complete by 23 years thus making it the last epiphysis to fuse.

1.2.3.2 Inferior angle epiphysis (*forms the inferior angle of the scapula*) appears between 15-17 years and fuses by 23 years thus forming the inferior angle of the scapula.

Thus, the medial border of the scapula continues to grow until the third decade of life whilst the coracoid and glenoid epiphysis usually cease growth by late teens.

1.2.3.3 Development of the Acromion

Medial Surface of the acromion including **the angle of the acromion** develops from the *primary ossification center*, which forms the acromial spine.

Acromial epiphyseal center (*forms the lateral edge of the acromion*) Multiple small island coalesce to form the lateral edge and anterior tip of the acromion. Fusion generally occurs by 18-20 years.

Failure of fusion of the medial (*spinous*) and lateral (*acromial ossification center*) results in the formation of a bi partite acromion (*os acromiale*).

Thus to summarise, scapular development is a complex process of origin and fusion of various growth centres. However, it is clear that the scapular body and the glenoid develop independent of each other and have very different mechanisms of maturation to reach the adult shape. The medial and inferior part of the scapula continue to grow till the early 3rd decade; making them one of the last regions to cease growth in the human skeleton. In addition, the glenoid develops from 2 very different growth centres, which ultimately unite in late teens to form the adult glenoid. This explains the difference in morphology of the superior and inferior part of the glenoid.

1.3 BIOMECHANICS

1.3.1 NORMAL SHOULDER JOINT BIOMECHANICS

The gleno-humeral joint is a synovial enarthrodial ball and socket joint. It allows poly axial movement of the humeral head relative to the scapula. Despite its ball and socket morphology, translation of the humeral head onto the glenoid occurs with movement. This is primarily due to the relative incongruence of the glenoid surface and the humeral head.

Sahara et al using a vertically open MRI, evaluated 3D position of the glenohumeral joint during abduction. The authors reported that in the supero-inferior direction the humeral head translated slightly inferiorly from +1.9 mm at 0° to +0.8 mm at maximal abduction. In the antero-posterior direction the humeral head translated anteriorly by +2.4 mm from 0° - 90° and posteriorly by -1.4 mm from 90°- 150° of abduction. Furthermore, the humeral head contact pattern with the glenoid changed from the central to posterior part of the humeral head in mid range of abduction.¹⁶

Normal kinematics of the shoulder are dependent on synergistic motion of the deltoid and the rotator cuff. The deltoid is considered the engine of the shoulder joint. The deltoid is the strongest abductor of the shoulder joint. Abduction is the key function of this large triangular multi pinnate muscle. Its anterior fibres contribute to forward flexion and internal rotation and whilst posterior fibres contribute to external rotation and extension.

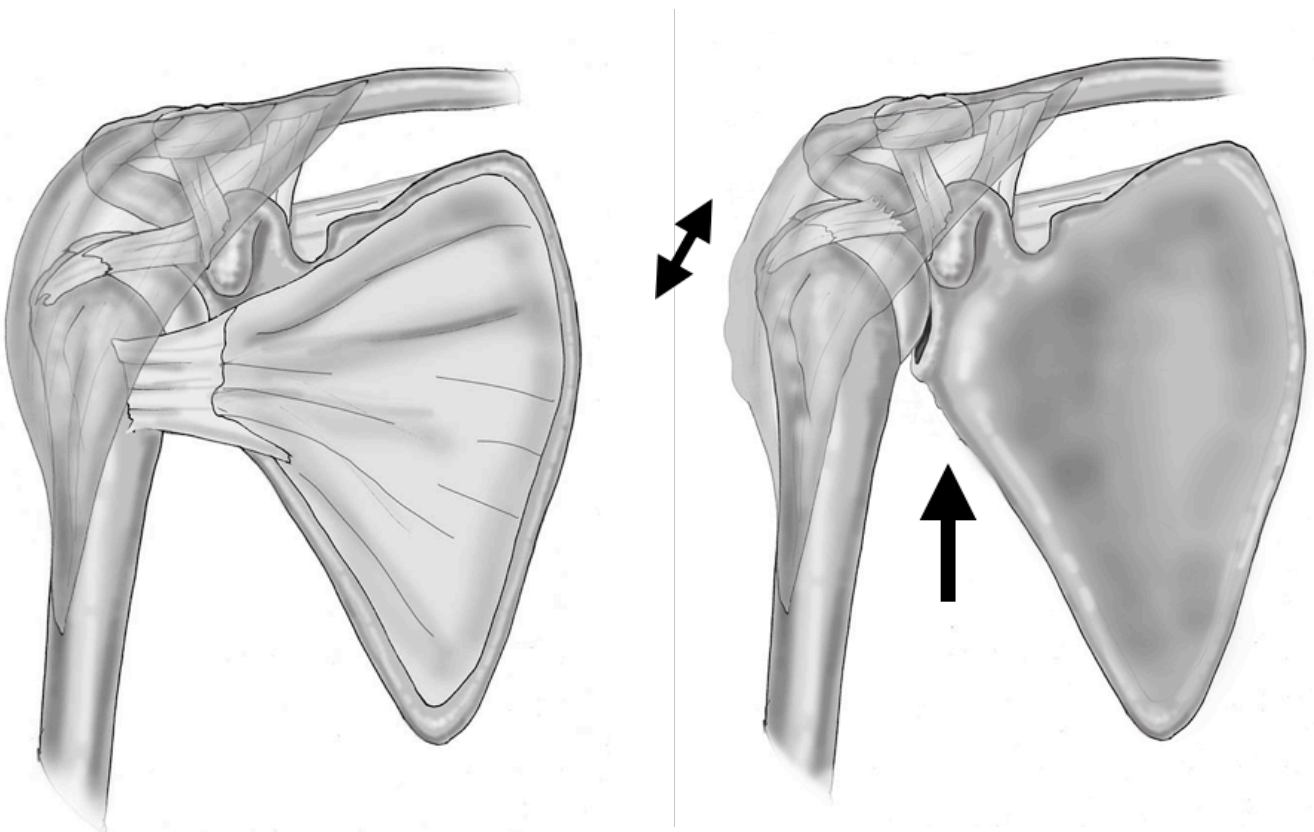


Figure 1.8 Normal Shoulder 1.8(A)The Deltoid Is Tensioned and The Rotator Cuff Stabilizes The Center Of Rotation (Balanced Force Couple). Figure 1.8(B) In A Rotator Cuff Deficient Shoulder; The Compressive Effect Of The Cuff Is Absent (Unbalanced Force Couple) Thereby Shortening The Deltoid Lever Arm

The rotator cuff is crucial for providing a balanced force couple, which compresses the humeral head onto the glenoid whilst the deltoid exerts an abduction force. Joint reaction forces of approximately 44% (335 N) – 85% (650 N) of total body weight are experienced at the GHJ at full abduction. The joint reaction forces increase with increasing abduction angle and peak at 90° of abduction. Forces at the GHJ vary according to ratio of forces in the supraspinatus and deltoid. The supraspinatus with its smaller moment arm generates a greater applied force (40% increase), to counterbalance the mass moment of the upper extremity with a non-functioning deltoid. On the contrary in a supraspinatus deficient shoulder a significantly larger deltoid force is required to initiate abduction than to maintain abduction. This may be explained by the fact that the

moment arm of the deltoid is short at the initiation of abduction and longer at the end of abduction.^{17,18}

The subscapularis and the infraspinatus/ teres minor provide a transverse force couple that is active during abduction of the shoulder; maintaining the center of rotation through abduction (Figure 1.8a). The subscapularis has an internal rotation moment arm of 23 mm in the resting position, making it the strongest internal rotator. Posteriorly the infraspinatus and teres minor have external rotation moment arms of 24 mm and 17 mm, respectively.^{15,19,20}

Furthermore, it is well understood that both the subscapularis and infraspinatus contribute to abduction of the arm with the humerus in external rotation and internal rotation respectively. This is clinically evident in patients who have good elevation of the arm with complete supraspinatus tears and therefore strengthening of the remainder of the cuff is the focus of rehabilitation in such patients.²¹

Joint reaction forces in the GHJ significantly decrease in the presence of rotator cuff tears (Figure 1.8b). Isolated incomplete or complete tears of supraspinatus lead to a marginal reduction in joint reaction force 296 ± 83 N and 300 ± 85 N respectively compared to a normal joint (337 ± 88 N) with all tendons intact. However, extension of the tear beyond the supraspinatus, to involve the infraspinatus and or subscapularis leads to a significant reduction of joint reaction force 126 ± 31 N. In addition, the force exerted in a very different direction. The resultant force couple depends on the size and extent of the remaining cuff. This leads to very abnormal GHJ kinematics. If the tear configuration disrupts the transverse force couple, the deltoid force by itself is unable to achieve maximal abduction. The loss of effective concavity compression prevents abduction above 90 degrees due to the loss of a stable fulcrum. In addition, the loss of the centring effect of concavity compression results in a decrease of the inferiorly directed force vector. This effect is also noted in the antero posterior direction where the head translates in the direction of the remaining cuff muscle. All these changes exaggerate load transmission across the GHJ and lead to accelerated chondral and later bony damage.²²

1.4 GLENOHUMERAL JOINT OSTEOARTHRITIS (GHJ OA)

Primary osteoarthritis (OA) is idiopathic. Secondary OA may be caused by trauma, infection, genetics or various other extraneous causes. Whatever the primary aetiology, OA is characterised by sub-chondral sclerosis, reduced joint space due to loss of articular cartilage, formation of osteophytes and sub-chondral cysts. Loss of articular cartilage, abnormal kinematics and an inflammatory response leads to pain and restriction of movement. This sets a vicious cycle causing further muscle weakness, stiffness, pain and loss of function.

Loss of glenoid articular cartilage ultimately leads to glenoid bone defects. The glenoid erosion might occur in a concentric or in an eccentric fashion. Eccentric glenoid erosion further causes subluxation of the humeral head and progression of OA. It is unknown whether primary humeral head subluxation leads to the erosion or vice versa; however, the end result is the same.

CLASSIFICATION OF GHJ-OA

Samilson and Prieto radiologically classified shoulder OA as grade 0 or normal, grade 1 or mild OA (inferior humeral or glenoid osteophyte <3 mm in height), grade 2 or moderate OA (slight GH irregularity with inferior humeral or glenoid osteophyte 3-7 mm) and grade 3 or severe (GHJ narrowing and sclerosis with inferior humeral or glenoid osteophyte >7 mm).²³ This classification has been used in this thesis to establish the inclusion criteria for the subjects. Only subjects with GHJ OA grade 0 to grade 2 were included for analysis.

Furthermore, advanced GHJ-OA classification systems exist, based upon the extent of bone loss and aetiology of arthritis (i.e. cuff tear, trauma, inflammatory etc.).

GLENOID BONE LOSS in OA

Primary OA

Walch et al. classified glenoid erosions in primary OA as Type A, B and C. Symmetric glenoid erosion is classified as Type A (A1= Minor and A2 = Major). Asymmetric glenoid erosion is classified as Type B (B1 = narrowed posterior joint space with no signs of glenoid posterior erosion and B2 = posterior glenoid erosion with a visible articular biconcavity). Dysplastic glenoids are classified as Type C (glenoid retroversion $>25^\circ$).²⁴

Cuff Tear Arthropathy

Chronic tear of the rotator cuff leads to altered joint mechanics. Depending upon the extent of the cuff tear there is a loss of the balanced force couple. The loss of the depressor effect of the rotator cuff results in proximal humeral head migration. Abnormal joint mechanics leads to chondral injury and development of secondary OA. Numerous classifications have been developed to define severity of cuff tear arthropathy.

Based upon humeral head migration

Hamada Classification²⁵ - Used the Acromio Humeral interval (distance between the humeral head and the acromion in a true anteroposterior shoulder radiograph)

Grade 1: Acromio Humeral interval $>6\text{mm}$

Grade 2: Acromio Humeral interval $\leq 5\text{mm}$

Grade 3: Grade 2 changes + acetabularization of the acromion (concave deformity of the under surface of the acromion caused by humeral head abutment).

Grade 4: Grade 3 changes + narrowing of GHJ

Grade 5: Bony destruction – humeral head collapse

Based Upon Glenoid Bone loss

Sirveaux et al.²⁶ classified cuff tear arthropathy as

E0 was defined as a normal glenoid

E1 was defined by a concentric erosion of the glenoid.

E2 erosion of the superior part of the glenoid

E3 the erosion extended to the inferior part of the glenoid

Based upon Humeral head migration and Glenoid Bone loss

Seebauer et al.²⁷ have classified cuff tear arthropathy based upon humeral head migration and glenoid bone loss as:

Type 1A - Centered stable, Minimal superior migration,

C-A arch acetabularization

Type 1B - Centered medialized, Minimal superior migration,

medial glenoid erosion, C-A arch acetabularization

Type 2 A - Decentered limited stable, superior translation,

superior-medial erosion

significant C-A arch acetabularization

Type 2 B - Decentered unstable, anterior superior escape,

C-A arch and anterior structures deficient

1.5 REVERSE SHOULDER ARTHROPLASTY (RSA)

Rupture of the rotator cuff causes a loss of the stabilizing fulcrum and results in an unbalanced shoulder. This leads to proximal (superior) migration of the humeral head, with deltoid contraction. The humeral head with time impinges upon the undersurface of the acromion, which now becomes the new fulcrum for abduction. Neer in 1983²⁸ described this process in detail and described the term ‘cuff tear arthropathy.’ He proposed the ‘preferred method appears to be a resurfacing total shoulder replacement with rotator-cuff reconstruction and special rehabilitation.’²⁸

Repair of the cuff in conjunction with a total shoulder replacement though; a rational idea was often not possible. Poor quality or irreparable rotator cuff tendons led to early failures of the total shoulder replacement.²⁹ Neer explored constrained shoulder designs, as he believed that constraint would obviate the need for a cuff repair. In an effort to create a fixed fulcrum prosthesis Neer developed the Mark I, Mark II and Mark III prostheses. These prostheses lateralized the center of rotation, which often made repair of the residual cuff difficult. Failure of these designs convinced Neer that rotator cuff repair, not constraint, was critical for improving shoulder function.³⁰

The concept of reversing the ball to the glenoid and socket to the humerus saw the development of various prosthesis designs.³¹ The most successful out of these was the design proposed by Grammont in 1987. Grammont^{32,33} popularized his novel idea, which was based upon 4 underlying principles: 1) the prosthesis must be inherently stable, 2) the weight bearing part must be convex and the supporting part concave, 3) the center of the sphere must be at or within the glenoid neck and 4) the center of rotation must be medialized and distalized.^{32,33} This led to the development of the Delta I, II, and III prosthesis. These fundamental concept still holds true and are the foundation of all the current reverse shoulder arthroplasty designs.³⁴

The Delta prosthesis has been implanted in Europe since the early 1990’s and received Heath Canada approval in 2003 and FDA approval in the USA in 2004. The Reverse Shoulder Arthroplasty (RSA) was initially developed to treat cuff tear arthropathy. Due to its widespread success, the pathologic indications and age limitations have decreased.

The present indications for RSA now include Cuff Tear Arthropathy, irreparable rotator cuff tears with or without glenohumeral arthritis, glenoid deformities, acute and chronic trauma, tumor, systemic/inflammatory arthritis and revision arthroplasty.³⁴

1.5.1 COMPONENTS OF AN RSA

A RSA consists of 4 main components (Figure 1.9). A base plate that is fixed onto the glenoid surface by varying configurations of screws. A glenosphere that is hemispherical in shape and is fixed on to the baseplate (by a Morse taper construct), and may be additionally, secured onto the baseplate with the aid of a central screw. The humeral component consists of a humeral stem that may be a single unit (mono block) or made up of multiple separate units, which can be assembled prior to insertion (modular stem). Modularity increases the various options available to the surgeon and helps match each prosthesis to the patient's individual anatomy. The humeral stem is composed of an epiphyseal component which fits into the humeral epiphysis and metaphysis and a diaphyseal stem. The 4th component is a polyethylene liner, which is inserted on the humeral epiphyseal tray and forms the articulation between the glenosphere and the humerus. Thus the RSA is a non-linked prosthesis relying primarily on the surrounding soft tissue and muscular structures to provide stability and function.

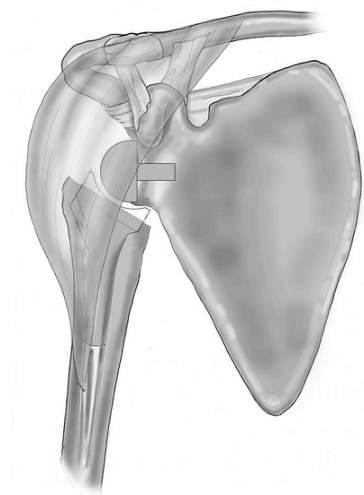


Figure 1.9 Reverse Shoulder Arthroplasty (RSA)

1.5.2 BIOMECHANICS OF A RSA

Medialization of the Center of Rotation (COR), large glenosphere size and the use of a 155° humeral neck inclination, which tensions and lengthens the deltoid arm are the hallmarks of the Grammont design RSA implants. To mitigate the problem of early baseplate loosening and failure in the earlier generations of RSA's, Grammont proposed shifting the COR medially and inferiorly. This significantly reduces the shear forces on the baseplate at the glenoid and prevents early implant loosening. In addition, this new COR lengthens the deltoid muscle by 20% and increases the deltoid moment arm by 42% to compensate for loss of rotator cuff function. This restores stability by reversing the envelope of joint contact forces and reacting to increased shear forces.³⁵ However, the net force exerted by the deltoid is in a different direction compared to the anatomical GHJ. This force is exerted as a superior pulling/ shearing force on the glenoid. The overall compressive forces are reduced and cumulatively the total joint contact force is reduced by 41% compared to a normal shoulder.³⁵ This is a fine balance, which the surgeon has to attain; the altered kinematics helps minimise implant loosening by reducing total joint forces, but in turn can lead to dislocation and instability if the balance is not struck right.

1.5.3 CURRENT BASEPLATE DESIGNS

There are 16 different RSA prosthesis which have FDA approval for use. The vast majority of these prosthesis use a circular designed baseplate. Few prostheses employ an elliptical baseplate design. Irrespective of the baseplate design utilised, the core principle needs to be upheld: the glenosphere needs to be positioned as low as possible; so as to allow overhang of the inferior part of the glenosphere over the scapular neck. The aim is to prevent scapular notching and increase the deltoid lever arm.³⁵

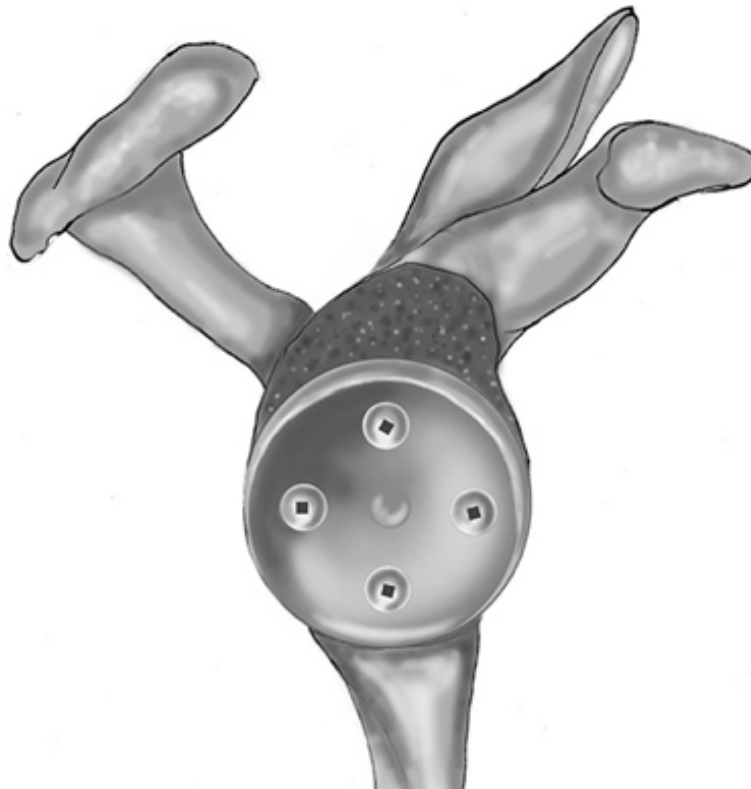


Figure 1.10 Current Circular Baseplate Design

Rationale for a circular baseplate

The inferior glenoid is circular in shape in the majority of patients and is typically preserved in cuff tear arthroplasty. Rigid primary fixation of the baseplate is therefore attainable. The circular baseplate design employs a central peg with or without a large central screw and an addition of 2 to 4 peripheral screw holes for fixation, by either locking or non locking screws. The disadvantage is that the good quality bone on the superior part of the glenoid face is not utilized (Figure 1.10).

Rationale for elliptical baseplate design

An elliptical baseplate allows larger coverage of the glenoid surface by increasing the surface area of the baseplate. Thus, the central peg/ screw can be of a larger diameter (up to 6.5 mm central screw with a 10 mm central peg). This allows the superior screw to be positioned higher, or allows the placement of > 4 screws for baseplate fixation. This design resists higher torques subjected by a laterally offset glenosphere design and provides stronger initial fixation.³⁶ The down side is that the baseplate tends to be bulkier and an eccentric lateralised glenosphere with inferior overhang needs to be used.

Screw positioning with the current baseplate designs

Fixation of the Current RSA Design

Primary base plate fixation and stability rely on the quality of bone in the glenoid vault and the position and length of peripheral screws and the central peg or screw. Micro-motion around the baseplate will increase as the surrounding bone density decreases. Most RSA are performed in the elderly where the glenoid vault has reduced bone density. Primary fixation by the central peg is imperative to attain initial implant stability. The central peg along with the superior and inferior screws provides 77% of the primary implant stability.³⁷ Finite element analysis (FEA) studies have demonstrated that increasing the screw length has the maximal effect on primary implant stability. Further increasing the angle of insertion of the screw fixing the baseplate to the bone improves implant stability.³⁸

Three column concept

In 2008, Norris et al popularised the Three Column Concept for glenoid baseplate fixation (Figure 1.11) in RSA.³⁹ The author conceptualised the scapula as 3 bony columns attached to the glenoid. The 3 columns include:

- 1 The base of the coracoid
- 2 The scapular spine
- 3 The lateral / scapular pillar

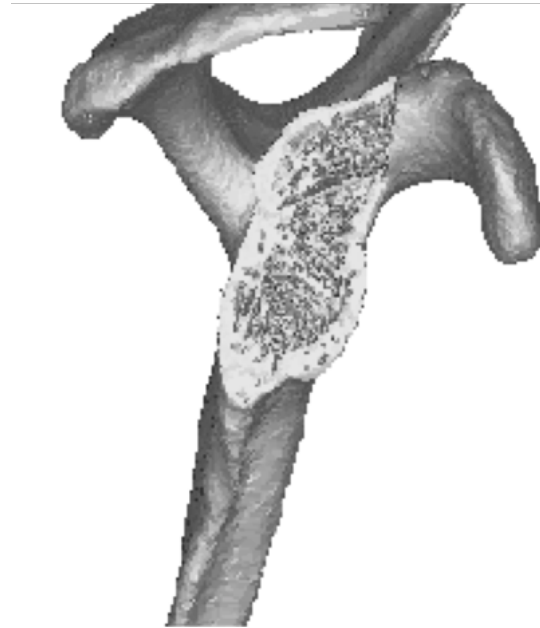


Figure 1.11 The 3 Columns Of The Scapula With Glenoid Subtraction

These columns of bone provide good quality bone stock for optimal screw fixation (ie. longest screw with bi-cortical fixation). The authors described the screw trajectory to target each column independently. They used a circular baseplate (Aequalis Reverse Prosthesis, Wright Medical Inc.) with 2 variable and 2 fixed angle screws. The authors defined the ideal screw trajectory for each column. The coracoid column ideal screw trajectory was 19° superior and 5° anterior. The average trajectory for the scapular spine was 14° superior and 13° posterior. The average trajectory for the inferior column/scapular pillar was 7° anterior and 14° inferior. Using the current implant design, the authors were unable to attain fixation in all 3 columns simultaneously.³⁹ Most surgeons in such a scenario would attempt screw purchase in the coracoid column and the scapular pillar. The remaining 2 holes of the base plate would be used to insert small screws into the glenoid vault. In addition, all the screw trajectories in the study are based upon placement of the baseplate on a normal glenoid face with normal bone stock.

Changes in glenoid morphology (version and inclination) or loss of bone stock would significantly alter these trajectories.

Numerous other studies have tried to identify the best screw trajectory by positioning the glenoid baseplate onto a normal glenoid face.⁴⁰⁻⁴³ The aim of all these studies is to attain ideal screw fixation in a safe manner, as to avoid injury to the neighbouring neurovascular structures. Authors have concluded that fixation into all the three columns of the scapula is not attainable with the current baseplate designs.^{40,41}

1.6 GLENOID BONE LOSS AND RSA

1.6.1 GLENOID BONE LOSS CAUSED BY CURRENT RSA DESIGN

Radiographic notching remains the commonest post-operative complication of the current 155° RSA designs. Notching is defined as bone loss in the lateral pillar of the scapula as a result of mechanical impingement of the medial surface of the humeral epiphysis or polyethylene onto the lateral pillar of the glenoid, during maximal adduction of the arm. Notching is classified from Grade 0 - 4 by Nerot⁴⁴ (Grade 0 No Notch, Grade 1 Small Notch, Grade 2= notch with condensation, Grade 3= Erosion up to the inferior screw and Grade 4 =erosion over the inferior screw and extension under the baseplate).

In a systematic review of 782 RSA procedures with a minimum 2 year follow-up, an overall notching rate of 35% was reported. It was as high as 48% in Grammont style prosthetic designs. However, the authors reported an overall aseptic glenoid loosening rate of only 3.5%.⁴⁵ The clinical significance of notching leading to poorer clinical outcome is debatable. Some studies have implicated scapular notching to aseptic glenoid

loosening.^{26,46-48} However, a large study of 337 RSA with a mean follow up of 47 months reported no such clinical effect.⁴⁹

1.6.2 MANAGEMENT OF GLENOID BONE LOSS USING THE CURRENT RSA DESIGNS

Glenoid bone loss is often encountered in patients undergoing reverse shoulder arthroplasty. Bone loss is encountered in patients with chronic gleno-humeral dislocation, in the setting of cuff tear arthropathy with glenoid bone erosion, as a consequence of failed prior arthroplasty, or as a result of failed proximal humeral fracture fixation with glenoid erosion due to hardware penetration.

Glenoid defects can range from small defects, which can be managed by eccentric reaming of the glenoid, to large complex centric and eccentric defects, which may require cortico-cancellous grafts. Significant bone loss requiring bone grafting during reverse shoulder arthroplasty is reported to occur in up to 38% of cases.¹¹

Bone grafting glenoid defects for total shoulder arthroplasty has demonstrated unpredictable results.⁵⁰⁻⁵³ A high rate of graft subsidence, graft resorption and instability has resulted in early glenoid component loosening and early failure. Further, asymmetric bone loss with retroversion beyond 15° cannot be managed by high side reaming.⁵⁴

Reverse shoulder arthroplasty is a promising alternative.⁵⁵⁻⁵⁷ The geometry of the prosthesis design along with a rigidly fixed base plate provide an axial compressive force to the bone graft, which promotes graft incorporation. However, reconstruction of the glenoid anatomy is a prerequisite for a successful RSA. Management of large glenoid defects remains a challenge. Options vary from impaction bone grafting of contained defects to large structural allografts for large vault defects, but graft subsidence still remains a problem.^{50,51,58}

Fixation of the glenoid baseplate in the presence of large bone defects remains a challenge. A paucity of bone stock available has led surgeons to search for bone stock beyond the glenoid vault. The three columns of the scapula provide such bone for glenoid baseplate fixation. The ideal screw trajectories for fixation have been described above. However, the current baseplate designs do not provide the surgeon with the flexibility to address all the above issues.

1.7 SCOPE OF THE PROBLEM

The number of shoulder arthroplasties performed each year is steadily increasing world wide. RSA has emerged as an alternative treatment for end stage GHJ arthritis. In 2002, in the USA, 24,677 patients underwent shoulder arthroplasty, of which 10,125 (41%) were Total Shoulder Arthroplasty (TSA) and 14,552 (59%) were Hemiarthroplasties (HA). RSA was not available in the US market until 2004. In 2011, 66,485 patients underwent shoulder arthroplasty procedures with 21,692 (32.6%) RSA, 29,359 (44%) TSA and 15,434 (23%) HA. Per capita utilization of shoulder arthroplasty has more than doubled from 2002-2011 from 24.5 per 100,000 people to 54.4 per 100,000.⁵⁹

The Australian Orthopaedic Association National Joint Replacement registry, in its analysis of 27,236 shoulder arthroplasties from 2008-2014, noted an increase of 71.9% in the number of procedures performed annually since 2008. The number of hemiarthroplasties is steadily declining. Most of the hemiarthroplasties were performed for fracture. The cumulative revision rate at 7 years was 8% each for fracture and OA. Of the revisions of HA, 92.4% were revised to RSA. Out of the 19,059 (8,906 TSA and 9,682 RSA) the reported cumulative revision rate at 7 years is 9.4% for TSA and 5.4% for RSA. The registry highlights a higher revision rate for uncemented metal back TSA glenoids, especially metal back glenoid with a modular insert (15.8% vs 3% for all poly glenoids).⁶⁰

As the global use of TSA and RSA increase the number of patients requiring revision arthroplasties will steadily increase. Tackling glenoid bone loss and achieving primary glenoid baseplate fixation are the challenges shoulder arthroplasty surgeons will routinely have to encounter. The current baseplate designs in RSA need modification and further development to face the demands of revision shoulder arthroplasty.

1.8 PROJECT OBJECTIVES AND HYPOTHESES

The aim of this thesis is to develop a better understanding of scapular morphology and its role in RSA design. We aim to study the effect of sexual dimorphism on scapular morphology. To accurately study the orientation of the acromion, coracoid, glenoid and the lateral pillar of the scapula, accurate analysis of the anthropometry is needed. A 3D generated computer model is created using fine cut computerised tomographic images.

While the scope of this thesis does not include a specific design of an implant, the objectives of this work were to establish the anatomical relationships that are relevant to screw placement, peg placement and positioning of a baseplate for revision shoulder arthroplasty.

The pursuit of understanding scapular morphology for RSA design led to **3 specific objectives**.

Objective 1 Analysis of the scapular body and glenoid firstly requires the development of reference co-ordinate planes / axis. The three current scapular co-ordinate systems are described to understand GHJ biomechanics. A discrepancy exists between the co-ordinate planes described by the International Society of Biomechanics (ISB) and the clinical plane used by the orthopaedic community. The clinically used scapular plane depends on referencing the center of the glenoid. This may be an issue in situations of glenoid bone loss where by this plane cannot be accurately recreated. Using the scapular plane, accurate implant positioning is not possible. The 3 different co-ordinate planes are evaluated and the relationship amongst them is established.

Hypothesis 1 *A scapular co-ordinate system can be developed independent of glenoid morphology.*

Objective 2 In chapter 3, scapular anthropometry is revisited and we aim to find correlations between the scapular body and glenoid dimensions. With significant glenoid bone loss, the restoration of normal glenoid anatomy remains a challenge. Clinically, the surgeon has to rely on the contralateral shoulder or attempt to restore anatomy based upon clinical judgement. The objective of this study is to study the anthropometric relationship between the scapular body and the glenoid. This will aid in restoration of glenoid bone stock and predicting the correct size and positioning of the glenoid component.

Hypothesis 2 *The glenoid dimensions can be predicted using the scapular body dimensions.*

Objective 3 In chapter 4, the three columns of the scapula are evaluated and the relationship between them is analysed. Sexual dimorphism of scapular anatomy has been reported, however, this has not translated into implant design. In this study, we attempt to understand the anatomy of the 3 columns of the scapula and establish the relationship of each column independent of glenoid anatomy. This will provide the foundation upon which an RSA glenoid baseplate can be built.

Hypothesis 3 *The location of the best bone stock beyond the glenoid vault varies between sexes.*

1.9 THESIS OVERVIEW

Following the background information and general discussion of Chapter 1, Chapter 2 evaluates the various co-ordinate planes of the scapula and defines the relationships between current scapular co-ordinate systems, so that a universal co-ordinate system can be applied. Chapter 3 describes the various anthropometric measurements of the scapular body and the glenoid, and sexual dimorphism is evaluated. In chapter 4, the scapular body anatomy is utilised to develop reference columns for fixation of glenoid baseplates, independent of glenoid anatomy, with the eventual aim to use these references to attain baseplate fixation in primary and revision RSA. Finally, in chapter 5, a general discussion about this work is undertaken in context with the current literature. The significance, strengths and limitations of this thesis are summarised and recommendations are made for the scope and future direction of work.

1.10 REFERENCES

1. Pectoral girdle, shoulder region and axilla. In: Standring S, ed. *Gray's anatomy : the anatomical basis of clinical practice* 40 ed: Churchill Livingstone/Elsevier, 2008; 2008:791-823.
2. Mochizuki T, Sugaya H, Uomizu M, et al. Humeral insertion of the supraspinatus and infraspinatus. New anatomical findings regarding the footprint of the rotator cuff. Surgical technique. *The Journal of bone and joint surgery. American volume*. 2009;91 Suppl 2 Pt 1:1-7.
3. Agrawal D, Singh B, Dixit SG, et al. Morphometry and variations of the human suprascapular notch. *Morphologie*. 2015;99(327):132-140.
4. Scheuer LB, S. Pectoral Girdle. In: Scheuer LB, S, ed. *Developmental Juvenile Osteology*. 1 ed: Elsevier; 2000:252-271.
5. Bhatia DN, de Beer JF, du Toit DF. Coracoid process anatomy: Implications in radiographic imaging and surgery. *Clinical Anatomy*. 2007;20(7):774-784.
6. Young AA, Baba M, Neyton L, Godeneche A, Walch G. Coracoid graft dimensions after harvesting for the open Latarjet procedure. *Journal of shoulder and elbow surgery / American Shoulder and Elbow Surgeons ... [et al.]*. 2013;22(4):485-488.
7. Fortun CM, Streit JJ, Horton SA, Muh SJ, Gillespie RJ, Gobezie R. Scapular neck length and implications for reverse total shoulder arthroplasty: An anatomic study of 442 cadaveric specimens. *International journal of shoulder surgery*. 2015;9(2):38-42.
8. Checroun AJ, Hawkins C, Kummer FJ, Zuckerman JD. Fit of current glenoid component designs: an anatomic cadaver study. *Journal of shoulder and elbow surgery / American Shoulder and Elbow Surgeons ... [et al.]*. 2002;11(6):614-617.
9. Churchill RS, Brems JJ, Kotschi H. Glenoid size, inclination, and version: an anatomic study. *Journal of shoulder and elbow surgery / American Shoulder and Elbow Surgeons ... [et al.]*. 2001;10(4):327-332.
10. Iannotti JP, Gabriel JP, Schneck SL, Evans BG, Misra S. The normal glenohumeral relationships. An anatomical study of one hundred and forty shoulders. *The Journal of bone and joint surgery. American volume*. 1992;74(4):491-500.
11. Frankle MA, Teramoto A, Luo ZP, Levy JC, Pupello D. Glenoid morphology in reverse shoulder arthroplasty: classification and surgical implications. *Journal of shoulder and elbow surgery / American Shoulder and Elbow Surgeons ... [et al.]*. 2009;18(6):874-885.
12. Friedman RJ, Hawthorne KB, Genes BM. The use of computerized tomography in the measurement of glenoid version. *The Journal of bone and joint surgery. American volume*. 1992;74(7):1032-1037.
13. Lewis GS, Armstrong AD. Glenoid spherical orientation and version. *Journal of shoulder and elbow surgery / American Shoulder and Elbow Surgeons ... [et al.]*. 2011;20(1):3-11.

14. Monk AP, Berry E, Limb D, Soames RW. Laser morphometric analysis of the glenoid fossa of the scapula. *Clin Anat.* 2001;14(5):320-323.
15. Sebastian H. Shoulder Biomechanics. In: Frankle M, ed. *Reverse Shoulder Arthroplasty.* 1 ed: Springer; 2016:21-30.
16. Sahara W, Sugamoto K, Murai M, Tanaka H, Yoshikawa H. The three-dimensional motions of glenohumeral joint under semi-loaded condition during arm abduction using vertically open MRI. *Clinical biomechanics.* 2007;22(3):304-312.
17. Apreleva M, Parsons IMt, Warner JJ, Fu FH, Woo SL. Experimental investigation of reaction forces at the glenohumeral joint during active abduction. *Journal of shoulder and elbow surgery / American Shoulder and Elbow Surgeons ... [et al.].* 2000;9(5):409-417.
18. Karlsson D, Peterson B. Towards a model for force predictions in the human shoulder. *J Biomech.* 1992;25(2):189-199.
19. Ackland DC, Richardson M, Pandy MG. Axial rotation moment arms of the shoulder musculature after reverse total shoulder arthroplasty. *The Journal of bone and joint surgery. American volume.* 2012;94(20):1886-1895.
20. Herrmann S, Konig C, Heller M, Perka C, Greiner S. Reverse shoulder arthroplasty leads to significant biomechanical changes in the remaining rotator cuff. *J Orthop Surg Res.* 2011;6:42.
21. Otis JC, Jiang CC, Wickiewicz TL, Peterson MG, Warren RF, Santner TJ. Changes in the moment arms of the rotator cuff and deltoid muscles with abduction and rotation. *The Journal of bone and joint surgery. American volume.* 1994;76(5):667-676.
22. Parsons IM, Apreleva M, Fu FH, Woo SL. The effect of rotator cuff tears on reaction forces at the glenohumeral joint. *J Orthop Res.* 2002;20(3):439-446.
23. Samilson RL, Prieto V. Dislocation arthropathy of the shoulder. *The Journal of bone and joint surgery. American volume.* 1983;65(4):456-460.
24. Walch G, Badet R, Boulahia A, Khoury A. Morphologic study of the glenoid in primary glenohumeral osteoarthritis. *J Arthroplasty.* 1999;14(6):756-760.
25. Hamada K, Fukuda H, Mikasa M, Kobayashi Y. Roentgenographic findings in massive rotator cuff tears. A long-term observation. *Clinical orthopaedics and related research.* 1990(254):92-96.
26. Sirveaux F, Favard L, Oudet D, Huquet D, Walch G, Mole D. Grammont inverted total shoulder arthroplasty in the treatment of glenohumeral osteoarthritis with massive rupture of the cuff. Results of a multicentre study of 80 shoulders. *The Journal of bone and joint surgery. British volume.* 2004;86(3):388-395.
27. Visotsky JL, Basamania C, Seebauer L, Rockwood CA, Jensen KL. Cuff tear arthropathy: pathogenesis, classification, and algorithm for treatment. *The Journal of bone and joint surgery. American volume.* 2004;86-A Suppl 2:35-40.
28. Neer CS, 2nd, Craig EV, Fukuda H. Cuff-tear arthropathy. *The Journal of bone and joint surgery. American volume.* 1983;65(9):1232-1244.
29. Neer CS, 2nd. Unconstrained shoulder arthroplasty. *Instr Course Lect.* 1985;34:278-286.
30. 2nd. NC. *Shoulder Reconstruction.* Philadelphia, PA: WB Saunders;. 1990.
31. Flatow EL, Harrison AK. A history of reverse total shoulder arthroplasty. *Clinical orthopaedics and related research.* 2011;469(9):2432-2439.
32. Grammont P TP, Laffay J, Deries X. Concept study and realization of a new total shoulder prosthesis. *Rhumatologie.* 1987(39):407-418.

33. Grammont PM, Baulot E. Delta shoulder prosthesis for rotator cuff rupture. *Orthopedics*. 1993;16(1):65-68.
34. Gupta A, Heani D, Lafosse L. Reverse Shoulder Arthroplasty. In: Dines DM, Edwards TB, Dines J, eds. *Reverse Shoulder Arthroplasty*. New York: Thieme; 2016.
35. Kontaxis A, Johnson GR. The biomechanics of reverse anatomy shoulder replacement--a modelling study. *Clinical biomechanics*. 2009;24(3):254-260.
36. Roche CP, Stroud NJ, Flurin PH, Wright TW, Zuckerman JD, DiPaola MJ. Reverse shoulder glenoid baseplate fixation: a comparison of flat-back versus curved-back designs and oval versus circular designs with 2 different offset glenospheres. *Journal of shoulder and elbow surgery / American Shoulder and Elbow Surgeons ... [et al.]*. 2014;23(9):1388-1394.
37. D. Seybold MKn, J. Geßmann, B. Jettkant,, Schildhauer TA. Wie viel Peg-Länge ist erforderlich zur einzeitigen Rekon- struktion von glenoidalen Defekten mit der inversen Schulterprothese. Eine klinische und biomechanische Studie. DVSE; 2013; Würzburg.
38. Hopkins AR, Hansen UN, Bull AM, Emery R, Amis AA. Fixation of the reversed shoulder prosthesis. *Journal of shoulder and elbow surgery / American Shoulder and Elbow Surgeons ... [et al.]*. 2008;17(6):974-980.
39. Humphrey CS, Kelly JD, 2nd, Norris TR. Optimizing glenosphere position and fixation in reverse shoulder arthroplasty, Part Two: The three-column concept. *Journal of shoulder and elbow surgery / American Shoulder and Elbow Surgeons ... [et al.]*. 2008;17(4):595-601.
40. Codsí MJ, Bennetts C, Powell K, Iannotti JP. Locations for screw fixation beyond the glenoid vault for fixation of glenoid implants into the scapula: an anatomic study. *Journal of shoulder and elbow surgery / American Shoulder and Elbow Surgeons ... [et al.]*. 2007;16(3 Suppl):S84-89.
41. DiStefano JG, Park AY, Nguyen TQ, Diederichs G, Buckley JM, Montgomery WH, 3rd. Optimal screw placement for base plate fixation in reverse total shoulder arthroplasty. *Journal of shoulder and elbow surgery / American Shoulder and Elbow Surgeons ... [et al.]*. 2011;20(3):467-476.
42. Hart ND, Clark JC, Wade Krause FR, Kissenberth MJ, Bragg WE, Hawkins RJ. Glenoid screw position in the Encore Reverse Shoulder Prosthesis: an anatomic dissection study of screw relationship to surrounding structures. *Journal of shoulder and elbow surgery / American Shoulder and Elbow Surgeons ... [et al.]*. 2013;22(6):814-820.
43. Molony DC, Cassar Gheiti AJ, Kennedy J, Green C, Schepens A, Mullett HJ. A cadaveric model for suprascapular nerve injury during glenoid component screw insertion in reverse-geometry shoulder arthroplasty. *Journal of shoulder and elbow surgery / American Shoulder and Elbow Surgeons ... [et al.]*. 2011;20(8):1323-1327.
44. Valenti PH BD, Nerot C. Delta 3 reversed prosthesis for osteoarthritis with massive rotator cuff tear: long term results. 2000 shoulder prostheses ... two to ten year follow-up. In: Walch G BP, Molé D, ed. Montpellier, Paris, France:: Sauramps Medical; 2001:253-259.
45. Zumstein MA, Pinedo M, Old J, Boileau P. Problems, complications, reoperations, and revisions in reverse total shoulder arthroplasty: a systematic review. *Journal of shoulder and elbow surgery / American Shoulder and Elbow Surgeons ... [et al.]*. 2011;20(1):146-157.

46. Boulahia A, Edwards TB, Walch G, Baratta RV. Early results of a reverse design prosthesis in the treatment of arthritis of the shoulder in elderly patients with a large rotator cuff tear. *Orthopedics*. 2002;25(2):129-133.
47. De Wilde L, Mombert M, Van Petegem P, Verdonk R. Revision of shoulder replacement with a reversed shoulder prosthesis (Delta III): report of five cases. *Acta orthopaedica Belgica*. 2001;67(4):348-353.
48. Valenti P BD, Nerot C. Delta 3 reversed prosthesis for arthritis with massive rotator cuff tear: long term results (> 5 years). In: Walch G BP, Mole´ P, ed. *2000 shoulder prosthesis: two to ten years follow up*. Montpellier: Sauramps Medical; 2001:253-259.
49. Levigne C, Boileau P, Favard L, et al. Scapular notching in reverse shoulder arthroplasty. *Journal of shoulder and elbow surgery / American Shoulder and Elbow Surgeons ... [et al.]*. 2008;17(6):925-935.
50. Hill JM, Norris TR. Long-term results of total shoulder arthroplasty following bone-grafting of the glenoid. *The Journal of bone and joint surgery. American volume*. 2001;83-A(6):877-883.
51. Scalise JJ, Iannotti JP. Bone grafting severe glenoid defects in revision shoulder arthroplasty. *Clinical orthopaedics and related research*. 2008;466(1):139-145.
52. Klika BJ, Wooten CW, Sperling JW, et al. Structural bone grafting for glenoid deficiency in primary total shoulder arthroplasty. *Journal of shoulder and elbow surgery / American Shoulder and Elbow Surgeons ... [et al.]*. 2014;23(7):1066-1072.
53. Denard PJ, Walch G. Current concepts in the surgical management of primary glenohumeral arthritis with a biconcave glenoid. *Journal of shoulder and elbow surgery / American Shoulder and Elbow Surgeons ... [et al.]*. 2013;22(11):1589-1598.
54. Clavert P, Millett PJ, Warner JJ. Glenoid resurfacing: what are the limits to asymmetric reaming for posterior erosion? *Journal of shoulder and elbow surgery / American Shoulder and Elbow Surgeons ... [et al.]*. 2007;16(6):843-848.
55. Neyton L, Boileau P, Nove-Josserand L, Edwards TB, Walch G. Glenoid bone grafting with a reverse design prosthesis. *Journal of shoulder and elbow surgery / American Shoulder and Elbow Surgeons ... [et al.]*. 2007;16(3 Suppl):S71-78.
56. Neyton L, Sirveaux F, Roche O, Mole D, Boileau P, Walch G. [Results of revision surgery for glenoid loosening: a multicentric series of 37 shoulder prosthesis]. *Revue de chirurgie orthopedique et reparatrice de l'appareil moteur*. 2004;90(2):111-121.
57. Boileau P, Moineau G, Roussanne Y, O'Shea K. Bony increased-offset reversed shoulder arthroplasty: minimizing scapular impingement while maximizing glenoid fixation. *Clinical orthopaedics and related research*. 2011;469(9):2558-2567.
58. Phipatanakul WP, Norris TR. Treatment of glenoid loosening and bone loss due to osteolysis with glenoid bone grafting. *Journal of shoulder and elbow surgery / American Shoulder and Elbow Surgeons ... [et al.]*. 2006;15(1):84-87.
59. Westermann RW, Pugely AJ, Martin CT, Gao Y, Wolf BR, Hettrich CM. Reverse Shoulder Arthroplasty in the United States: A Comparison of National Volume, Patient Demographics, Complications, and Surgical Indications. *Iowa Orthop J*. 2015;35:1-7.
60. AOANJRR. AOANJRR Shoulder Registry. Australia: South Australian Health and Medical Reserch Institute; 2015.

Chapter 2- Comparison Of Three Scapular Co-Ordinate Systems In The Context Of Glenoid Fixation In Shoulder Arthroplasty

Overview: Currently there is a discrepancy between the scapular plane used by the orthopaedic surgical community and the planes suggested by the International Society of Biomechanics; to evaluate shoulder biomechanics and guide implant positioning. This chapter aims to compare the described scapular co-ordinate planes to determine which should be used as the reference plane for all future analyses in this thesis.

2.1 INTRODUCTION

In 2006 the International Society of Biomechanics (ISB) defined a scapular plane in an attempt to localise the gleno-humeral centre of rotation. The scapular plane was formed by three points: the medial scapular point, inferior scapular point and the posterolateral acromial point. This plane has been referred to as the New ISB scapular plane¹ (Figure 2.1a). Prior to 2006, the scapular plane was defined as a plane formed by the medial scapular point, the inferior scapular point and the acromio-clavicular (AC) joint point – termed the Old ISB plane (Figure 2.1b). The gleno-humeral center of rotation is calculated by regression analysis or by calculating the pivot point of instantaneous helical axis of gleno-humeral motion. The new ISB was chosen to reduce the occurrence of complications due to gimbal lock.¹

In the clinical orthopaedic literature, the scapular axis has been described by Friedman² and Randelli³. This axis is defined in a 2D view, and is widely used in the orthopaedic literature to determine glenoid version in the axial plane. It connects the center of the glenoid to the medial angle of the scapula at the medial border of the scapula. This was later modified by Kwon⁴ who developed the concept of the ‘scapular plane’ by adding the inferior point on the scapula (Figure 2.1c). Scalise⁵ and Budge⁶ have demonstrated that 3D analysis of the scapular plane allows for a more accurate estimation of the glenoid version, despite differences in scapular positioning in the CT gantry.

The construction of the scapular plane is dependent on localising the center of the glenoid. This is often not possible in cases with glenoid erosion or bone loss. Thus, the surgeon faces the clinical problem of positioning an implant accurately without the ability to estimate the scapular plane accurately.

The purpose of this study was to investigate relationships among the old and new ISB planes, as well as the currently used clinical scapular plane. Secondly, anatomical gender differences were determined. Thirdly, of the planes compared, the most clinically applicable plane was chosen, allowing for evaluation of patients with glenoid bone defects.

2.2 MATERIALS AND METHODS

Computed tomography (CT) scans were obtained for 50 fresh-frozen cadaveric shoulders (age 71 ± 14 yrs; 25 males: 72 ± 15 yrs, 25 females: 69 ± 13 yrs). The CT scans were acquired with a multi slice scanner with standardised clinical settings. The CT scans were classified by fellowship trained orthopaedic surgeons according to the classification proposed by Samilson – Prieto.⁷ Shoulders with glenohumeral arthritis with Grade 0-2 were included for analysis. Cases with Grade 3 arthritic changes and any case with evidence of fractures, surgery or glenoid bone loss were excluded from analysis.

The CT images were then uploaded in Digital Imaging in Communications in Medicine format (DICOM) to Mimics medical imaging software (Mimics 17.0®, Materialise, Leuven, Belgium). Thresholding was set to a minimum value of 200 Hounsfield Units (HU) to preserve scapular anatomy during segmentation and to obtain both cancellous and cortical bone models.⁸

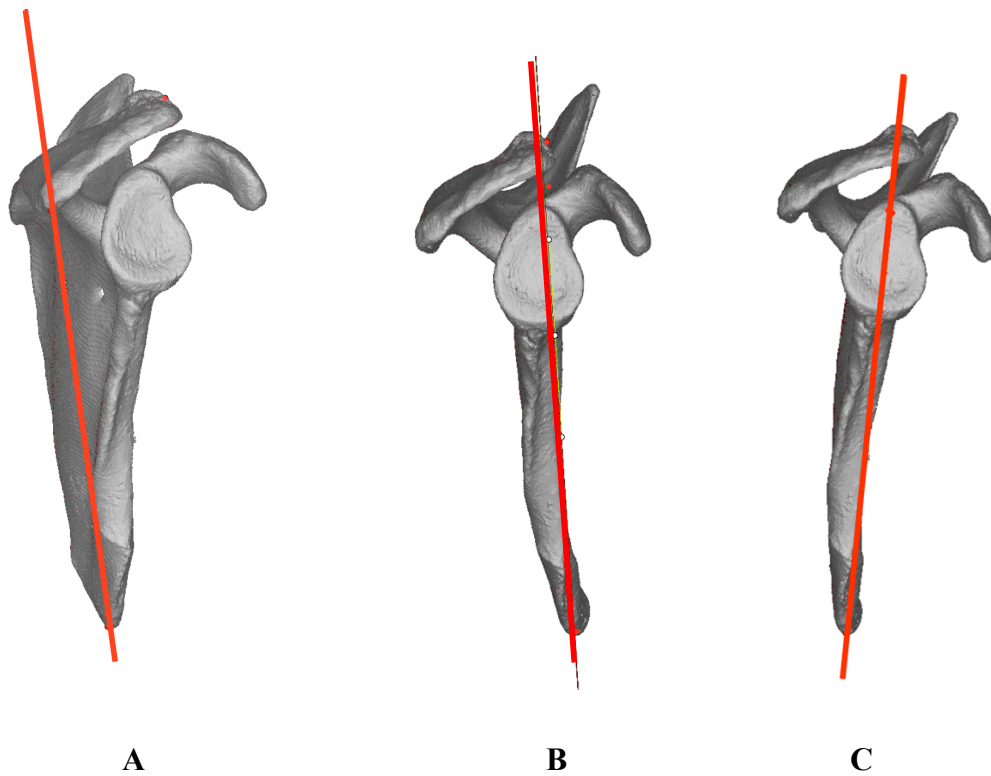


Figure 2.1 Scapular Co- Ordinate Systems A) New ISB, B) Old ISB, C) Scapular Plane

Utilising the built in med-CAD module in Mimics® various surface points were extracted from the scapula by multiple observers. Four standardised views were chosen to extract the surface anatomy points: superior axial view, posterior view, sagittal view (glenoid enface view), and inferior para axial view (parallel to the lateral pillar of the scapula) (Figure 2.2). The superior (axial) view of the scapula was used to extract the most medial point on the medial vertebral surface of the scapula - Medial scapular point (MSP). This point, termed the Trigonum Spinae Scapulae, lies in the medial scapular angle (attachment of the levator scapulae muscle) which corresponds to the intersection of the scapular spine with the medial border of the scapula.¹ Additionally, in the superior axial view the acromio-clavicular joint (AC Joint) was identified. The most prominent antero-medial point of the articular surface within the joint was extracted as the ACJ point.

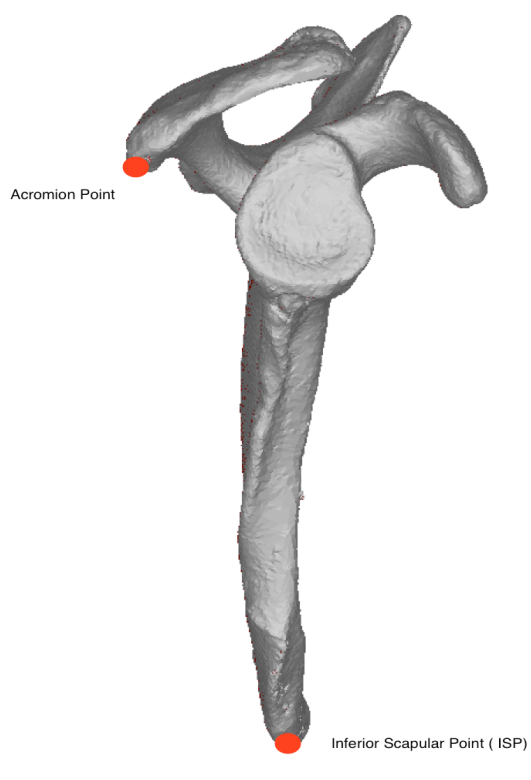
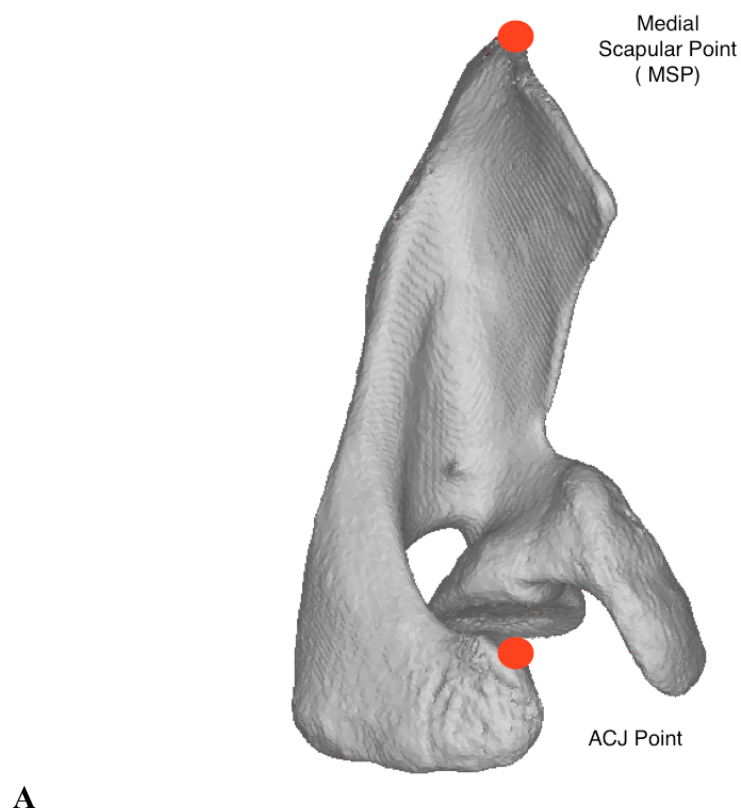


Figure 2.2 A) Superior Axial View - Medial Scapular Point and ACJ Point Are Established, B) Scapular Y View- Inferior Scapular Point And Acromial Point Are Established

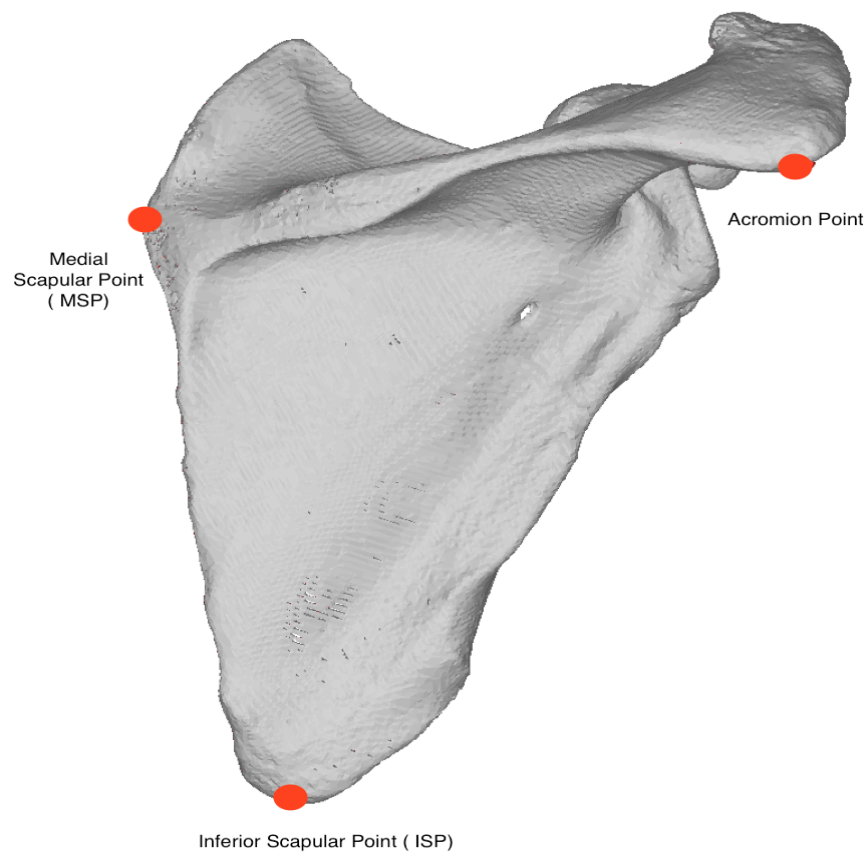


Figure 2.2 C Posterior View Demonstrating The Points

Various surface points were extracted on the sagittal (Y-view) of the scapula (Figure 2.2 b). The most inferior point of the scapular body was extracted; this was the lowermost and most posterior projection of the inferior angle of the scapula - Inferior Scapular Point (ISP).^{4,9} The second point extracted was the most posterolateral point on the posterior angle of the acromion (Acromial point). The MSP, ISP and Acromial Points correspond to the most prominent landmarks felt during palpation of the medial, inferior border of the scapula, and the postero-lateral margin of the acromion.^{1,4,9}

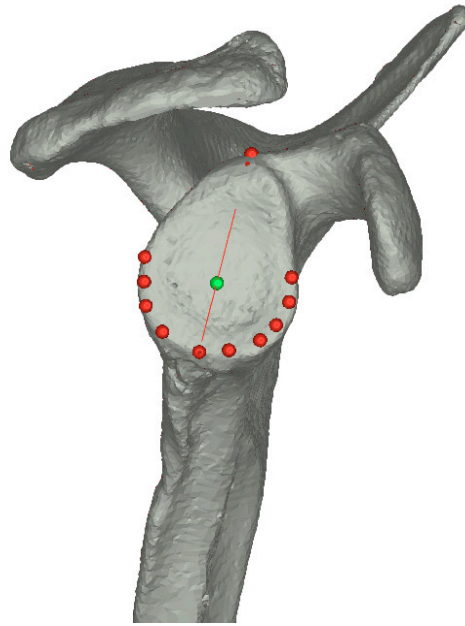


Figure 2. 3 Calculation Of The Glenoid Center Point And SI Glenoid Axis (SI Axis Of The Glenoid Is Formed By The Line Joining The Superior Glenoid Point And The Glenoid Center Point And Intersects The Inferior Rim Of The Glenoid Demarcating The 6 O'clock Position)

The inferior curvature of the glenoid (Figure 2.3) was evaluated on the enface view of the glenoid. The circular inferior rim of the glenoid was marked by 10 surface points placed on the inferior cortical rim. Custom code was developed in Matlab® (Math works, Natick, MA, USA) to transform this semicircle to a complete circle, using a least square circle fit, and the centre point of the circle was ascertained. This central point corresponds to the centre of the glenoid (Glenoid Centre point). The superior (12 o'clock) point was identified as per the descriptions of Chuang¹⁰, Saito¹¹ and Kany¹² and its apex extracted as the Superior Glenoid Point (SGP). A line was then passed through the SGP and Glenoid centre. This line was extended until it intersected the inferior glenoid rim. This intersection point was extracted as the Inferior Glenoid point (IGP, 6 o'clock). This axis was used as the longitudinal axis of the glenoid (Superior-Inferior –SI Glenoid axis).

The Scapular plane, as described by Kwon et al.,⁴ was created. This was the plane connecting the Medial Scapular point, the Inferior Scapular Point and the Glenoid Center. This served as the (scapular) coordinate plane against which an orthogonal

glenoid plane was created. The points extracted were used to establish a scapular and glenoid co-ordinate system. (Figure 2.4)

Next the New ISB scapular axis was created by extraction of the MSP, ISP and the Acromion point (Figure 2.4b). Lastly the Old ISB Scapular axis was recreated by extraction of the MSP, ISP and ACJ point (Figure 2.4c).

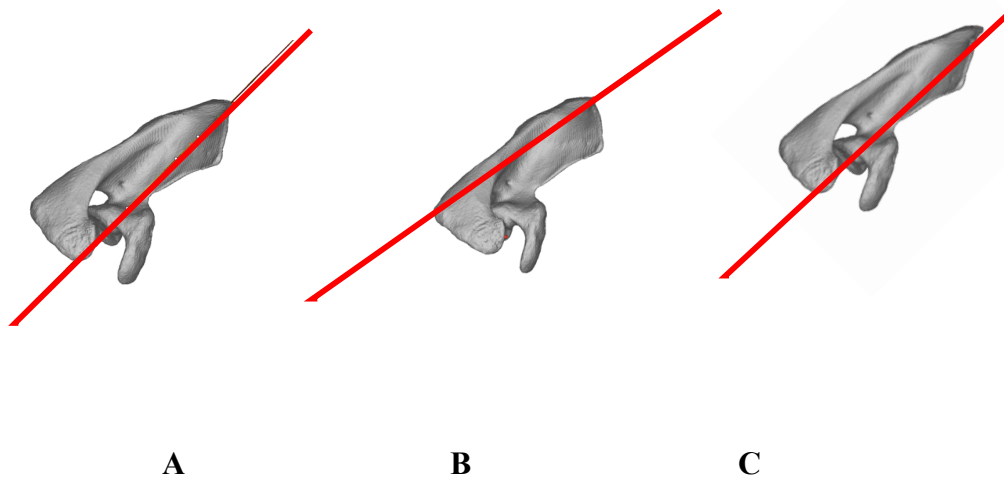


Figure 2. 4: Old ISB Plane (A), New ISB Plane (B), and Scapular Plane (C).

An orthogonal plane to the scapular plane was created parallel to the glenoid face and the three axes (Scapular axis, Old ISB axis and New ISB axis) were projected onto this plane. The relationships of these axes with respect to the scapular axis were calculated. The scapular axis was used as the index axis due to its widespread use by the orthopaedic surgeons and prosthetic design engineers. The axis was represented as (+) if it lay posterior to the scapular axis and (-) if it lay anterior to the scapular axis.

Statistical analysis (SPSS software®, 15.0; IBM Inc. USA) was performed and mean and standard deviations for each subgroup was calculated. Analysis to determine the

difference between the orientation of each axis with respect to scapular axis was carried out by performing a t-test for all cases and separated by subgroups. The relationship of the orientation of each axis in males and females was analysed by t-test. All differences were considered significant at a probability level of 95% ($P < 0.05$).

2.3 RESULTS

There were 23 right and 27 left scapulae analysed. Our results demonstrate that the New ISB is directed $17.0 \pm 2.0^\circ$ posterior to the scapular axis. Subgroup analysis between males and females demonstrates that the axis is 0.6° more posterior in males ($17.3 \pm 1.7^\circ$) compared to females ($16.7 \pm 2.3^\circ$). This was not significant ($p = 0.28$) (Figure 2.9). The Old ISB passes much closer to the scapular axis, being just $1.3^\circ \pm 2.2^\circ$ anterior to the scapular axis. Similar to the results of the New ISB, the Old ISB demonstrates a non-significant ($p = 0.68$) sexual variability.

| | Male (n=25) | Female (n=25) | Combined Mean (n=50) | <i>p value</i> * |
|----------------|----------------------------|-----------------------|----------------------|------------------|
| New ISB | $17.3^\circ \pm 1.7^\circ$ | $16.7 \pm 2.3^\circ$ | $17.0 \pm 2.0^\circ$ | $p = 0.28$ |
| Old ISB | $-1.2 \pm 2.4^\circ$ | $-1.4 \pm 2.07^\circ$ | $-1.3 \pm 2.2^\circ$ | $p = 0.68$ |

(-) Denotes the Axis is anterior to the Scapular Axis)

* t-Test, significance is denoted by $P < 0.05$

Table 2.1-Relationship to the Scapular Axis of the NEW ISB and Old ISB Axis

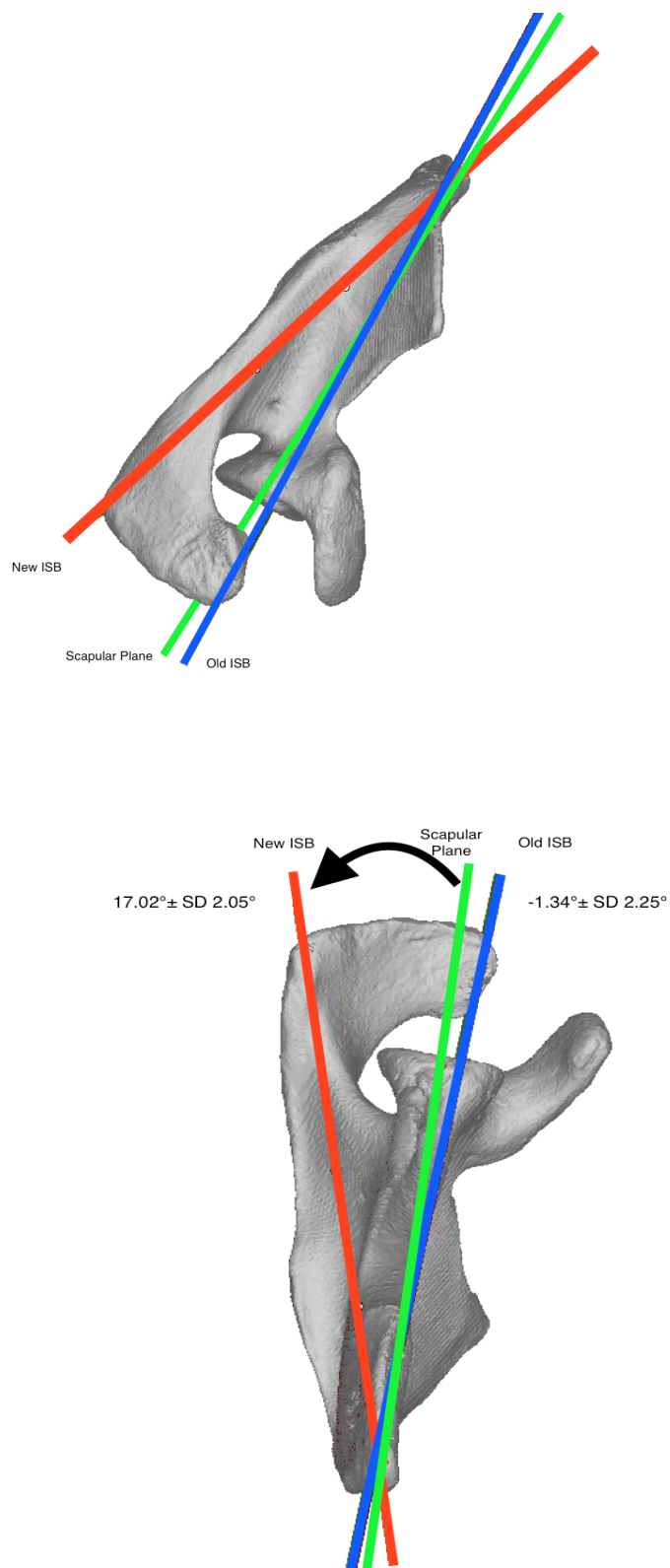


Figure 2.5 *The New ISB Is The Most Posterior Axis. The Old ISB Is The Most Anterior Axis. The Mean For Male And Females Combined Is $17.0 \pm 2.0^\circ$*

2.4 DISCUSSION

Recreation of normal joint kinematics is the goal of anatomic TSA. With RSA the mechanics of the joint are considerably altered. Both of these surgical procedures; however, rely on correct positioning of the glenoid component. Malpositioning of the components leads to abnormal biomechanics and altered joint loading, which may result in early aseptic loosening and is often associated with poorer clinical results.^{13,14} For each degree of change in glenoid version there is a reported 0.5 mm displacement of the humeral head in a anatomic shoulder arthroplasty.¹⁵ Farron in their finite element analysis study reported an exponential increase in mean micro motion (669%) with glenoid placement beyond 10 of retroversion.¹³ Ho et al have reported component positioning in greater than 15 of retroversion correlated with early signs of radiographic loosening of the glenoid implant.¹⁶

Shoulder arthroplasty poses significant challenges to the orthopaedic surgeon. Difficult surgical access, a large soft tissue envelope and a small amount of working bone stock makes the procedure challenging. In addition, the surgeon is not able to visualise the scapula and has to decide implant positioning by relying on the enface view of a pathologic glenoid. This has led to the importance of preoperative templating and CT guided analysis of the glenoid version and scapular axis.

The 2-D axial scapular axis is most commonly calculated by the method described by Friedman² and Randelli³. Kwon et al⁴ further elaborated on this by developing a 3D plane called the scapular plane; this plane is currently used by the orthopaedic fraternity. Suitable CT scanning protocols have been developed to scan the scapula parallel to the scapular axis so as to enable the orthopaedic surgeon to accurately calculate the glenoid version and guide positioning of the glenoid component.^{6,17,18} Utilising the scapular axis, numerous studies have documented the ideal method to calculate glenoid version for correct implant positioning.^{5,19,20} Budge et al have demonstrated the superiority of glenoid version calculation by 3D CT scans rather than using a 2D axial image.⁶

Even in experienced hands, accurate guide pin positioning in RSA has a large degree of variability. Throckmorton et al in a multi surgeon study of 70 orthopaedic surgeons demonstrated an average variability of 8° in version and 7° in inclination from the target.²¹ The accuracy further deteriorated in the presence of glenoid bone defects.²² This has led to the development of patient specific guides. These custom guides are based upon preoperative CT templating of the patient's scapulae.

Numerous recent studies have reported the superiority of patient specific guides over traditional instrumentation.²³⁻²⁶ Some implant companies have developed proprietary software programs to develop patient specific guides. Despite the obvious advantage of improving implant positioning, there are some disadvantages. Firstly, there is an additional cost involved in producing and manufacturing these guides. Secondly, the added logistics of generating, fabricating, and delivering guides can pose a challenge, especially in public health systems with limited resources. Thirdly, the accuracy of each software system is proprietary and details of axis calculation may be variable. Lastly, most guidance software systems rely on the presence of a partially intact glenoid rim, however, in cases of massive bone loss or revision, these local landmarks may be distorted or absent.

The ISB has standardised the joint coordinate system used for all the joints of the human body and describes the GHJ axis to be passing through a plane independent of glenoid anatomy. The center of GH motion is calculated by regression analysis²⁷ or by calculating the pivot point of instantaneous helical axes (IHA) of GH motions.²⁸ The IHA method is the preferred method due to its higher accuracy and because it has been validated in patients with GH bone loss due to degeneration or a prosthetic implant.⁹ The rationale behind selecting this axis is that it is impossible to delineate GHJ motion without accounting for scapula-thoracic motion and motion in the acromio-clavicular joint and the sterno-clavicular joints. Unlike other joints in the body the movement in the GHJ is reliant upon the movement of the pectoral girdle against the thorax. Thus arbitrarily choosing just the glenoid and the humeral head to define motion is fraught with errors. Thus the ISB axis is widely utilised in the biomechanical literature as the GHJ / shoulder axis.

The use of the Old ISB, as proposed by van der Helm²⁹, was aborted in 2006 due to gimbal lock. However, many biomechanical papers refer to the use of the Old ISB. Ludewig et al in their study compared the New ISB and the Old ISB and concluded that The New ISB interprets the same scapular motion with less internal rotation and upward rotation and more posterior tilting than the Old ISB. They also highlighted that the Old ISB under represents the scapular plane and the New ISB over represents it. They, however, concluded that the New ISB should be considered for measurements as shoulder kinematic measurement evolves.³⁰

There is a mismatch between the scapular reference planes used by engineers and the orthopaedic community. Our study is an attempt to fill this lacuna. We have demonstrated that the New ISB has a mean 17.0° posterior deviation from the scapular plane. As the New ISB is a biomechanical plane for GHJ motion, variations in gender should not play a role. In accordance to this principle, in our study we did not find a statistical difference between males and females ($p=0.28$). The Old ISB lies in very close proximity to the scapular plane 1.3° anterior to the scapular plane. However, this axis relies on a normal ACJ and this may be difficult to ascertain in all patients especially patients with a prior ACJ arthritis or excision.

The strength of our study lies in describing the relationship between the New ISB and the scapular plane, which may be utilised for templating and implant positioning. As the New ISB is independent of glenoid morphology, it can be readily employed in calculation of the scapular axis for implant positioning in cases of severe glenoid bone loss or in revision arthroplasty.

One of the limitations of this study is that some of the specimens chosen did have ACJ arthritis and thus the measurements of the Old ISB may be different if our entire cohort had healthy ACJs. We compensated for this problem by digitally subtracting anterior and superior ACJ osteophytes. The articular surfaces were now deemed normal for

measurement purposes and manual extraction of the ACJ point was then carried out as per the protocol.

2.5 CONCLUSION

Our study demonstrates that the New ISB scapular plane can be reliably utilised as a reference plane for glenoid implant positioning. The plane can be used in the presence of glenoid bone loss and in revision shoulder arthroplasty.

2.6 REFERENCES

1. Wu G, van der Helm FCT, Veeger HEJ, et al. ISB recommendation on definitions of joint coordinate systems of various joints for the reporting of human joint motion—Part II: shoulder, elbow, wrist and hand. *Journal of Biomechanics*. 2005;38(5):981-992.
2. Friedman RJ, Hawthorne KB, Genez BM. The use of computerized tomography in the measurement of glenoid version. *The Journal of bone and joint surgery. American volume*. 1992;74(7):1032-1037.
3. Randelli M, Gambrioli PL. Glenohumeral osteometry by computed tomography in normal and unstable shoulders. *Clinical orthopaedics and related research*. 1986(208):151-156.
4. Kwon YW, Powell KA, Yum JK, Brems JJ, Iannotti JP. Use of three-dimensional computed tomography for the analysis of the glenoid anatomy. *Journal of shoulder and elbow surgery / American Shoulder and Elbow Surgeons ... [et al.]*. 2005;14(1):85-90.
5. Scalise JJ, Codsì MJ, Bryan J, Brems JJ, Iannotti JP. The influence of three-dimensional computed tomography images of the shoulder in preoperative planning for total shoulder arthroplasty. *The Journal of bone and joint surgery. American volume*. 2008;90(11):2438-2445.
6. Budge MD, Lewis GS, Schaefer E, Coquia S, Flemming DJ, Armstrong AD. Comparison of standard two-dimensional and three-dimensional corrected glenoid version measurements. *Journal of shoulder and elbow surgery / American Shoulder and Elbow Surgeons ... [et al.]*. 2011;20(4):577-583.
7. Samilson RL, Prieto V. Dislocation arthropathy of the shoulder. *The Journal of bone and joint surgery. American volume*. 1983;65(4):456-460.
8. Bryce CD, Pennypacker JL, Kulkarni N, et al. Validation of three-dimensional models of in situ scapulae. *Journal of shoulder and elbow surgery / American Shoulder and Elbow Surgeons ... [et al.]*. 2008;17(5):825-832.
9. Wu G, van der Helm FC, Veeger HE, et al. ISB recommendation on definitions of joint coordinate systems of various joints for the reporting of human joint

- motion--Part II: shoulder, elbow, wrist and hand. *J Biomech.* 2005;38(5):981-992.
10. Chuang TY, Adams CR, Burkhart SS. Use of preoperative three-dimensional computed tomography to quantify glenoid bone loss in shoulder instability. *Arthroscopy : the journal of arthroscopic & related surgery : official publication of the Arthroscopy Association of North America and the International Arthroscopy Association.* 2008;24(4):376-382.
 11. Saito H, Itoi E, Sugaya H, Minagawa H, Yamamoto N, Tuoheti Y. Location of the glenoid defect in shoulders with recurrent anterior dislocation. *The American journal of sports medicine.* 2005;33(6):889-893.
 12. Kany J, Flamand O, Grimberg J, et al. Arthroscopic Latarjet procedure: is optimal positioning of the bone block and screws possible? A prospective computed tomography scan analysis. *Journal of shoulder and elbow surgery / American Shoulder and Elbow Surgeons ... [et al.].* 2016;25(1):69-77.
 13. Farron A, Terrier A, Buchler P. Risks of loosening of a prosthetic glenoid implanted in retroversion. *Journal of shoulder and elbow surgery / American Shoulder and Elbow Surgeons ... [et al.].* 2006;15(4):521-526.
 14. Hasan SS, Leith JM, Campbell B, Kapil R, Smith KL, Matsen FA, 3rd. Characteristics of unsatisfactory shoulder arthroplasties. *Journal of shoulder and elbow surgery / American Shoulder and Elbow Surgeons ... [et al.].* 2002;11(5):431-441.
 15. Nyffeler RW, Sheikh R, Atkinson TS, Jacob HA, Favre P, Gerber C. Effects of glenoid component version on humeral head displacement and joint reaction forces: an experimental study. *Journal of shoulder and elbow surgery / American Shoulder and Elbow Surgeons ... [et al.].* 2006;15(5):625-629.
 16. Ho JC, Sabesan VJ, Iannotti JP. Glenoid component retroversion is associated with osteolysis. *The Journal of bone and joint surgery. American volume.* 2013;95(12):e82.
 17. Bokor DJ, O'Sullivan MD, Hazan GJ. Variability of measurement of glenoid version on computed tomography scan. *Journal of shoulder and elbow surgery / American Shoulder and Elbow Surgeons ... [et al.].* 1999;8(6):595-598.
 18. Iannotti JP, Ricchetti ET, Rodriguez EJ, Bryan JA. Development and validation of a new method of 3-dimensional assessment of glenoid and humeral component position after total shoulder arthroplasty. *Journal of shoulder and elbow surgery / American Shoulder and Elbow Surgeons ... [et al.].* 2013;22(10):1413-1422.
 19. Rouleau DM, Kidder JF, Pons-Villanueva J, Dynamidis S, Defranco M, Walch G. Glenoid version: how to measure it? Validity of different methods in two-dimensional computed tomography scans. *Journal of shoulder and elbow surgery / American Shoulder and Elbow Surgeons ... [et al.].* 2010;19(8):1230-1237.
 20. Scalise JJ, Codsí MJ, Bryan J, Iannotti JP. The three-dimensional glenoid vault model can estimate normal glenoid version in osteoarthritis. *Journal of shoulder and elbow surgery / American Shoulder and Elbow Surgeons ... [et al.].* 2008;17(3):487-491.
 21. Throckmorton TW, Gulotta LV, Bonnarens FO, et al. Patient-specific targeting guides compared with traditional instrumentation for glenoid component placement in shoulder arthroplasty: a multi-surgeon study in 70 arthritic cadaver specimens. *Journal of shoulder and elbow surgery / American Shoulder and Elbow Surgeons ... [et al.].* 2015;24(6):965-971.
 22. Eraly K, Stoffelen D, Vander Sloten J, Jonkers I, Debeer P. A patient-specific guide for optimizing custom-made glenoid implantation in cases of severe

- glenoid defects: an in vitro study. *Journal of shoulder and elbow surgery / American Shoulder and Elbow Surgeons ...* [et al.]. 2016;25(5):837-845.
23. Dallalana RJ, McMahon RA, East B, Geraghty L. Accuracy of patient-specific instrumentation in anatomic and reverse total shoulder arthroplasty. *International journal of shoulder surgery*. 2016;10(2):59-66.
 24. Walch G, Vezeridis PS, Boileau P, Deransart P, Chaoui J. Three-dimensional planning and use of patient-specific guides improve glenoid component position: an in vitro study. *Journal of shoulder and elbow surgery / American Shoulder and Elbow Surgeons ...* [et al.]. 2015;24(2):302-309.
 25. Iannotti JP, Weiner S, Rodriguez E, et al. Three-dimensional imaging and templating improve glenoid implant positioning. *The Journal of bone and joint surgery. American volume*. 2015;97(8):651-658.
 26. Lewis GS, Stevens NM, Armstrong AD. Testing of a novel pin array guide for accurate three-dimensional glenoid component positioning. *Journal of shoulder and elbow surgery / American Shoulder and Elbow Surgeons ...* [et al.]. 2015;24(12):1939-1947.
 27. Meskers CG, van der Helm FC, Rozendaal LA, Rozing PM. In vivo estimation of the glenohumeral joint rotation center from scapular bony landmarks by linear regression. *J Biomech*. 1998;31(1):93-96.
 28. Stokdijk M, Nagels J, Rozing PM. The glenohumeral joint rotation centre in vivo. *J Biomech*. 2000;33(12):1629-1636.
 29. van der Helm FC, Pronk GM. Three-dimensional recording and description of motions of the shoulder mechanism. *J Biomech Eng*. 1995;117(1):27-40.
 30. Ludewig PM, Hassett DR, Laprade RF, Camargo PR, Braman JP. Comparison of scapular local coordinate systems. *Clinical biomechanics*. 2010;25(5):415-421.

Chapter 3- Morphologic Analysis of the Scapular Body and the Glenoid.

***Overview:** In cases of severe glenoid bone loss, glenoid size estimation is important for accurate reconstruction and implant selection.*

This chapter evaluates the anthropometric measurements of the scapular body and glenoid and determines the gender dimorphism between males and females. In addition, linear regression analysis aims to ascertain the glenoid dimensions by using the scapular body height.

3.1 INTRODUCTION

The scapula has a large flat body with numerous muscular attachments and a lateral pear shaped glenoid with its pyramidal vault. Degenerative joint disease results in alteration of the glenoid morphology. Glenoid bone loss ranges from minor glenoid rim erosions to complete destruction of the glenoid vault. Reconstruction of the glenoid in the setting of bone loss poses a challenging problem. To restore the glenoid to its premorbid anatomy, the contralateral scapula may be used as a template. Quite often, however, the contralateral glenoid is diseased or has undergone an arthroplasty, and thus an accurate estimation of glenoid dimensions is not possible. The current solution to this problem remains the subjective reconstruction of the glenoid vault based upon the remaining bony landmarks noted pre-operatively and intraoperatively. The development of patient-specific guides has been shown to improve the accuracy of baseplate positioning¹. However, accurate recreation of a normal joint line remains a challenge in conditions of severe bone loss.

The aim of this study was to determine the dimension of the scapular body and the glenoid. Our second objective was to ascertain whether glenoid dimensions can be reliably predicted by the scapular body measurements. Thirdly, we compared morphologic gender dimorphism between the male and female scapulae.

3.2 MATERIALS AND METHODS

Computed tomography (CT) scans were obtained from 50 cadaveric shoulders (25 male and 25 female; age 71 ± 14 years). The CT scans were acquired with a multi slice scanner with standardised clinical settings (120 to 140 kVp, 512X512 resolution). The CT scans were classified by fellowship trained orthopaedic surgeon according to the classification proposed by Samilson and Prieto.² Shoulders with glenohumeral arthritis with Grade 0-2 were included for analysis. Cases with Grade 3 arthritic changes, or any case with evidence of trauma, surgery or glenoid bone loss, were excluded from analysis.

The CT images were then uploaded in Digital Imaging and Communications in Medicine format (DICOM) to Mimics medical imaging software (Mimics 17.0®, Materialise, Leuven, Belgium). Thresholding was set to a minimum value of 200 Hounsfield Units (HU) to preserve scapular anatomy during segmentation and to obtain both cancellous and cortical bone models.³

Various osseous landmarks were located on the scapula using the Mimics® med-CAD module. Four standardised views were chosen to extract the surface anatomy points; superior axial view, sagittal view (glenoid enface view) and posterior view (Figure 3.1). The superior (axial) view of the scapula was used to extract the most medial point on the medial vertebral surface of the scapula - Medial scapular point (MSP). MSP, termed the Trigonum spinae scapulae, lies in the medial scapular angle (attachment of the levator scapulae muscle) which corresponds to the intersection of the scapular spine with the medial border of the scapula.⁴

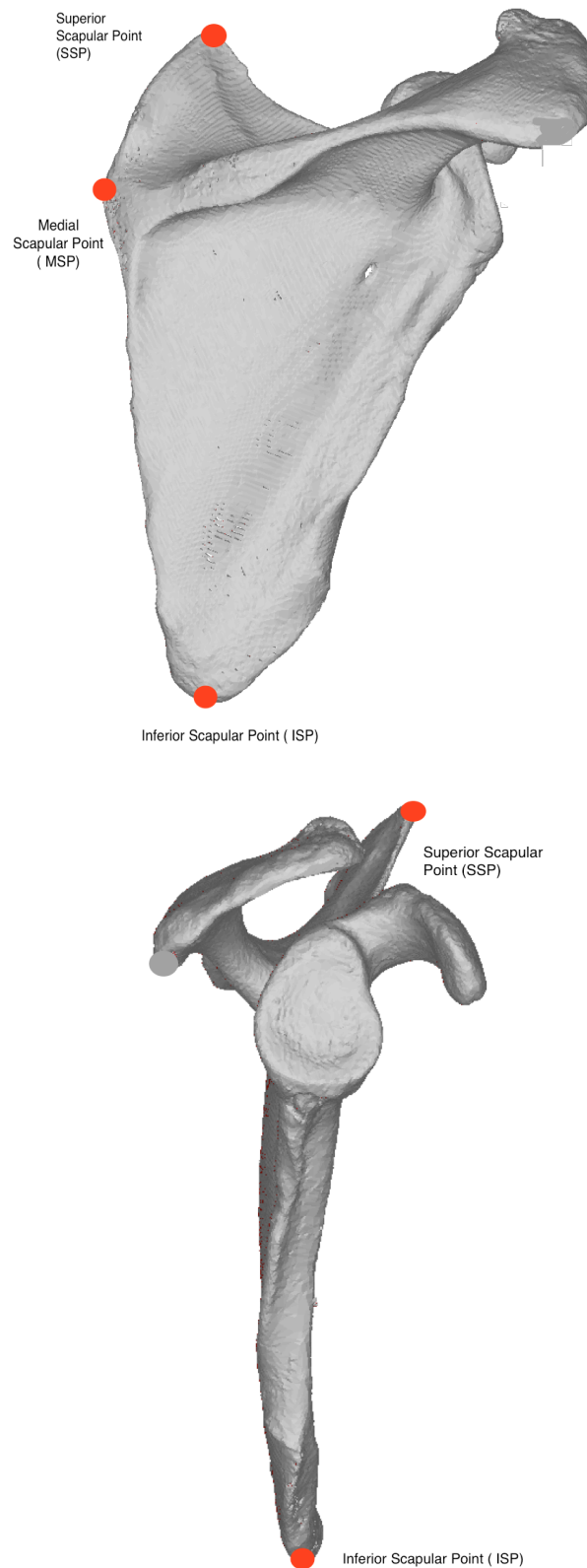


Figure 3.1 Coronal View Of The Scapula And The Sagittal Y View Demonstrating The Superior Scapular Point- SSP, Inferior Scapular Point ISP And Medial Scapular Point MSP

Various surface points were extracted on the sagittal or Y-view of the scapula. The most inferior point on the scapular body was extracted, which was the lowest and most posterior projection of the inferior angle of the scapula - Inferior Scapular Point (ISP).^{5,6} Next, the most cephalad point on the scapular body was extracted, which corresponds to the superior angle of the scapula - Superior Scapular Point (SSP).

Evaluation of the enface view of the glenoid, the circular rim of the glenoid was delineated and 10 surface points were extracted from the inferior cortical rim (Figure 3.2a). This defined the inferior curvature of the circular glenoid. Custom code was developed in Matlab® (Math works, Natick, MA, USA) to transform this semicircle to a complete circle and the centre point of the circle was ascertained. This point corresponds to the centre of the Glenoid (Glenoid Centre point). The superior 12 o'clock point, was identified as per the descriptions of Chuang⁷, Saito⁸ and Kany⁹ and its apex extracted as the Superior Glenoid Point (SGP). A line was then passed through the SGP and Glenoid centre. This line was extended till it intersected the inferior glenoid rim. This intersection point was extracted as the Inferior Glenoid point (IGP, 6 o'clock). This axis was used as the longitudinal axis of the glenoid (Superior Inferior –SI Glenoid axis).

Glenoid width was calculated as the maximal antero-posterior width of the glenoid perpendicular to the SI axis of the glenoid. Glenoid height was calculated as the distance between SGP and IGP (Figure 3.2b).

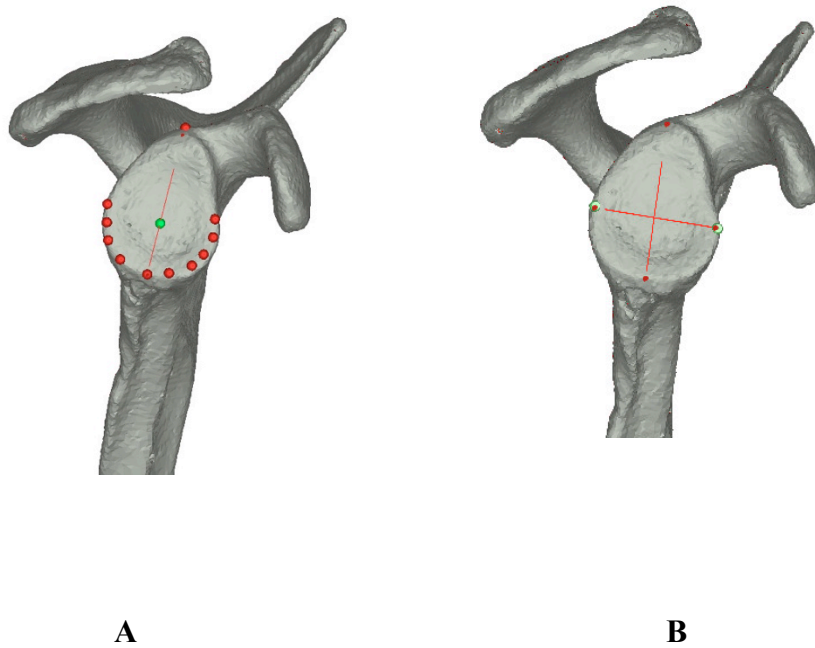


Figure 3.2a Glenoid Enface View. Center Point Of Glenoid Is Calculated. Superior-Inferior (SI) axis of the glenoid is calculated by connecting the Superior Glenoid Point (SGP) and the glenoid center point (Green dot). The intersection of this line to the inferior glenoid rim defines the 6 o'clock point. Figure 3.2 b defines the maximal width and height of the glenoid. The width of the glenoid is calculated by the maximal glenoid width measured perpendicular to the Glenoid SI axis.

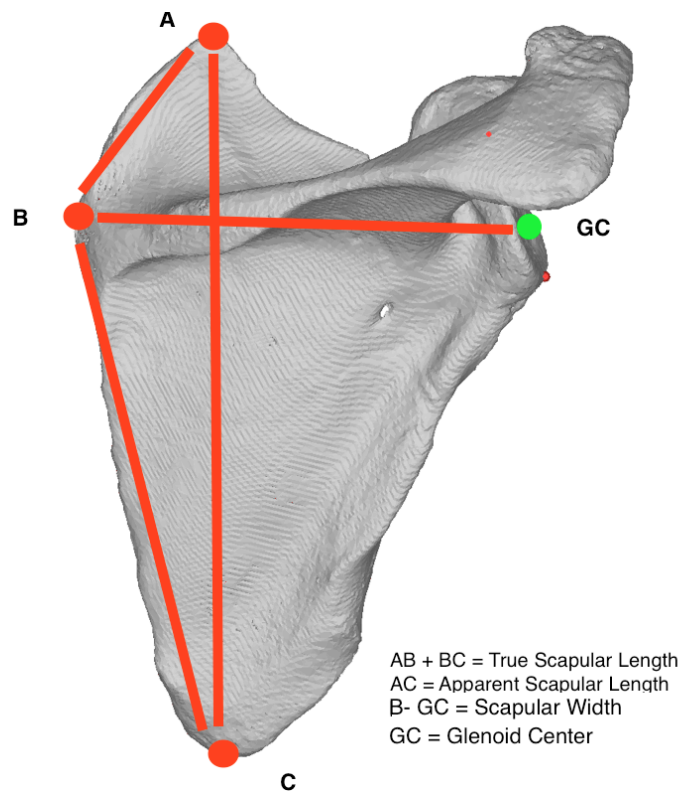


Figure 3. 3 Posterior View (Coronal View) of the Scapula

A= Superior Scapular Point (SSP), B= Medial Scapular Point (MSP)

C= Inferior Scapular Point (ISP), GC = Glenoid center

Scapular body measurements were carried out (Figure 3.3). The Distance between the superior scapular point and medial scapular point was defined as length AB. The distance between the Medial scapular point and Inferior scapular point was defined as BC. True scapular height was calculated as AB+BC. In addition, the traditional method of calculating scapular height from SSP to ISP = AC (Apparent Scapular height) was also calculated. The scapular width was calculated as the distance between MSP and Glenoid Center = Medial Lateral Length (Figure 3.3)

Statistical analysis (SPSS software®, 15.0; IBM Inc. USA) was performed and mean and standard deviations for each subgroup were calculated. Analysis to determine the difference in proportion between male and females was carried out by performing a t-test separated by subgroups. Values were considered significant at a probability level of 95% ($P < 0.05$). A Spearman rank order correlation was carried out to assess the relationship between the scapular body and the glenoid. Data analysis was performed for males and females and both sexes grouped together.

3.3 RESULTS

The male scapular body is much larger than the female scapular body in both height and width ($p < 0.001$) (Appendix B). The overall mean scapular height (the Superior Scapular Point to the Inferior Scapular Point) was 152 ± 17 mm. The medial border of the scapula (AB + BC) was 29 mm larger in the males (183.4 ± 13.4 mm) than in the females (154.1 ± 10.9); $p < 0.001$. The male scapula (114.5 ± 6.0 mm) was noted to be wider than the female (99.5 ± 4.8 mm) by 14.9 mm. (Table 3.1) The angle between the upper one third and lower two thirds of the medial border of the scapula was found to be 57° ; there was no sex difference of significance in this measurement ($p = 0.25$). Thus the female scapula was noted to be a scaled down version of the male scapula with statistically significant differences in anthropometric measurements.

The male glenoid was 6.1 mm longer and 5.4 mm wider than the female ($p < 0.001$).

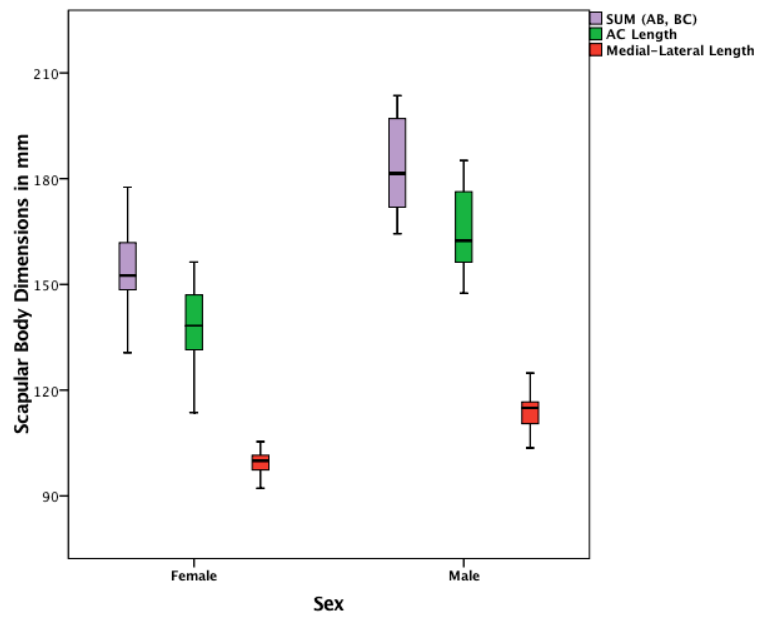
Glenoid measurements were not normally distributed as measured by the Shapiro Wilk test ($p < 0.05$). Thus, a Spearman (rho) correlation test was performed to ascertain the association between the scapular and glenoid dimensions (Appendix B). There was a moderate positive correlation between the height of the scapula and the glenoid height $r_{s,(98)} = 0.750$, $p < 0.001$. Glenoid width was strongly associated with scapular height $r_{s,(98)} = 0.766$, $p < 0.001$.

A linear regression was performed to predict glenoid height from scapular height. The regression equation $\text{Glenoid Height} = \text{Constant} + \text{Slope} \times \text{Value of Predictor}$ ($\text{Glenoid Height} = 15.156 + \text{Slope} \times \text{Scapular Height}$) established that scapular height could not reliably predict glenoid height (p value = ns) (Appendix B). When an analysis for males and females combined was conducted the R^2 value = 54.3% for the entire cohort. However, on subgroup analysis of males and females the R^2 reduced to 1.2% and 16%, respectively. Similar results were obtained while trying to predict glenoid width by linear regression. The R^2 value = 10.4% for females and 23.9% for males.

Table 3.1 Glenoid And Scapular Dimensions

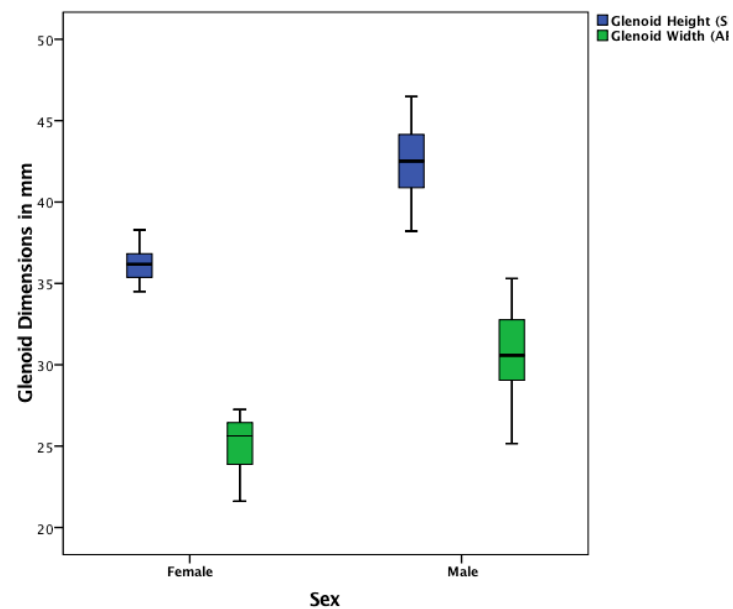
| | Male (n=25) | Female (n=25) | Mean (n=50) | P value* |
|--------------------------------|----------------|----------------|----------------|----------|
| Glenoid | | | | |
| Glenoid Height (SI) (mm) | 42.46 ± 2.14 | 36.38 ± 2.35 | 39.42 ± 3.72 | P< 0.001 |
| Glenoid Width (AP) (mm) | 30.77 ± 2.73 | 25.36 ± 2.35 | 28.06 ± 3.71 | P< 0.001 |
| Scapular Body | | | | |
| AB Length (mm) | 56.66 ± 13.83 | 41.95 ± 6.88 | 49.30 ± 13.11 | P< 0.001 |
| BC Length (mm) | 126.74 ± 15.72 | 112.23 ± 8.67 | 119.49 ± 14.54 | P< 0.001 |
| AC Length (mm) | 165.61 ± 11.57 | 138.61 ± 9.49 | 152.11 ± 17.19 | P< 0.001 |
| AB + BC Length (mm) | 183.40 ± 13.43 | 154.19 ± 10.92 | 168.80 ± 19.09 | P< 0.001 |
| AB and BC Angle | 56.10° ± 6.44° | 58.68° ± 9.06° | 57.39° ± 7.89° | P= 0.25 |
| Medio-Lateral (ML) Length (mm) | 114.52 ± 6.09 | 99.59 ± 4.86 | 107.05 ± 9.30 | P< 0.001 |
| Ratio | | | | |
| Glenoid Height/ AB+BC | 0.23 ± 0.15 | 0.23 ± 0.19 | 0.23 ± 0.19 | P= 0.41 |

* t-Test



Scapular Dimensions

Figure 3.4 Box Plot Demonstrates The Sexual Dimorphism In The Scapular Body Dimensions Dimensions Between Gender.



Glenoid Dimensions

Figure 3.5 Box Plot Demonstrates The Sexual Dimorphism In The Glenoid Dimensions Dimensions Between Gender.

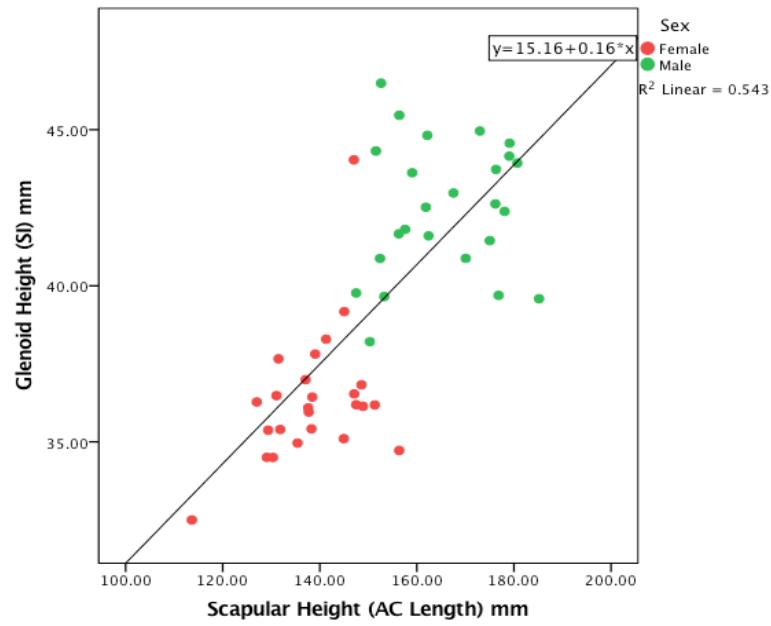


Figure 3.6

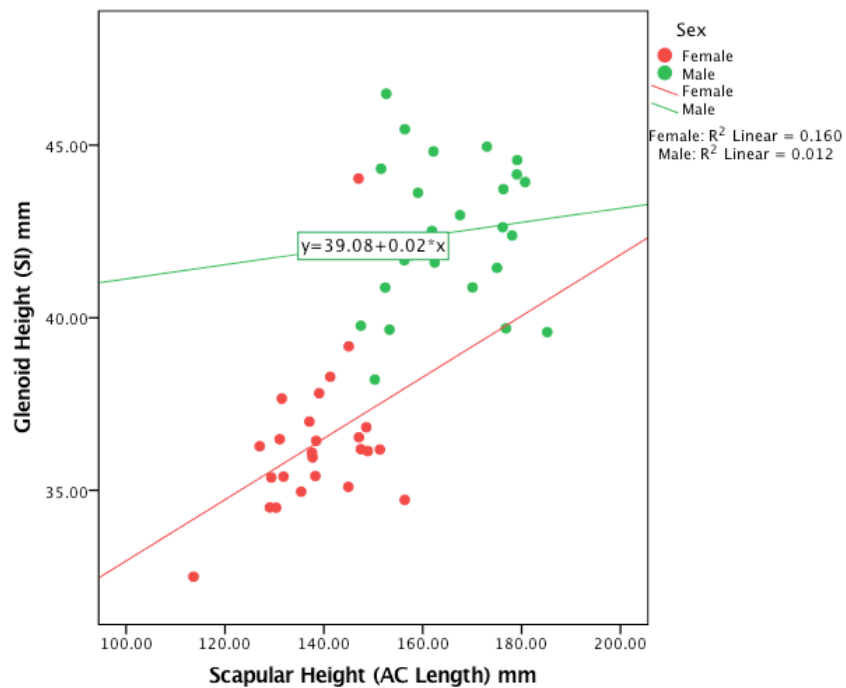


Figure 3.7

Scatter Plot Demonstrating The Correlation Between Estimation Of Glenoid Height By Apparent Scapular Height (AC) $R^2 = 0.54$

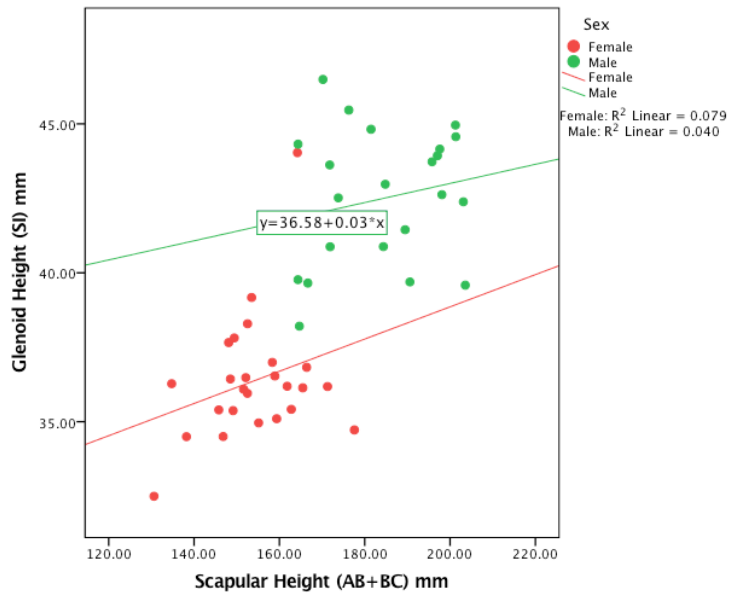


Figure 3.8 Scatter Plot Demonstrating Poor Correlation Between Estimation Of Glenoid Height By Apparent Scapular Height (AC) Amongst Sexes. Apparent Scapular Height Is A Poor Predictor Of Glenoid Height When Evaluated For Each Sex Individually.

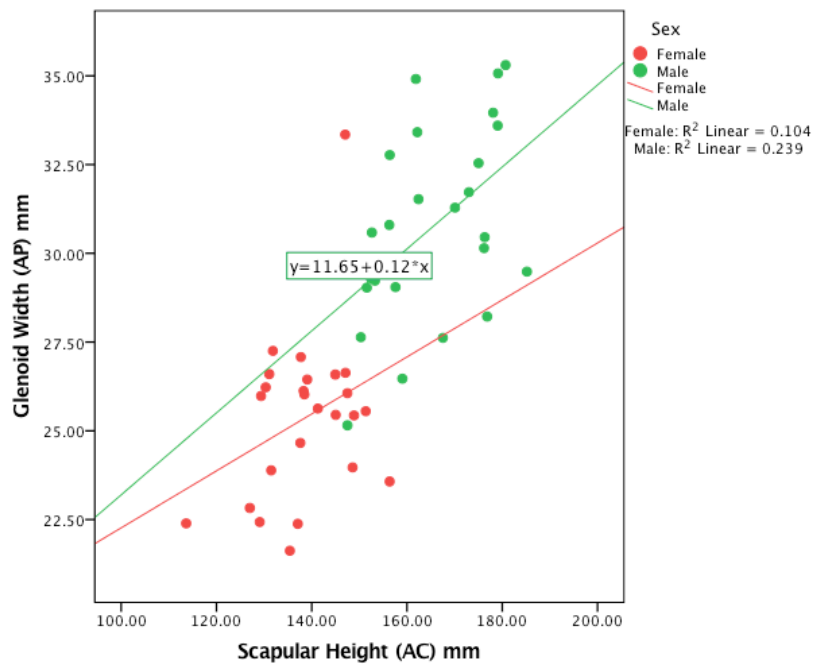


Figure 3.9 Scatter Plot Demonstrating The Poor Correlation Between Estimation Of Glenoid Width By Apparent Scapular Height (AC) R^2 0.10 And 0.23 For Females And Males Respectively.

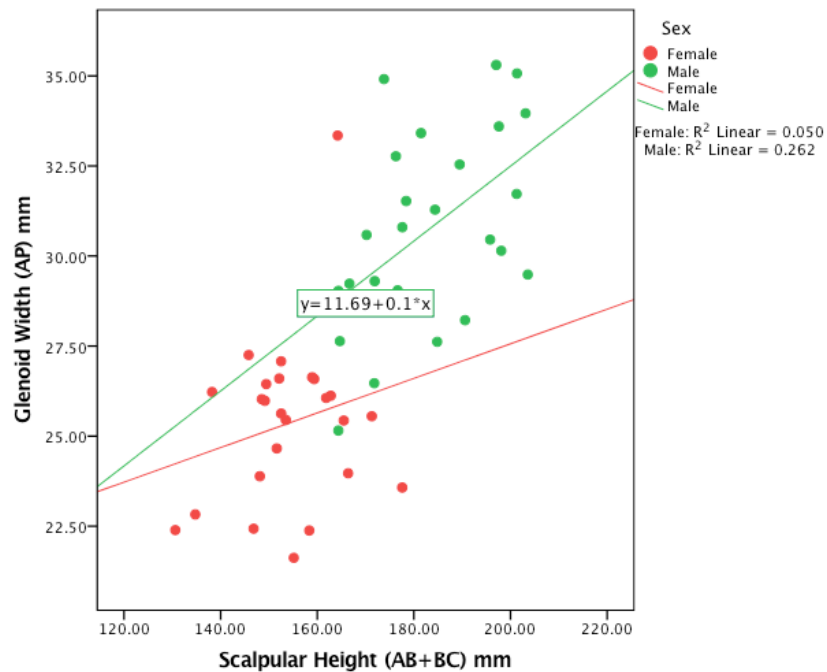


Figure 3.10 Scatter Plot Demonstrating The Poor Correlation Between Estimation Of Glenoid Width By True Scapular Height (AC) $R^2 = 0.05$ And 0.26 For Females And Males Respectively.

3.4 DISCUSSION

Sexual dimorphism between the male and female scapulae has been previously reported.¹⁰⁻¹² Studies have demonstrated a significant difference in the height of the scapulae between male and females. von Schroder et al described the mean scapular height as 155 ± 16 mm and the mean scapular width as 106 ± 8 mm. Our study found similar results with the mean scapular height 152.1 ± 17.1 mm and the mean scapular width 107.0 ± 9.3 mm (Figure 3.4). In addition to the above findings we measured the true height of the scapulae, by individually measuring the superior one third and the inferior two thirds of the medial border of the scapulae. The true height (AB + BC measurement) measured 18 mm longer (mean $183. \pm 13$ mm) than the relative height (mean 152 ± 17 mm) of the scapula (AC measurement). In accordance with previous

reports our study identified significant variation in size between the male and females. The male scapulae were 29 ± 2 mm larger in height and 15 ± 1 mm in width than the females ($p < 0.001$).

The glenoid morphology demonstrated variation between sexes (Figure 3.5) with the male glenoid measuring 6 mm longer and 5 mm wider than the females ($p < 0.001$) (Table 1). The mean glenoid height of 39 ± 4 mm found is similar to the report by Iannotti¹³ (glenoid height 39 ± 3 millimeters). The mean glenoid width of 28 mm was similar to the studies reported by von Schroder¹² (28.6 ± 3.3 mm) and Frankle et al¹⁴ (28.9 ± 3.3 mm). Churchill et al¹⁵ in their study of 172 cadaveric scapulae compared glenoid dimensions between Africa-American and Caucasian men and women. They reported statistically significant differences in the height and width of glenoid between men and women ($p < 0.001$), however they did not find any statistical difference in dimensions between the two races.

Our results highlight that a family of glenoid baseplate sizes are needed both for total shoulder arthroplasty (TSA) and reverse shoulder arthroplasty (RSA) designs. The glenoid width varies from 23 mm to 27 mm in females and 28 mm to 33 mm in males. Thus the overall variability in dimension lies from 23 mm to 33 mm. One standard baseplate size is insufficient to provide adequate implant coverage to the whole glenoid surface and design changes are needed to accommodate the male and female anthropometric measurements.

The aim of this study was to find a correlation between the scapular body and the glenoid morphology. Our analysis of the bony morphology of 50 scapulae failed to demonstrate any significant correlation between the scapular body and glenoid dimensions. The Spearman rho coefficient demonstrated moderately positive correlation between the glenoid height and scapular height $r_s(98) = 0.750$, $p < 0.001$. Glenoid width was strongly associated with scapular height $r_s(98) = 0.766$, $p < 0.001$. A linear regression performed to estimate glenoid height from scapular height demonstrated an R^2 value = 0.54 for the entire cohort (Figure 3.6). However, on further subgroup analysis between males and females the R^2 value dropped to 0.012 for males and 0.016 for females. (Figure 3.7). Further analysis to predict the glenoid height from the true scapular height (AB+BC) demonstrated a R^2 value of 0.04 for males and 0.07 for

females (Figure 3.8). Similar results were obtained whilst trying to predict the glenoid width from true scapular height ($R^2 = 0.26$ and 0.05 for male and females respectively) (Figure 3.9-3.10).

These findings may be explained by the development of the scapula. The scapula largely develops by membranous ossification whereas the glenoid largely develops by enchondral ossification. The secondary ossification centers in the glenoid contribute to the growth of the glenoid. The superior one third of the glenoid (triangular part) develops in conjunction with the base of the coracoid from the sub-coracoid ossification center, whereas the bottom two thirds or circular part of the glenoid develops as a result of fusion of numerous small islands of ossification. Fusion of the upper triangular and lower circular part results in the adult pear shaped glenoid.¹⁶ This fusion occurs >16 years in males and >14 years in females¹⁷⁻¹⁹ thus accounting for the larger glenoid dimensions in males than in females. The scapula body attains most of its growth by intra membranous ossification; however, the medial border and the inferior angle grow by secondary ossification centers, which appear in the late teens. These centers continue to grow much beyond puberty both in males and females and fusion occurs by the age of 23 years making them one of the last ossific centers in the body to fuse.²⁰ Thus, the medial border of the scapula continues to grow long after the glenoid has attained maturity. This can explain the inability in our study to predict the glenoid dimensions in our cohort of elderly patients. Regression analysis if carried out before the age of 20 years may yield different results.

The strength of our study lies in the accuracy of measurements carried out by custom code rather than mechanical methods. In addition, our study highlights that the true length of the medial border of the scapula is 18 mm longer than the traditionally measured distance from the SSP to ISP. Our study is one of the first that has demonstrated that glenoid dimensions cannot be reliably predicted by the scapular body dimensions and that the gender dimorphism has a significant role to play in scapular and glenoid dimensions.

A weakness of our study is the small sample size of 50 patients. Most of the cadavers were Caucasian in ethnicity thus our results may not be applicable to different races. However, our results are quite similar to those reported by other authors with much larger sample sizes and in studies conducted comparing anthropometric measurements in African-Americans and Caucasians.

3.5 CONCLUSION

Our study quantifies the gender dimorphism between the male and female scapular body and the glenoid. Significant size variations of note are reported between the male and female glenoids thus necessitating the need for a family of glenoid sizes for TSA and glenoid baseplate sizes for RSA. Further regression analysis has demonstrated that the glenoid size cannot be reliably predicted by the scapular body. Further studies are needed to develop methods to accurately predict glenoid size from the ipsilateral scapula.

Acknowledgement

The authors thank Dr. Yves Bureau for his assistance in statistical analysis of the data.

3.6 REFERENCES

1. Dallalana RJ, McMahon RA, East B, Geraghty L. Accuracy of patient-specific instrumentation in anatomic and reverse total shoulder arthroplasty. *International journal of shoulder surgery*. 2016;10(2):59-66.
2. Samilson RL, Prieto V. Dislocation arthropathy of the shoulder. *The Journal of bone and joint surgery. American volume*. 1983;65(4):456-460.
3. Bryce CD, Pennypacker JL, Kulkarni N, et al. Validation of three-dimensional models of in situ scapulae. *Journal of shoulder and elbow surgery / American Shoulder and Elbow Surgeons ... [et al.]*. 2008;17(5):825-832.
4. Wu G, van der Helm FCT, Veeger HEJ, et al. ISB recommendation on definitions of joint coordinate systems of various joints for the reporting of human joint motion—Part II: shoulder, elbow, wrist and hand. *Journal of Biomechanics*. 2005;38(5):981-992.
5. Kwon YW, Powell KA, Yum JK, Brems JJ, Iannotti JP. Use of three-dimensional computed tomography for the analysis of the glenoid anatomy. *Journal of shoulder and elbow surgery / American Shoulder and Elbow Surgeons ... [et al.]*. 2005;14(1):85-90.
6. Wu G, van der Helm FC, Veeger HE, et al. ISB recommendation on definitions of joint coordinate systems of various joints for the reporting of human joint motion--Part II: shoulder, elbow, wrist and hand. *J Biomech*. 2005;38(5):981-992.

7. Chuang TY, Adams CR, Burkhart SS. Use of preoperative three-dimensional computed tomography to quantify glenoid bone loss in shoulder instability. *Arthroscopy : the journal of arthroscopic & related surgery : official publication of the Arthroscopy Association of North America and the International Arthroscopy Association*. 2008;24(4):376-382.
8. Saito H, Itoi E, Sugaya H, Minagawa H, Yamamoto N, Tuoheti Y. Location of the glenoid defect in shoulders with recurrent anterior dislocation. *The American journal of sports medicine*. 2005;33(6):889-893.
9. Kany J, Flamand O, Grimberg J, et al. Arthroscopic Latarjet procedure: is optimal positioning of the bone block and screws possible? A prospective computed tomography scan analysis. *Journal of shoulder and elbow surgery / American Shoulder and Elbow Surgeons ... [et al.]*. 2016;25(1):69-77.
10. Mallon WJ, Brown HR, Vogler JB, 3rd, Martinez S. Radiographic and geometric anatomy of the scapula. *Clinical orthopaedics and related research*. 1992(277):142-154.
11. Penning R, Muller S. [Sexual dimorphism of the scapula]. *Z Rechtsmed*. 1988;101(3):183-196.
12. von Schroeder HP, Kuiper SD, Botte MJ. Osseous anatomy of the scapula. *Clinical orthopaedics and related research*. 2001(383):131-139.
13. Iannotti JP, Gabriel JP, Schneck SL, Evans BG, Misra S. The normal glenohumeral relationships. An anatomical study of one hundred and forty shoulders. *The Journal of bone and joint surgery. American volume*. 1992;74(4):491-500.
14. Frankle MA, Teramoto A, Luo ZP, Levy JC, Pupello D. Glenoid morphology in reverse shoulder arthroplasty: classification and surgical implications. *Journal of shoulder and elbow surgery / American Shoulder and Elbow Surgeons ... [et al.]*. 2009;18(6):874-885.
15. Churchill RS, Brems JJ, Kotschi H. Glenoid size, inclination, and version: an anatomic study. *Journal of shoulder and elbow surgery / American Shoulder and Elbow Surgeons ... [et al.]*. 2001;10(4):327-332.
16. Scheuer LB, S. Pectoral Girdle. In: Scheuer LB, S, ed. *Developmental Juvenile Osteology*. 1 ed: Elsevier; 2000:252-271.
17. Coqueugniot H, Weaver TD. Brief communication: infracranial maturation in the skeletal collection from Coimbra, Portugal: new aging standards for epiphyseal union. *Am J Phys Anthropol*. 2007;134(3):424-437.
18. Schaefer M. A summary of epiphyseal union timings in Bosnian males. *International Journal of Osteoarchaeology*. 2008.
19. McKern TWaS, T.D. Skeletal age changes in young American males, analysed from the standpoint of age identification. Natick, MA. 1957.
20. Saunders S, Hoppa, R. and Southern, R. Diaphyseal growth in a nineteenth-century skeletal sample of sub adults from St Thomas' Church, Belleville, Ontario. *International Journal of Osteoarchaeology*. 1993;3:265-281.

Chapter 4- Morphologic Analysis of the Three Columns of the Scapula: Surgical Implications in Reverse Shoulder Arthroplasty

Overview: Success of Reverse Shoulder Arthroplasty hinges on attaining primary stability by rigid fixation of the glenoid baseplate. This can be challenging when the procedure is performed in osteoporotic bone or in the setting of severe glenoid bone loss. In such a scenario, the surgeon relies on adequate screw fixation beyond the glenoid vault. The three columns of the scapula host dense bone for screw fixation. This chapter evaluates the relationship of these three columns of the scapula and the ability of the screw holes in current baseplate designs to engage these columns.

4.1 INTRODUCTION

Reverse shoulder arthroplasty (RSA) was initially developed for the treatment of cuff tear arthropathy.^{1,2} Due to its widespread success, the indications and age limitations have expanded. The indications for RSA now include cuff tear arthropathy, irreparable rotator cuff tears with or without glenohumeral arthritis, glenoid deformities, acute and chronic trauma, tumor, systemic/inflammatory arthritis and revision arthroplasty.³

In the setting of poor or limited glenoid bone stock, total shoulder arthroplasty (TSA) has had disappointing results.⁴⁻⁸ Glenoid retroversion beyond 15-20 degrees has been described as unsuitable for attaining primary fixation of a polyethylene glenoid component without severely compromising glenoid bone stock.⁹ This has led to the development of augmented glenoid components, with recent studies showing encouraging short-term results. However, long term data is necessary to establish the efficacy of augmented glenoid components.^{10,11} RSA is currently the implant of choice for most revision procedures and is the current implant used to treat advanced glenoid bone loss.^{8,12-16} This is further highlighted in the Australian Joint registry, which reports a steady increase in the number of RSA performed for revision arthroplasty.¹⁷

Rigid primary fixation of the glenoid baseplate with correct positioning is a prerequisite for a successful RSA outcome. It is widely accepted that the baseplate needs to be positioned as low as possible on the glenoid to avoid notching.¹⁸ In addition, rigid fixation of at least two angled screws with a well seated central peg is imperative for primary stability of the baseplate.^{19,20} In the elderly population, the glenoid bone stock is often poor and satisfactory screw purchase may be of concern.²¹ This has led to numerous studies attempting to locate the best bone beyond the glenoid vault.²²⁻²⁴

The “Tri Pillar model” of the scapula proposed by Bhatia et al.²⁵ and popularised as the “Three Column concept” by Humphrey et al.²⁶ delineates the columns of bone beyond the glenoid which may be utilised to attain rigid screw fixation. So far, the relationship

of the coracoid base, the acromial spine and the lateral border/pillar of the scapula, has not been clearly defined, especially in the setting of glenoid deficiency. Large variability exists in the description of angular measurements due to the differences in the reference planes utilised.

The purpose of this study is to quantitatively establish the relationship of the three columns of the scapula by utilizing standardised, clinically applicable reference planes. Secondly, we aim to ascertain the relationship of these columns with and without a glenoid co-ordinate system and to find the relationship between the two methods. Thirdly, we aim to evaluate gender dimorphism and its implications on current baseplate design.

4.2 MATERIALS AND METHODS

Computed tomography (CT) scans were obtained from the shoulders of 50 cadavers. There were 25 male and 25 female cadavers (age 71 ± 14 years). The mean age of the subjects was 71 ± 14 yrs (men 72 ± 15 yrs and women 69 ± 13 yrs). There were 23 right and 27 left scapulae analysed. The CT scans were acquired with a multi slice scanner with standardised clinical settings (120 to 140 kVp, 512X512 resolution). The CT scans were classified by fellowship trained orthopaedic surgeon according to the classification proposed by Samilson – Prieto²⁷. Shoulders with glenohumeral arthritis with Grade 0-2 were included for analysis.²⁷ Cases with Grade 3 arthritic changes and any case with evidence of trauma, surgery or glenoid bone loss were excluded from analysis.

The CT images were then uploaded in Digital Imaging and Communications in Medicine format (DICOM) to Mimics medical imaging software (Mimics 17.0®, Materialise, Leuven, Belgium). Thresholding was set to a minimum value of 200 Hounsfield Units (HU) to preserve scapular anatomy during segmentation and to obtain both cancellous and cortical bone models.²⁸

Utilising the built in med-CAD module in Mimics®, various surface points were extracted from the scapula. Four standardised views were chosen to extract the surface anatomy points; superior axial view, posterior view, sagittal view (glenoid en face view)

and inferior para axial view (parallel to the lateral pillar of the scapula) (Figure 4.1). The superior (axial) view of the scapula was used to extract the most medial point on the medial vertebral surface of the scapula - Medial scapular point (MSP) this corresponds to the Trigonum spinae scapulae. This point is localised to the medial scapular angle (attachment of the levator scapulae muscle) which corresponds to the intersection of the scapular spine with the medial border of the scapula.²⁹

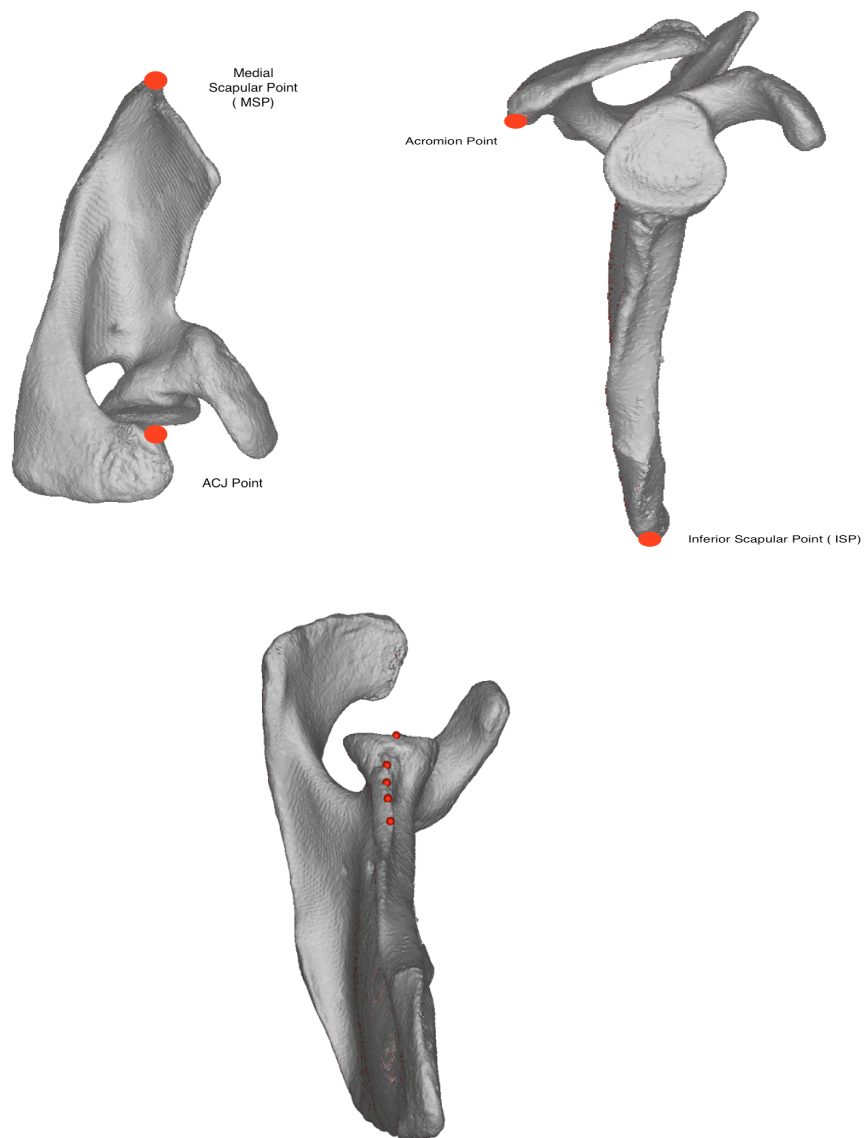


Figure 4. 1 Superior Axial View, Scapular Y View And Inferior Para-Axial View.

Various surface points were extracted on the sagittal “Y” view of the scapula. The most inferior point of the scapular body was extracted. This was the lowermost and most posterior projection of the inferior angle of the scapula - Inferior Scapular Point (ISP).^{30,31}

Whilst evaluating the enface view of the glenoid; the circular rim of the glenoid was delineated and 10 surface points were extracted from the inferior cortical rim (Figure 4.2). This defined the inferior curvature of the circular glenoid rim. Custom code was developed in Matlab (Math works, Natick, MA, USA) to transform this semicircle to a complete circle, using a least square circle fit, and the centre point of the circle was ascertained. This point corresponds to the centre of the glenoid (Glenoid Centre point). The superior 12 o’clock point, was identified as per the descriptions of Chuang³², Saito³³ and Kany³⁴ and its apex extracted as a point Superior Glenoid Point (SGP). A line was then passed through the SGP and Glenoid centre. This line was extended until it intersected the inferior glenoid rim. This intersection point was extracted as the Inferior Glenoid point (IGP, 6 o’clock). This axis was used as the longitudinal axis of the glenoid (Superior Inferior – SI Glenoid axis).

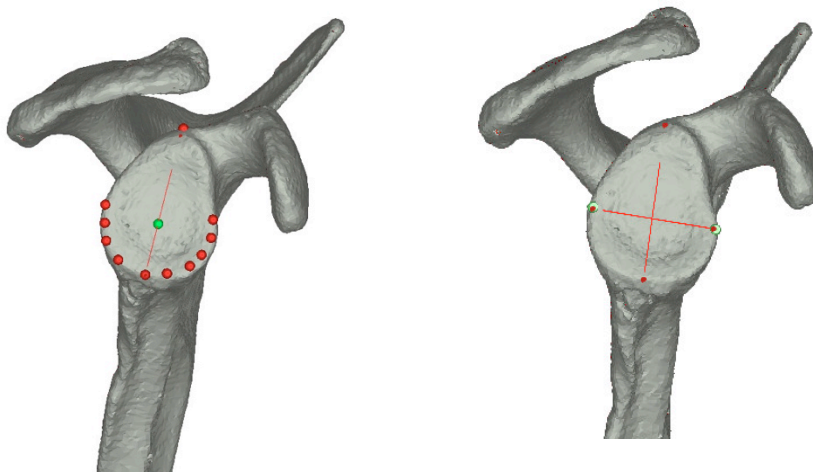


Figure 4. 2 Calculation Of The Glenoid Center Point And Establishment Of The Superior Inferior (SI) Glenoid Axis

The Scapular plane as described by Kwon et al.³⁰ was created using the previously defined points. This was the plane connecting the Medial scapular point, the inferior scapular point and the glenoid center (Please refer to Chapter 2 Figure 2.1C). This served as the (scapular) coordinate plane against which an orthogonal glenoid plane was created.

To delineate the position of the coracoid and the scapular spine column, the coracoid surface and scapular spine anatomy was evaluated on the sagittal enface view. Eight points (4 points each from the acromion and coracoid) were extracted from the inferior cortex of the coracoid and the scapular spine (Figure 4.3). Tangential views to the inferior cortex of the coracoid and scapular spine were obtained. Fixed segmentation angles were used in the Mimics® software so as to evaluate all specimens in a similar fashion. This line was then projected to a sagittal plane perpendicular to the scapular plane.

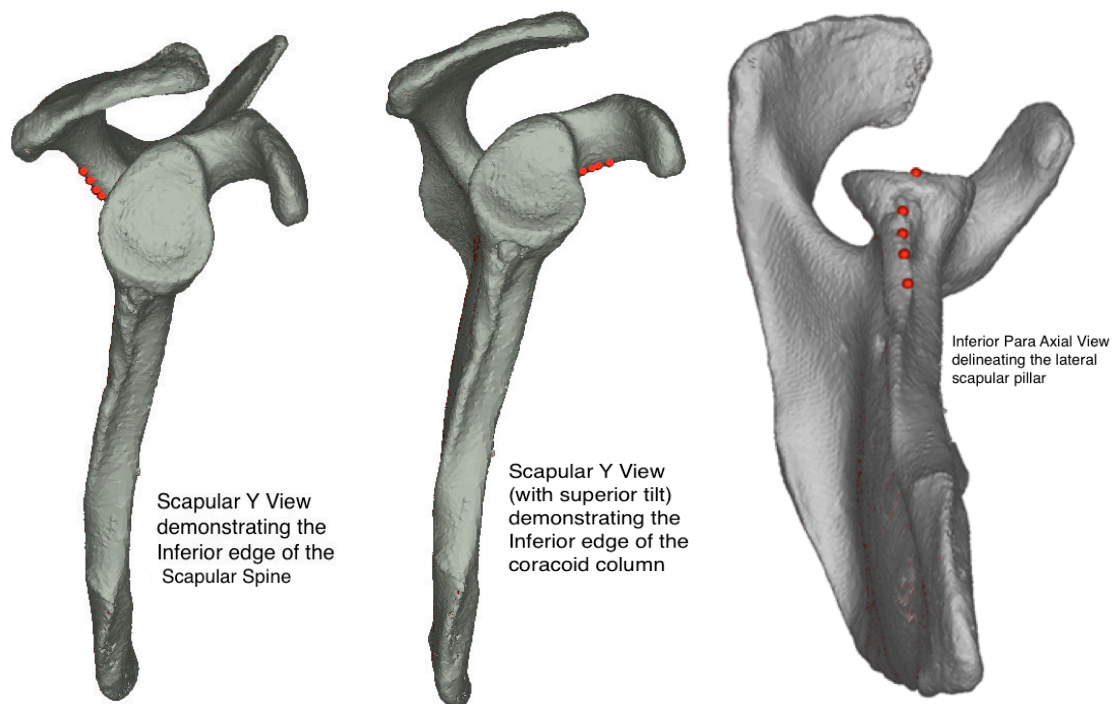


Figure 4.3 The Images Demonstrate The 3 Standardized Views Chosen In All 50 Scapulae To Delineate The Posterior Cortical Edge Of The Scapular Spine, The Inferior Cortical Margin Of The Coracoid Base, And The Lateral Scapular Pillar (Inferior Para Axial Plane).

The lateral scapular column was best evaluated from the inferior para axial plane. This is a plane in line with the long axis of the lateral scapular pillar. The surface anatomy of the proximal 7 cm of the lateral scapular pillar formed by the origins of the long head of triceps and the origin of teres minor until the groove of the circumflex scapular artery was demarcated.³⁵ Four points were extracted. The first point was located at the junction of the glenoid rim and the lateral scapular pillar. The most caudal point was extracted 7 cm caudal (Figure 4.3).

The long axis of the three columns of the scapula, in the sagittal plane were calculated using custom code developed in Matlab®. An orthogonal plane to the scapular plane was developed parallel to the glenoid face (Figure 4.4). The axis representing each of the three columns of the scapula and the SI axis of the glenoid, were projected onto this plane. The relationship between each column was analysed with respect to each other and with respect to the SI glenoid axis. Thus, measurements obtained gave the relationships of the three columns of the scapula (independent of the glenoid) and their relationships to the long axis of the glenoid (dependant on the glenoid).

Statistical analysis (SPSS software®, 15.0; IBM Inc. USA) was performed and mean and standard deviations for each subgroup was calculated. Analysis to determine the difference between the position and orientation of each column with respect to each other and the SI axis respectively was carried out by performing a t-test for all cases and separated by subgroups. The relationship of the orientation of each column, between males and females was analysed by a t-test. All differences were considered significant at a probability level of 95% ($P < 0.05$).

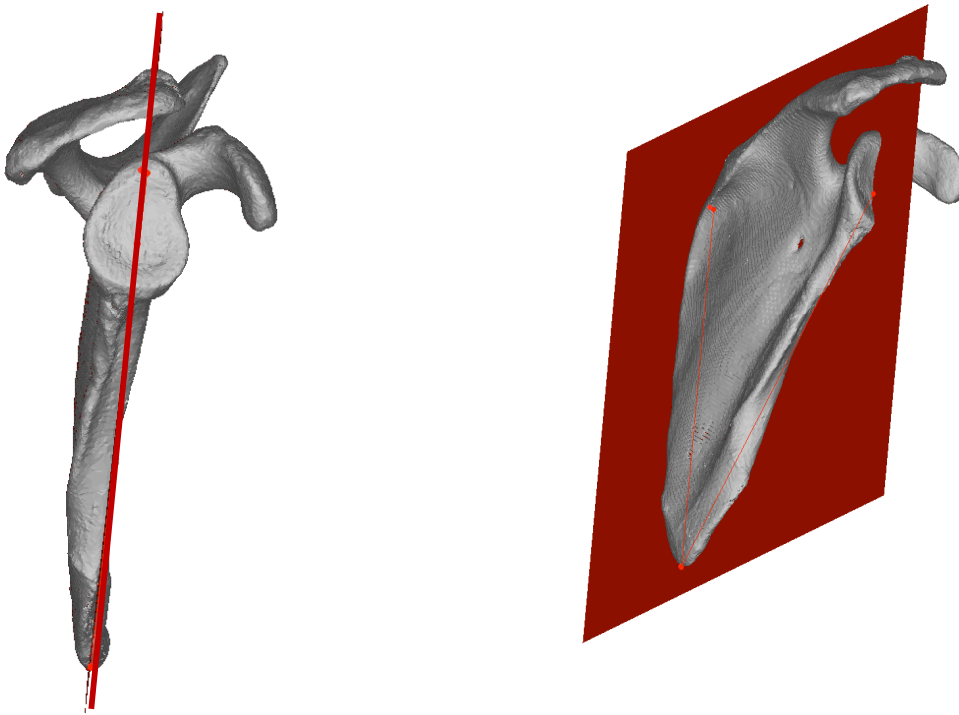


Figure 4. 4 Orthogonal Plane Developed Parallel To The Glenoid Face An Perpendicular To The Scapular Plane Using Med CAD Algorithm

Inter observer reliability was used to assess the point selection in angle measurements of the coracoid, acromion, and inferior spine by two independent observers (A.G & N.K.K) using intra class correlation coefficients (ICC) with a 2-way random effects model and absolute agreement. Classifications were interpreted according to Fleiss and Cicchetti and Sparrow as poor (ICC < 0.40), fair (ICC = 0.40-0.59), good (ICC = 0.60-0.74), and excellent (ICC > 0.74).

4.3 RESULTS

The analysis of the relationship of the three columns of the scapula in relation to the glenoid axis demonstrated a mean scapular spine SI glenoid angle of $48.4 \pm 8.8^\circ$. The angle between the lateral pillar and the SI glenoid axis was $1.1 \pm 10.0^\circ$. The angle between the coracoid pillar and the SI glenoid axis was noted to be $44.7 \pm 11.3^\circ$. No significant sex difference was found between the acromial spine/glenoid axis ($p=0.26$) and the inferior scapular pillar/SI glenoid axis ($p=0.27$) (Table 4.1). However, the female coracoid was found to be more horizontal than the male coracoid in relation to the SI axis of the glenoid ($p=0.037$).

Table 4.1: Relationship between the 3 Columns and SI- Glenoid Axis

| | Male (n=25) | Female (n=25) | Total (n=50) | <i>p value</i> |
|---|--------------------|---------------------|--------------------|----------------|
| Acromial Spine-SI Glenoid axis angle | $49.8 \pm 9^\circ$ | $46.9 \pm 8^\circ$ | $48.4 \pm 9^\circ$ | <i>p=0.26</i> |
| Lateral Pillar-SI Glenoid axis Angle | $3 \pm 9^\circ$ | $-0.4 \pm 11^\circ$ | $1 \pm 10^\circ$ | <i>p=0.27</i> |
| Coracoid-SI Glenoid axis Angle | $41 \pm 13^\circ$ | $48 \pm 8^\circ$ | $45 \pm 11^\circ$ | <i>p=0.037</i> |

Negative values denote a posteriorly directed inferior column.

The mean angle between the acromial spine and the coracoid column was $93 \pm 13^\circ$ with no significant difference between males ($91 \pm 15^\circ$) and females ($95 \pm 10^\circ$) ($p=0.29$). The angle between the inferior scapular column and the scapular spine was 6.5° greater ($p=0.03$) in females ($134 \pm 10^\circ$) than in males ($128 \pm 11^\circ$). Similarly, the angle between the inferior scapular column and the coracoid column was 11° greater ($p=0.009$) in males ($141 \pm 15^\circ$) than in females ($130 \pm 12^\circ$) (Table 4.2) (Appendix C).

Table 4.2 Relationship between the 3 Columns of the Scapula

| | Male (n=25) | Female (n=25) | Total (n=50) | <i>p value</i> |
|-----------------------------------|--------------------|--------------------|--------------------|----------------|
| Acromial Spine- Coracoid | $91 \pm 15^\circ$ | $95 \pm 10^\circ$ | $93 \pm 13^\circ$ | <i>p=0.29</i> |
| Acromial Spine- Lateral Pillar | $128 \pm 11^\circ$ | $134 \pm 10^\circ$ | $131 \pm 11^\circ$ | <i>p=0.030</i> |
| Coracoid-Lateral Pillar | $141 \pm 15^\circ$ | $130 \pm 12^\circ$ | $136 \pm 14^\circ$ | <i>p=0.009</i> |

Inter observer reliability was excellent for the acromion (ICC = 0.870, 95% CI: 0.464-0.968), coracoid (ICC = 0.878, 95% CI: 0.371-0.972), and inferior spine (ICC = 0.938, 95% CI: 0.745-0.985) relative to the glenoid centre axis. Similarly, reliability was excellent for the acromion (ICC = 0.832, 95% CI: 0.302-0.959), coracoid (ICC = 0.873, 95% CI: 0.352-0.970), and inferior spine (ICC = 0.933, 95% CI: 0.725-0.984) relative to the glenoid SI axis. Interobserver reliability was also excellent for the acromion-coracoid angle (ICC = 0.811, 95% CI: 0.306-0.952), acromion-inferior spine angle (ICC = 0.899, 95% CI: 0.586-0.975), and coracoid-inferior spine angle (ICC = 0.875, 95% CI: 0.528-0.968).

4.4 DISCUSSION

The shape of the scapula has been widely studied with osteology studies reporting gender dimorphism between male and female scapular borders for forensic identification.³⁶⁻³⁸ The female scapula has been reported as a scaled down version of the male scapula.³⁹ Scholtz reported that female scapulae have straighter lateral and medial borders, and that the supraspinous fossae is more convex than in males.³⁸ The coraco acromial arch anatomy has been of recent interest. Alobaidy et al. reported on the various characteristics of the bony morphology of the acromion and coracoid. They evaluated the position of the coracoid column with reference to the glenoid face and termed it as ‘scapular angle of the coracoid root’. They reported this angle to be $115 \pm 14^\circ$.⁴⁰ In our study we have found this angle to be $135 \pm 11^\circ$. This difference may arise in the different methodology of estimation of the SI axis of the glenoid and calculation of direction of the coracoid column. However, the authors also found a gender difference between men and women in regards to the position of the coracoid, which agrees with the current study.

In their detailed analysis of coracoid geometry, Bhatia et al. noted statistically significant gender dimorphism in the length, breadth, thickness and projections of the coracoid, with the male coracoid being larger. However, they did not find any significant difference in angular measurements. They reported a coracoid glenoid axis angle of 126.1 degrees.²⁵

This sexual dimorphism noticed may be attributed to the developmental anatomy. Phylogenetic studies of the scapula demonstrate that the scapular body and the glenoid develop relatively independent of each other.^{41,42} The acromial spine and the lateral pillar of the scapula develop from the primary ossification center located in the scapular neck in the foetus. After birth, the growth and development of the scapular body is dependent upon the surrounding muscles. The scapular spine and lateral pillar develop by intramembranous ossification, a characteristic of all flat bones in the human body.^{43,44}

The development from two very different ossification centres thus explains the glenoid pear shape. The superior 1/3 of the glenoid develops from the sub-coracoid center, which is also responsible for the development of the base of the coracoid. This center is located at the dorso medial aspect of the base of the coracoid and is visualised in the adult as the supra glenoid tubercle. The body of the coracoid develops from an independent nucleus and fuses to the root of the coracoid at maturity. Thus, the development of the superior 1/3 of glenoid and coracoid base is mutually dependent. The inferior circular part of the glenoid develops from two or more secondary ossific centres which fuse amongst themselves and later to the upper 1/3 of the glenoid, forming the mature adult glenoid.^{44,45}

Fusion of the physal plate and completion of growth is dependant upon hormonal, genetic and nutritive factors. Generally, between 15-17 years of age, the upper 1/3 of the glenoid and the coracoid fuse whilst the lower 2/3 of the glenoid fuses by 17-18 yrs. Earlier physal fusion in women may lead to the more horizontal position of the female coracoid compared to males. In keeping with our findings, we noted the angle between the inferior scapular column and the coracoid column was 11° greater ($p=0.009$) in males ($141\pm 15^\circ$) than in females ($130\pm 12^\circ$).

Previous radiographic studies have measured the angle between the acromial spine and the lateral pillar of the scapula.^{46,47} These studies were 2-dimensional x-ray based radiographic studies and with a lack of consistency amongst studies in defining the axis against which measurements are made. We have attempted to address this by using a clinically applied and validated method for measurement of the SI axis of the glenoid, using 3-dimensional models, which has been shown to avoid perspective errors caused by 2D measurements. In addition to this, we have measured the relationship of each column independent of the glenoid anatomy.

Our study demonstrates that the measurements between the three columns are similar in both of our subgroups (ie. using the SI glenoid axis or independent of the glenoid). This may be attributable to our selection, where specimens with only normal glenoid and scapular anatomy were used for this study. These findings may vary in the case of glenoid bone defects and retroversion of the glenoid.

The triple pillar concept of Bhatia et al.²⁵ or 3 column concept of Humphrey et al.²⁶ alludes to the supportive bony framework of the scapular body which provides sufficient mechanical stability to implant a glenoid baseplate, especially in cases with poor glenoid bone quality and in glenoid vault bone loss. Di Setafno²³ quantitatively analysed bone quality for screw placement for baseplate fixation in RSA. In their computer modelling study of screw placement in commercially available base plate designs they were only able to insert the superior and inferior screw in regions of good bone stock. The posterior and anterior screw were unable to attain the desired trajectories and thus were inserted in weaker bone.²³ Stephens et al.⁴⁸ in their study found similar difficulties in inserting screws into all the three columns. They found an optimal solution might be to internally rotate the base plate by $11\pm 1^\circ$ to attain maximal peripheral screw fixation. They reported the mean position for screw fixation from the 12 o'clock position as $6\pm 2^\circ$ for the coracoid pillar, $198\pm 2^\circ$ for the inferior pillar, and $295\pm 3^\circ$ for the scapular spine pillar. Both authors commented that implant design changes need to be made to allow surgeons to safely insert screws in the regions of best bone stock. In a cadaveric study of fixation of a custom baseplate beyond the glenoid, Codsì et al., were only able to attain fixation in all three columns by removing the central peg and enlarging all the screw holes of a glenoid baseplate. The authors summarized that if the glenoid vault is deficient the current implant systems cannot be implanted.²²

Based on our study we have demonstrated that the mean angle between coracoid column and the lateral pillar is $136 \pm 14^\circ$ and coracoid and scapular spine is $93 \pm 13^\circ$. Using commercially available baseplate designs with 90° screw constructs despite using variable angle screws it would be very challenging to insert more than 2 screws in good bone stock. Especially in women where the anatomy is considerably different. This may not be of much concern in a primary RSA with sufficient bone stock however, this

becomes a considerable problem in cases of glenoid bone loss which necessitate structural bone grafts.

Our study evaluates the three columns of the scapula independent of the glenoid morphology. The strengths of this study include: firstly, we used 3-dimensional measurements and mathematical algorithms which improve accuracy. Secondly, a standardized reference axis was used to analyze angular measurements. The scapular axis utilized is currently the most clinically used axis for calculation of glenoid version and serves as the platform for patient specific implant software. Lastly, this study highlights the gender dimorphism in the human scapula and questions the need for further implant design which caters to differences in male and female anatomy.

The limitations of our study are that it is a small cohort of 50 specimens. The majority of the cadavers are of Caucasian ethnic origin and further research would be required to evaluate the applicability of our findings to different racial subgroups.

4.5 CONCLUSION

Our study demonstrates that the 3 columns of the scapula demonstrate significant sexual dimorphism. The female scapula the coracoid is positioned lower; as a result the coracoid and the lateral scapular pillar are closer in females than in males. In addition, the 3 columns of the scapula are positioned at an angle of 93° between the acromion and the coracoid and 136° degrees between the coracoid and the lateral pillar and 131° degrees between the acromion spine and the lateral pillar. This structural relationship should be considered while inserting screws to fix a baseplate in a RSA.

4.6 REFERENCES

1. Neer CS, 2nd. Replacement arthroplasty for glenohumeral osteoarthritis. *The Journal of bone and joint surgery. American volume.* 1974;56(1):1-13.
2. Neer CS, 2nd, Craig EV, Fukuda H. Cuff-tear arthropathy. *The Journal of bone and joint surgery. American volume.* 1983;65(9):1232-1244.
3. Gupta A, Heani D, Lafosse L. Reverse Shoulder Arthroplasty. In: Dines DM, Edwards TB, Dines J, eds. *Reverse Shoulder Arthroplasty.* New York: Thieme; 2016.
4. Deutsch A, Abboud JA, Kelly J, et al. Clinical results of revision shoulder arthroplasty for glenoid component loosening. *Journal of shoulder and elbow surgery / American Shoulder and Elbow Surgeons ... [et al.].* 2007;16(6):706-716.
5. Hill JM, Norris TR. Long-term results of total shoulder arthroplasty following bone-grafting of the glenoid. *The Journal of bone and joint surgery. American volume.* 2001;83-A(6):877-883.
6. Ho JC, Sabesan VJ, Iannotti JP. Glenoid component retroversion is associated with osteolysis. *The Journal of bone and joint surgery. American volume.* 2013;95(12):e82.
7. Klika BJ, Wooten CW, Sperling JW, et al. Structural bone grafting for glenoid deficiency in primary total shoulder arthroplasty. *Journal of shoulder and elbow surgery / American Shoulder and Elbow Surgeons ... [et al.].* 2014;23(7):1066-1072.
8. Neyton L, Sirveaux F, Roche O, Mole D, Boileau P, Walch G. [Results of revision surgery for glenoid loosening: a multicentric series of 37 shoulder prosthesis]. *Revue de chirurgie orthopedique et reparatrice de l'appareil moteur.* 2004;90(2):111-121.
9. Clavert P, Millett PJ, Warner JJ. Glenoid resurfacing: what are the limits to asymmetric reaming for posterior erosion? *Journal of shoulder and elbow surgery / American Shoulder and Elbow Surgeons ... [et al.].* 2007;16(6):843-848.
10. Sabesan V, Callanan M, Sharma V, Iannotti JP. Correction of acquired glenoid bone loss in osteoarthritis with a standard versus an augmented glenoid component. *Journal of shoulder and elbow surgery / American Shoulder and Elbow Surgeons ... [et al.].* 2014;23(7):964-973.
11. Knowles NK, Ferreira LM, Athwal GS. Augmented glenoid component designs for type B2 erosions: a computational comparison by volume of bone removal and quality of remaining bone. *Journal of shoulder and elbow surgery / American Shoulder and Elbow Surgeons ... [et al.].* 2015;24(8):1218-1226.
12. Bell RH, Noble JS. The management of significant glenoid deficiency in total shoulder arthroplasty. *Journal of shoulder and elbow surgery / American Shoulder and Elbow Surgeons ... [et al.].* 2000;9(3):248-256.
13. Boileau P, Moineau G, Roussanne Y, O'Shea K. Bony increased-offset reversed shoulder arthroplasty: minimizing scapular impingement while maximizing glenoid fixation. *Clinical orthopaedics and related research.* 2011;469(9):2558-2567.
14. Neyton L, Boileau P, Nove-Josserand L, Edwards TB, Walch G. Glenoid bone grafting with a reverse design prosthesis. *Journal of shoulder and elbow surgery / American Shoulder and Elbow Surgeons ... [et al.].* 2007;16(3 Suppl):S71-78.

15. Bateman E, Donald SM. Reconstruction of massive uncontained glenoid defects using a combined autograft-allograft construct with reverse shoulder arthroplasty: preliminary results. *Journal of shoulder and elbow surgery / American Shoulder and Elbow Surgeons ... [et al.]*. 2012;21(7):925-934.
16. Melis B, Bonneville N, Neyton L, et al. Glenoid loosening and failure in anatomical total shoulder arthroplasty: is revision with a reverse shoulder arthroplasty a reliable option? *Journal of shoulder and elbow surgery / American Shoulder and Elbow Surgeons ... [et al.]*. 2012;21(3):342-349.
17. AOANJRR. AOANJRR Shoulder Registry. Australia: South Australian Health and Medical Research Institute; 2015.
18. Simovitch RW, Zumstein MA, Lohri E, Helmy N, Gerber C. Predictors of scapular notching in patients managed with the Delta III reverse total shoulder replacement. *The Journal of bone and joint surgery. American volume*. 2007;89(3):588-600.
19. Hopkins AR, Hansen UN, Bull AM, Emery R, Amis AA. Fixation of the reversed shoulder prosthesis. *Journal of shoulder and elbow surgery / American Shoulder and Elbow Surgeons ... [et al.]*. 2008;17(6):974-980.
20. D. Seybold MKn, J. Geßmann, B. Jettkant, Schildhauer TA. Wie viel Peg-Länge ist erforderlich zur einzeitigen Rekonstruktion von glenoidalen Defekten mit der inversen Schulterprothese. Eine klinische und biomechanische Studie. DVSE; 2013; Würzburg.
21. Wall B, Nove-Josserand L, O'Connor DP, Edwards TB, Walch G. Reverse total shoulder arthroplasty: a review of results according to etiology. *The Journal of bone and joint surgery. American volume*. 2007;89(7):1476-1485.
22. Codsí MJ, Bennetts C, Gordiev K, et al. Normal glenoid vault anatomy and validation of a novel glenoid implant shape. *Journal of shoulder and elbow surgery / American Shoulder and Elbow Surgeons ... [et al.]*. 2008;17(3):471-478.
23. DiStefano JG, Park AY, Nguyen TQ, Diederichs G, Buckley JM, Montgomery WH, 3rd. Optimal screw placement for base plate fixation in reverse total shoulder arthroplasty. *Journal of shoulder and elbow surgery / American Shoulder and Elbow Surgeons ... [et al.]*. 2011;20(3):467-476.
24. Frankle MA, Teramoto A, Luo ZP, Levy JC, Pupello D. Glenoid morphology in reverse shoulder arthroplasty: classification and surgical implications. *Journal of shoulder and elbow surgery / American Shoulder and Elbow Surgeons ... [et al.]*. 2009;18(6):874-885.
25. Bhatia DN, de Beer JF, du Toit DF. Coracoid process anatomy: Implications in radiographic imaging and surgery. *Clinical Anatomy*. 2007;20(7):774-784.
26. Humphrey CS, Kelly JD, 2nd, Norris TR. Optimizing glenosphere position and fixation in reverse shoulder arthroplasty, Part Two: The three-column concept. *Journal of shoulder and elbow surgery / American Shoulder and Elbow Surgeons ... [et al.]*. 2008;17(4):595-601.
27. Samilson RL, Prieto V. Dislocation arthropathy of the shoulder. *The Journal of bone and joint surgery. American volume*. 1983;65(4):456-460.
28. Bryce CD, Pennypacker JL, Kulkarni N, et al. Validation of three-dimensional models of in situ scapulae. *Journal of shoulder and elbow surgery / American Shoulder and Elbow Surgeons ... [et al.]*. 2008;17(5):825-832.
29. Wu G, van der Helm FCT, Veeger HEJ, et al. ISB recommendation on definitions of joint coordinate systems of various joints for the reporting of human joint motion—Part II: shoulder, elbow, wrist and hand. *Journal of Biomechanics*. 2005;38(5):981-992.

30. Kwon YW, Powell KA, Yum JK, Brems JJ, Iannotti JP. Use of three-dimensional computed tomography for the analysis of the glenoid anatomy. *Journal of shoulder and elbow surgery / American Shoulder and Elbow Surgeons ... [et al.]*. 2005;14(1):85-90.
31. Wu G, van der Helm FC, Veeger HE, et al. ISB recommendation on definitions of joint coordinate systems of various joints for the reporting of human joint motion--Part II: shoulder, elbow, wrist and hand. *J Biomech*. 2005;38(5):981-992.
32. Chuang TY, Adams CR, Burkhart SS. Use of preoperative three-dimensional computed tomography to quantify glenoid bone loss in shoulder instability. *Arthroscopy : the journal of arthroscopic & related surgery : official publication of the Arthroscopy Association of North America and the International Arthroscopy Association*. 2008;24(4):376-382.
33. Saito H, Itoi E, Sugaya H, Minagawa H, Yamamoto N, Tuoheti Y. Location of the glenoid defect in shoulders with recurrent anterior dislocation. *The American journal of sports medicine*. 2005;33(6):889-893.
34. Kany J, Flamand O, Grimberg J, et al. Arthroscopic Latarjet procedure: is optimal positioning of the bone block and screws possible? A prospective computed tomography scan analysis. *Journal of shoulder and elbow surgery / American Shoulder and Elbow Surgeons ... [et al.]*. 2016;25(1):69-77.
35. Pectoral girdle, shoulder region and axilla. In: Standring S, ed. *Gray's anatomy : the anatomical basis of clinical practice* 40 ed: Churchill Livingstone/Elsevier, 2008; 2008:791-823.
36. Molony DC, Cassar Gheiti AJ, Kennedy J, Green C, Schepens A, Mullett HJ. A cadaveric model for suprascapular nerve injury during glenoid component screw insertion in reverse-geometry shoulder arthroplasty. *Journal of shoulder and elbow surgery / American Shoulder and Elbow Surgeons ... [et al.]*. 2011;20(8):1323-1327.
37. Penning R, Muller S. [Sexual dimorphism of the scapula]. *Z Rechtsmed*. 1988;101(3):183-196.
38. Scholtz Y, Steyn M, Pretorius E. A geometric morphometric study into the sexual dimorphism of the human scapula. *Homo*. 2010;61(4):253-270.
39. von Schroeder HP, Kuiper SD, Botte MJ. Osseous anatomy of the scapula. *Clinical orthopaedics and related research*. 2001(383):131-139.
40. Alobaidy MA, Soames RW. Evaluation of the coracoid and coracoacromial arch geometry on Thiel-embalmed cadavers using the three-dimensional MicroScribe digitizer. *Journal of shoulder and elbow surgery / American Shoulder and Elbow Surgeons ... [et al.]*. 2015.
41. Huang R, Zhi Q, Patel K, Wilting J, Christ B. Dual origin and segmental organisation of the avian scapula. *Development*. 2000;127(17):3789-3794.
42. Voisin JL, Ropars M, Thomazeau H. The human acromion viewed from an evolutionary perspective. *Orthopaedics & traumatology, surgery & research : OTSR*. 2014;100(8 Suppl):S355-360.
43. Williams PL BL, Berry MM, Collins P, Dyson M, Dussek JE, MWJ. F. *Skeletal System:Scapula*. In: Williams PL, Bannister LH BM, Collins P, Dyson M, Dussek JE, Ferguson, MWJ, eds. *Grays Anatomy*. 38 ed: Churchill Livingstone; 1995.
44. Scheuer LB, S. *Pectoral Girdle*. In: Scheuer LB, S, ed. *Developmental Juvenile Osteology*. 1 ed: Elsevier; 2000:252-271.
45. Hodges P. An epiphyseal chart. *American Journal of Roentgenology*. 1933;30:809-810.

46. Anetzberger H, Putz R. The scapula: principles of construction and stress. *Acta Anat (Basel)*. 1996;156(1):70-80.
47. Mallon WJ, Brown HR, Vogler JB, 3rd, Martinez S. Radiographic and geometric anatomy of the scapula. *Clinical orthopaedics and related research*. 1992(277):142-154.
48. Stephens BF, Hebert CT, Azar FM, Mihalko WM, Throckmorton TW. Optimal baseplate rotational alignment for locking-screw fixation in reverse total shoulder arthroplasty: a three-dimensional computer-aided design study. *Journal of shoulder and elbow surgery / American Shoulder and Elbow Surgeons ... [et al.]*. 2015;24(9):1367-1371.

Chapter 5- General Discussion and Conclusion

Overview: *This chapter evaluates the objectives and findings of our research. The strengths and limitations are addressed. Better understanding of the scapular morphology and its impact on future implant design is discussed.*

5.1 SUMMARY

Shoulder arthroplasty has experienced an exponential rise in numbers since the last decade. After hip and knee arthroplasty it is the most common joint replacement performed worldwide. The current Grammont concept Reverse Shoulder Arthroplasty (RSA) is entering its third decade of use. The primary total shoulder arthroplasty (TSA) and RSA is entering a new era, whereby patients are requiring revision of their primary arthroplasty. As our understanding of the biomechanics and long term complications of TSA and RSA improves; the orthopaedic community is faced with new challenges which revision shoulder arthroplasty poses. Aseptic glenoid component loosening in a TSA remains the most common cause for revision and failure (infections excluded). Prosthesis notching in a standard 155 degree RSA design is common and leads to varying degrees of glenoid bone loss. Deficiency of glenoid bone stock is emerging as a significant clinical problem. Poor glenoid host bone stock is a relative contra indication for TSA and in severe bone loss primary baseplate fixation for a RSA remains a problem.

The current clinical orthopaedic literature illustrates the native glenoid for estimation of joint kinematics and implant positioning. Reference systems currently used (Scapular plane) utilise the glenoid to estimate the amount of bone loss and guide implant positioning. Estimation of the scapular plane in the presence of loss of glenoid bone stock is inaccurate and often not possible.

Chapter 2 focused on development of a scapular co-ordinate system independent of the glenoid morphology. The International Society of Biomechanics (ISB) has reported on the ISB scapular plane to define shoulder joint kinematics. ISB believes that the glenohumeral joint kinematics cannot be studied independent of the contribution of the scapula thoracic, acromio clavicular and sterno clavicular movements. In the chapter we compared the scapular plane used by the clinicians with the New ISB and Old ISB planes. Our study demonstrated that there is a constant relationship between the two coordinate systems; scapular plane vs ISB. Also this relationship is independent of the

sexual dimorphism which exists between male and female scapulae. This is one of the first studies of its kind whereby a relationship between the various scapular co-ordinate systems has been found. Thus a co-ordinate system independent of the glenoid morphology can be reliably used to guide implant positioning.

Chapter 3 analysed the anthropometric measurements of normal scapulae to evaluate the gender dimorphism and size of the scapular body and glenoid. Studies have highlighted that even though the scapular body and glenoid are part of the scapula they develop quite independent of each other. More importantly the development of the glenoid and scapular body from infancy to adulthood follows very different physiologic processes. Thus in fact these two parts of the same bone are 2 distinct units. This might explain the why as postulated by the ISB the scapular body has a much more important role to play in GH kinematics than previously thought. Our study found significant differences in the morphology of the male and female scapular body and glenoid. This has been reported by other authors as well. However, our study compared the true and apparent heights of the scapular body and we found that the true height of the scapular body is 17.79 mm longer than the apparent height reported by other similar studies. In this chapter we attempted to calculate the glenoid dimensions from the scapular body dimensions by using linear regression. However, this yielded a R^2 value of 0.04 for males and 0.07 for females. Our study has demonstrated that the glenoid and scapular body develop differently and the glenoid dimensions cannot be reliably predicted by the scapular body size alone.

The main underlying objective of this thesis is to establish methods to securely fix the glenoid baseplate for a RSA onto a deficient glenoid. Chapter 2 has demonstrated that an alternate co-ordinate system can be used to guide the baseplate position and chapter 3 establishes the appropriate size of the implant and bone graft can be estimated by the gender of the patient and templating the contralateral shoulder if available. The aim of chapter 4 was to find regions of best bone stock for fixation of the baseplate or baseplate bone graft construct beyond the glenoid vault. Other studies have looked at screw trajectories beyond the vault to provide dense bone for rigid fixation of the baseplate. In our study we have defined the position of the three columns of the scapula with respect

to the glenoid face (Superior Inferior glenoid axis) our findings are supported by the recent literature. In addition, we have described the relationship of each column with respect to each other. Our study has demonstrated that there is significant sexual dimorphism between the male and the female scapulae and this impacts the relative position of each column. This has a bearing on the screw trajectories for baseplate fixation of as RSA.

The body of knowledge associated with our understanding of the scapular anatomy and its clinical implications for shoulder arthroplasty has been improved by fulfilling the objectives of this thesis. Better understanding of the relationship of biomechanics of the GHJ and the Scapulo- Thoracic articulation has been highlighted in the use of the ISB axis to implant a RSA baseplate. This beckons the surgeon to widen their horizon and look beyond the glenoid to attain accurate baseplate positioning. The knowledge disseminated from the published articles of this thesis may lead the path for the development of implants which accurately match the patient's anatomy. Accurate implant positing tailored to each individual's anatomy and biomechanics may lead to better functional results and a longer overall prosthesis survival.

5.2 STRENGTHS AND LIMITATIONS

An important strength of this work is the relatively large patient cohort. 50 cadaveric patients were analysed. Evaluation of a larger patient cohort allows for more robust conclusions based on accurate characterization of bone morphology. This increases the clinical relevance and the ability to positively impact surgical technique and implant positioning.

Another strength of this thesis lies in the utilisation of 3D computer modelling using Mimics®. Creation of virtual bone models permits accurate delineation of anatomical

reference points. In addition, using standardized segmentation techniques and thresholding set above 200 HU minimises soft tissue and cartilaginous artefact further enhancing the accuracy of measurement. All the measurements were carried out using custom code developed in MatLab ® this allows for precise anthropometric measurements which were carried out using standardised reference planes.

Another strength of this thesis lies in the incorporation of knowledge from various fields of medical and engineering literature. The embryology and anatomy of the scapula has been studied in detail to better understand its development. This has helped us understand the different process for developmental of the scapular body and the glenoid and explains the significant of sexual dimorphism that exists. Further incorporation of this knowledge and pairing it with the biomechanical literature highlights the importance of understanding the movement of the scapula as a whole to predict GHJ motion. Incorporation of these findings to the realm of clinical orthopaedics guides us towards more accurate placement of implants with the overall aim of improving patient outcomes.

A limitation of this thesis is that most of the cadavers were of Caucasian and African American origin. Anthropometric measurements may vary considerably in patients of different races and the results of the studies should be applied to patients of other races with caution. However estimation of the scapular axis has been shown to be independent of sexual dimorphism.

5.3 FUTURE DIRECTION

The studies completed in this thesis have highlighted some key issues. The aim of this thesis was to develop tools to help the orthopaedic surgeon successfully perform a RSA in the setting of glenoid bone loss. Firstly chapter 2 has highlighted that reliance on the scapular plane to position a baseplate may suffice in a normal glenoid however the scapular plane cannot be recreated if there is volumetric loss of the glenoid vault. Thus the New ISB plane should be utilised for calculation of implant positioning. Utilization of this plane is critical for baseplate positioning in glenoid vault deficiency. The current industry standards utilise the scapular plane for navigation and patient specific implant guides. The body of knowledge from this thesis beckons the development of navigation software and patient guides which utilise the New ISB.

Anthropometric measurements demonstrate significant size variations between the male and female glenoid face. Size variations are well understood in the orthopaedic implant industry thus a plethora of sizing options exist to match patient anatomy for hip and knee arthroplasty. Shoulder arthroplasty has not seen a change in sizing of the baseplate. Most implant companies still manufacture either a 28 mm or a 25 mm baseplate. This is often insufficient to match the patient's anatomy. Thus the results of chapter 3 beckon the future development of a range of glenoid baseplate sizes which would match different patient characteristics. This would enable better implant host bone contact and avoid under reaming or over reaming of the glenoid thereby improving implant survival. Secondly an appropriately sized baseplate will enable the surgeon to attain screw purchase in the scapular columns. Significant baseplate and native glenoid size mismatch leads to significant alteration of the screw trajectories.

Lastly chapter 4 has highlighted the need for modification of the current baseplate design. The current screw configurations are insufficient to attain adequate screw purchase in the three scapular columns. Based upon the results of this paper modification of the screw hole position will enable better screw trajectories and enable the surgeon to attain fixation of a baseplate beyond the glenoid vault.

Improved understanding of the internal cancellous bone density characteristics in each of the 3 scapular columns needs to be evaluated. Improved understanding of the volumetric analysis of bone stock in these columns will enable multiple screw to be inserted. This would further lead to changes in the baseplate design for revision RSA. This analysis was beyond the scope of this thesis but lends itself to future studies.

The thesis has highlighted the importance of the scapular body in shoulder biomechanics. Thus it is imperative that further studies are carried out to understand the positioning of the scapula in a patient with GHJ pathology. Future research may indicate specific patterns of scapular dyskinesia which could help us understand the reason behind various patterns for glenoid bone erosion.

5.4 CONCLUSION

The work presented in this thesis demonstrates that the New ISB and Old ISB has a constant relationship with the scapular plane and can be reliably utilised to guide implant positioning (Chapter2). The different pathway of development of the scapular body and the glenoid highlighted in chapter 1 is further highlighted by the inability to predict the glenoid size by utilizing the scapular body measurements (Chapter3). Further considerable differences in size of the scapula body and the glenoid face has been demonstrated, between males and females. Sexual dimorphism is further highlighted in the relative position of the 3 columns of the scapula. Chapter 4 has highlighted that in the female scapula the coracoid and the inferior scapular column are closer together. The relationship between the acromial spine and coracoid is relatively constant amongst males and females however variation in anatomy exists in respect to the inferior part of the glenoid. This has important ramifications for screw trajectories to fix a baseplate in a RSA.

Appendix A – Scapular Co-Ordinate System Data Analysis

Figure A-1 Relationship between the Scapular Plane and the New ISB and Old ISB Axis (Degrees).

| Rt0/Lt 1 | Sex | Age | Height | New_ISB_Angle (Degrees) | Old_ISB_Angle (Degrees) |
|-----------------|-------------|------------|---------------|------------------------------------|------------------------------------|
| 0 | Male | 58 | 70 | 16.15 | 1.85 |
| 0 | Male | 62 | 66 | 16.32 | 1.92 |
| 1 | Male | 92 | 73 | 19.45 | 0.84 |
| 1 | Male | 87 | 66 | 20.09 | -3.24 |
| 0 | Male | 81 | 73 | 16.11 | -2.58 |
| 1 | Male | 77 | 66 | 17.92 | -1.53 |
| 1 | Male | 88 | 66 | 17.63 | -2.28 |
| 1 | Male | 75 | 70 | 14.36 | 2.07 |
| 0 | Male | 77 | 69 | 17.74 | -2.06 |
| 0 | Male | 71 | 66 | 18.17 | -0.44 |

| | | | | New_ISB_Angle | Old_ISB_Angle |
|-----------------|------------|------------|---------------|----------------------|----------------------|
| Rt0/Lt 1 | Sex | Age | Height | (Degrees) | (Degrees) |
| 0 | Male | 57 | 72 | 15.36 | -1.98 |
| 0 | Male | 73 | 69 | 13.12 | 2.67 |
| 1 | Male | 82 | 65 | 19.27 | -2.38 |
| 0 | Male | 69 | 70 | 17.14 | -3.59 |
| 0 | Male | 80 | 71 | 18.38 | -0.12 |
| 0 | Male | 84 | 66.5 | 17.62 | -3.58 |
| 0 | Male | 62 | 68 | 17.23 | -0.77 |
| 1 | Male | 76 | 68 | 15.55 | 2.97 |
| 0 | Male | 70 | 73 | 18.27 | -5.13 |
| 1 | Male | 55 | 71 | 18.8 | -2.42 |
| 0 | Male | 56 | 73 | 19.02 | -3.55 |
| 1 | Male | 21 | 74 | 15.14 | 2.94 |
| 0 | Male | 91 | 67 | 17.64 | -2.03 |
| 0 | Male | 81 | 75 | 19.07 | -4.26 |
| 1 | Male | 64 | 71 | 17.86 | -3.64 |
| 1 | Female | 76 | 64 | 20.31 | -1.2 |
| 1 | Female | 49 | 67 | 19.46 | -1.61 |
| | | | | | |

| Rt0/Lt 1 | Sex | Age | Height | New_ISB_Angle (Degrees) | Old_ISB_Angle (Degrees) |
|-----------------|---------------|------------|---------------|------------------------------------|------------------------------------|
| 1 | Female | 77 | 64 | 13.82 | -0.94 |
| 0 | Female | 69 | 60 | 14.81 | -0.15 |
| 0 | Female | 47 | 66 | 15.59 | -0.68 |
| 0 | Female | 66 | 62 | 17.32 | -2.69 |
| 0 | Female | 74 | 55 | 14.71 | -1.1 |
| 0 | Female | 55 | 64 | 14.78 | 0.15 |
| 0 | Female | 70 | 64 | 15.86 | -2.84 |
| 1 | Female | 87 | 62 | 17.08 | -1.4 |
| 1 | Female | 64 | 63 | 11.94 | 0.95 |
| 1 | Female | 68 | 65 | 18.3 | -2.69 |
| 1 | Female | 63 | 62 | 16.14 | 2.01 |
| 1 | Female | 75 | 65 | 14.79 | -1.51 |
| 1 | Female | 76 | 64 | 20.44 | -6.99 |
| 1 | Female | 65 | 65 | 15.85 | -2.22 |
| 1 | Female | 66 | 67 | 15.55 | -2.02 |
| 1 | Female | 62 | 62 | 18.11 | -3.03 |
| 1 | Female | 58 | 66 | 16.33 | -1.51 |

| Rt0/Lt 1 | Sex | Age | Height | New_ISB_Angle (Degrees) | Old_ISB_Angle (Degrees) |
|-----------------|---------------|--------------------|--------------------|------------------------------------|------------------------------------|
| 1 | Female | 91 | 58 | 17.82 | -1.19 |
| 1 | Female | 94 | 63 | 16.63 | -3.16 |
| 1 | Female | 68 | 64 | 19.95 | -3.8 |
| 1 | Female | 72 | 64 | 21.48 | -3.76 |
| 1 | Female | 88 | 60 | 13.92 | 2.91 |
| 0 | Female | 49 | 65 | 16.8 | 1.51 |
| Average | | 70.36 | 66.39 | 17.024 | -1.3456 |
| SD | | 13.90457273 | 4.270556528 | 2.056679511 | 2.25828557 |
| Average | | 71.56 | 69.54 | 17.3364 | -1.2128 |
| SD | | 15.3136105 | 2.992769063 | 1.708015125 | 2.460027981 |
| Average | | 69.16 | 63.24 | 16.7116 | -1.4784 |
| SD | | 12.53887289 | 2.758018612 | 2.348504276 | 2.079356231 |

Appendix B – Scapular Anthropometric Measurements and Data Analysis

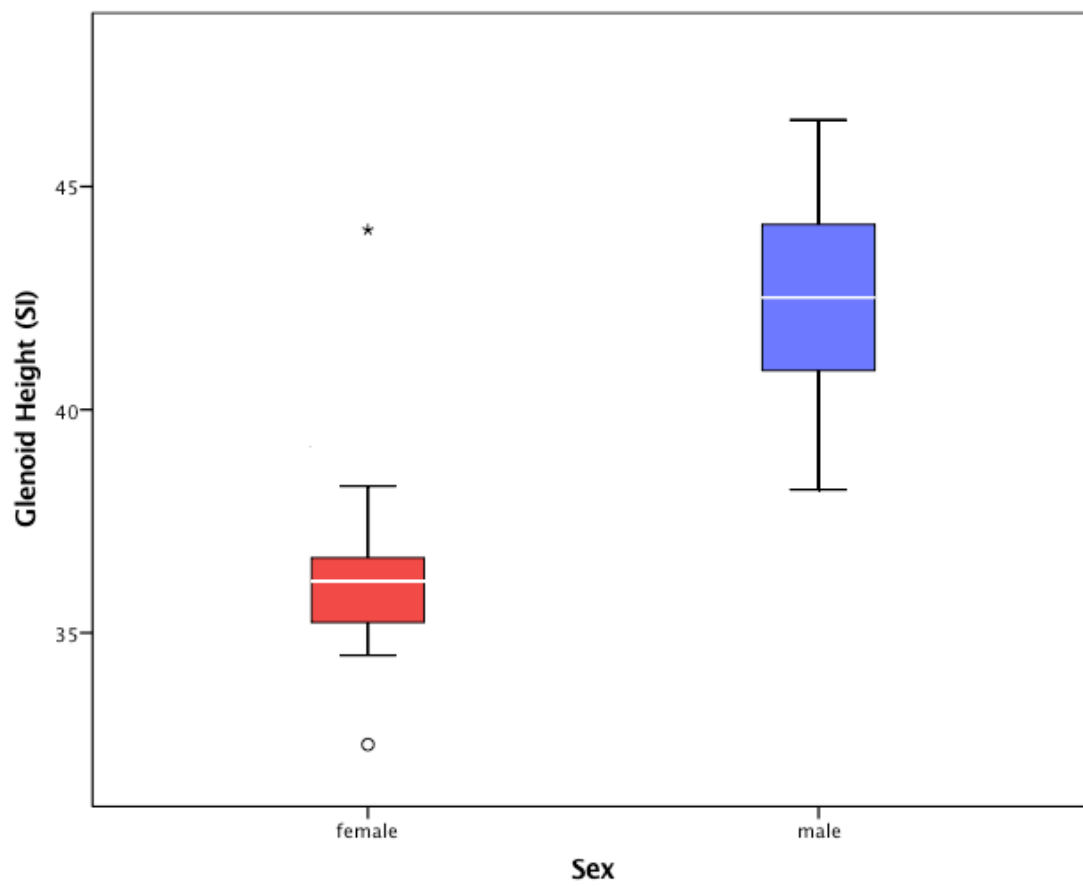


Figure B.1 Glenoid Height measurement in Females and Males

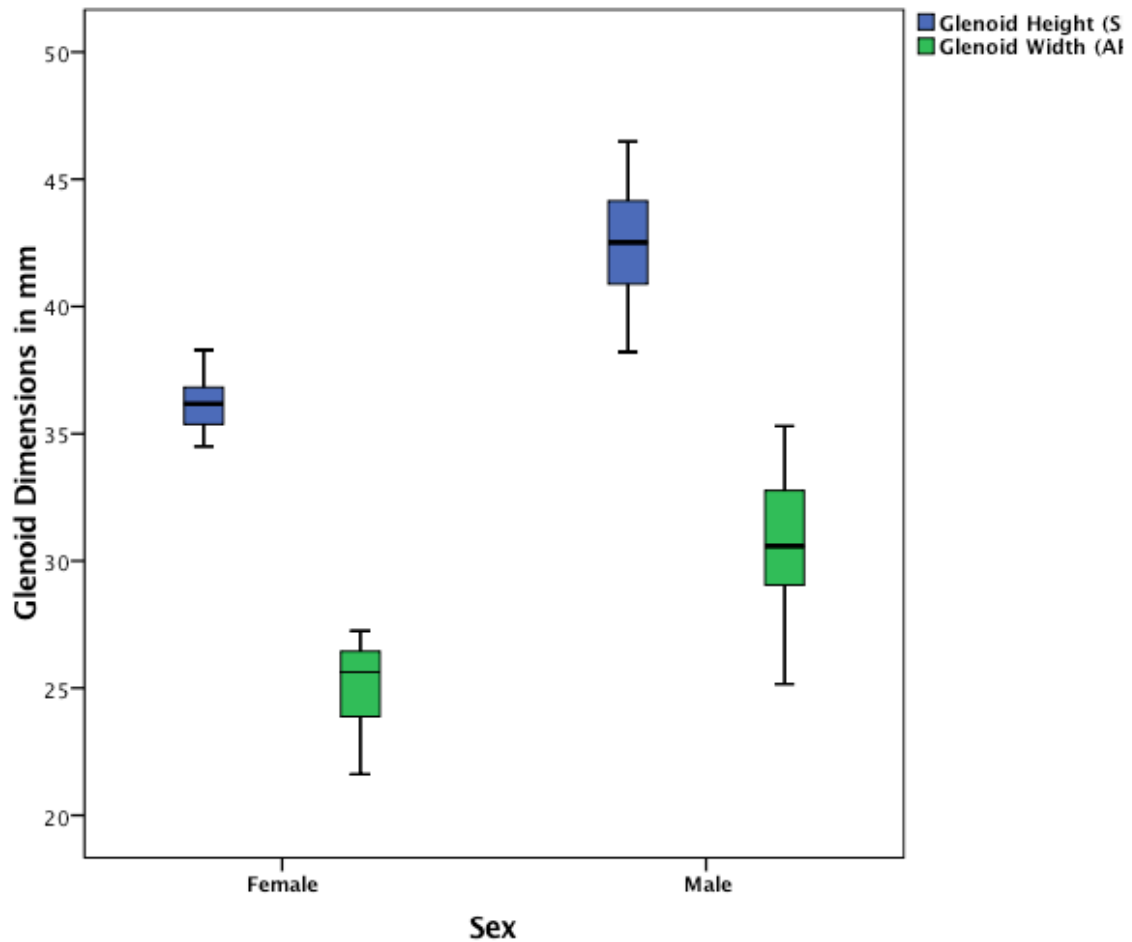


Figure B.2A Glenoid Measurements in Females and Males

Glenoid Height = Distance between the Superior Glenoid Tubercle and the 6 O'Clock Point on the Inferior Glenoid Rim.

Glenoid Width = Maximum distance between the Anterior and the Posterior Glenoid Rim measured Perpendicular to the SI Axis of the Glenoid (FigureB-3)

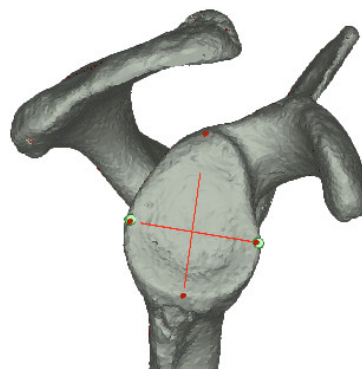


Figure B.2B

| Group Statistics | | | | | |
|-------------------------|-----|----|-------------------------|-------------------------|-----------------------|
| | Sex | N | Mean | Std. Deviation | Std. Error Mean |
| Glenoid Height (SI) | 0 | 25 | 36.3812400 00000000 | 2.10305906 7000000 | .420611813 000000 |
| | 1 | 25 | 42.4688400 00000000 | 2.14316297 9000000 | .428632596 000000 |
| Glenoid Width (AP) | 0 | 25 | 25.3660800 00000000 | 2.35719312 1000000 | .471438624 000000 |
| | 1 | 25 | 30.7712800 00000000 | 2.73244343 5000000 | .546488687 000000 |
| AB Length | 0 | 25 | 41.9554400 00000000 | 6.88143007 8000000 | 1.37628601 6000000 |
| | 1 | 25 | 56.6612400 00000000 | 13.8316239 20000000 | 2.76632478 3000000 |
| BC Length | 0 | 25 | 112.239319 999999990 | 8.67431448 2000000 | 1.73486289 6000000 |
| | 1 | 25 | 126.745120 000000000 | 15.7204943 300000001 | 3.14409886 6000000 |
| AC Length | 0 | 25 | 138.614800 000000000 | 9.49294480 1000000 | 1.89858896 0000000 |
| | 1 | 25 | 165.614800 000000000 | 11.5785193 10000000 | 2.31570386 1000000 |
| Medial-Lateral Length | 0 | 25 | 99.5916400 000000000 | 4.86963326 7000000 | .973926653 000000 |
| | 1 | 25 | 114.523199 999999990 | 6.09054234 00000001 | 1.21810846 8000000 |

| | | | | | |
|-------------------|---|----|-------------------------|------------------------|-----------------------|
| v_AB - v_BC Angle | 0 | 25 | 58.6835600 00000000 | 9.06836212 3000000 | 1.81367242 5000000 |
| | 1 | 25 | 56.1055600 00000004 | 6.44416078 1000001 | 1.28883215 6000000 |
| SUM (AB, BC) | 0 | 25 | 154.194760 00000000 | 10.9239893 90000001 | 2.18479787 7000000 |
| | 1 | 25 | 183.406359 999999980 | 13.4359045 70000000 | 2.68718091 3000000 |

Figure B.3 Anthropometric measurements of the Scapula and Glenoid

Sex 0= Female, 1= Male

AB = Length of the Medial Scapular Border between the Superior Scapular Point (SSP) and the Medial Scapular Point (MSP)

BC= Length of the Medial Scapular Border between the MSP and the Inferior Scapular Point (ISP)

AC= Apparent Scapular Height between the SSP and ISP

AB+ BC= True Scapular Height

Medio-Lateral Length of the Scapula= Distance between the MSP and the Glenoid Center Point (GC)

Analysis of Data and Correlations Of The Whole Cohort (Male and Females Combined)

| | | Correlations | | | | | | |
|-----------------------|---------------------|---------------------|--------------------|-----------|-----------|-----------|-----------------------|--------------|
| | | Glenoid Height (SI) | Glenoid Width (AP) | AB Length | BC Length | AC Length | Medial-Lateral Length | SUM (AB, BC) |
| Glenoid Height (SI) | Pearson Correlation | 1 | .821** | .505** | .493** | .737** | .744** | .722** |
| | Sig. (2-tailed) | | .000 | .000 | .000 | .000 | .000 | .000 |
| | N | 50 | 50 | 50 | 50 | 50 | 50 | 50 |
| Glenoid Width (AP) | Pearson Correlation | .821** | 1 | .600** | .425** | .756** | .793** | .736** |
| | Sig. (2-tailed) | .000 | | .000 | .002 | .000 | .000 | .000 |
| | N | 50 | 50 | 50 | 50 | 50 | 50 | 50 |
| AB Length | Pearson Correlation | .505** | .600** | 1 | -.050 | .665** | .760** | .649** |
| | Sig. (2-tailed) | .000 | .000 | | .730 | .000 | .000 | .000 |
| | N | 50 | 50 | 50 | 50 | 50 | 50 | 50 |
| BC Length | Pearson Correlation | .493** | .425** | -.050 | 1 | .681** | .344* | .727** |
| | Sig. (2-tailed) | .000 | .002 | .730 | | .000 | .015 | .000 |
| | N | 50 | 50 | 50 | 50 | 50 | 50 | 50 |
| AC Length | Pearson Correlation | .737** | .756** | .665** | .681** | 1 | .816** | .976** |
| | Sig. (2-tailed) | .000 | .000 | .000 | .000 | | .000 | .000 |
| | N | 50 | 50 | 50 | 50 | 50 | 50 | 50 |
| Medial-Lateral Length | Pearson Correlation | .744** | .793** | .760** | .344* | .816** | 1 | .784** |
| | Sig. (2-tailed) | .000 | .000 | .000 | .015 | .000 | | .000 |
| | N | 50 | 50 | 50 | 50 | 50 | 50 | 50 |
| SUM (AB, BC) | Pearson Correlation | .722** | .736** | .649** | .727** | .976** | .784** | 1 |
| | Sig. (2-tailed) | .000 | .000 | .000 | .000 | .000 | .000 | |
| | N | 50 | 50 | 50 | 50 | 50 | 50 | 50 |

** . Correlation is significant at the 0.01 level (2-tailed).
* . Correlation is significant at the 0.05 level (2-tailed).

Figure B.4 Pearson Correlation Coefficients demonstrating Good correlation between the various measurements when male and female data is combined.

Tests of Normality

| | Kolmogorov-Smirnov ^a | | | Shapiro-Wilk | | |
|-----------------------|---------------------------------|----|-------------------|--------------|----|------|
| | Statistic | df | Sig. | Statistic | df | Sig. |
| Glenoid Height (SI) | .143 | 50 | .012 | .939 | 50 | .012 |
| Glenoid Width (AP) | .130 | 50 | .034 | .960 | 50 | .092 |
| AB Length | .164 | 50 | .002 | .890 | 50 | .000 |
| BC Length | .087 | 50 | .200 [*] | .969 | 50 | .210 |
| AC Length | .089 | 50 | .200 [*] | .967 | 50 | .168 |
| Medial-Lateral Length | .117 | 50 | .083 | .969 | 50 | .208 |
| v_AB - v_BC Angle | .084 | 50 | .200 [*] | .977 | 50 | .435 |
| SUM (AB, BC) | .084 | 50 | .200 [*] | .967 | 50 | .176 |

*. This is a lower bound of the true significance.

a. Lilliefors Significance Correction

Figure B.5 Tests of Normality to assess distribution of the data

Analysis of Data and Correlations Of The Whole Cohort (Male and Females Combined)

| | | | Correlations | | | | | | |
|----------------|-----------------------|-------------------------|---------------------|--------------------|-----------|-----------|-----------|-----------------------|--------------|
| | | | Glenoid Height (SI) | Glenoid Width (AP) | AB Length | BC Length | AC Length | Medial-Lateral Length | SUM (AB, BC) |
| Spearman's rho | Glenoid Height (SI) | Correlation Coefficient | 1.000 | .787** | .563** | .507** | .750** | .715** | |
| | | Sig. (2-tailed) | . | .000 | .000 | .000 | .000 | .000 | |
| | | N | 50 | 50 | 50 | 50 | 50 | 50 | |
| | Glenoid Width (AP) | Correlation Coefficient | .787** | 1.000 | .577** | .448** | .766** | .796** | |
| | | Sig. (2-tailed) | .000 | . | .000 | .001 | .000 | .000 | |
| | | N | 50 | 50 | 50 | 50 | 50 | 50 | |
| | AB Length | Correlation Coefficient | .563** | .577** | 1.000 | .131 | .735** | .735** | |
| | | Sig. (2-tailed) | .000 | .000 | . | .364 | .000 | .000 | |
| | | N | 50 | 50 | 50 | 50 | 50 | 50 | |
| | BC Length | Correlation Coefficient | .507** | .448** | .131 | 1.000 | .655** | .396** | |
| | | Sig. (2-tailed) | .000 | .001 | .364 | . | .000 | .004 | |
| | | N | 50 | 50 | 50 | 50 | 50 | 50 | |
| | AC Length | Correlation Coefficient | .750** | .766** | .735** | .655** | 1.000 | .849** | |
| | | Sig. (2-tailed) | .000 | .000 | .000 | .000 | . | .000 | |
| | | N | 50 | 50 | 50 | 50 | 50 | 50 | |
| | Medial-Lateral Length | Correlation Coefficient | .750** | .796** | .735** | .396** | .849** | 1.000 | |
| | | Sig. (2-tailed) | .000 | .000 | .000 | .004 | .000 | . | |
| | | N | 50 | 50 | 50 | 50 | 50 | 50 | |
| | SUM (AB, BC) | Correlation Coefficient | .715** | .731** | .737** | .707** | .974** | .804** | |
| | | Sig. (2-tailed) | .000 | .000 | .000 | .000 | .000 | .000 | |
| | | N | 50 | 50 | 50 | 50 | 50 | 50 | |

** . Correlation is significant at the 0.01 level (2-tailed).

Figure B.6 Spearman's Rho Correlation Coefficients (for Non Parametric Data) demonstrating Good correlation between the various measurements when male and female data is combined.

Subgroup Analysis of Data and Correlations between Males and Females

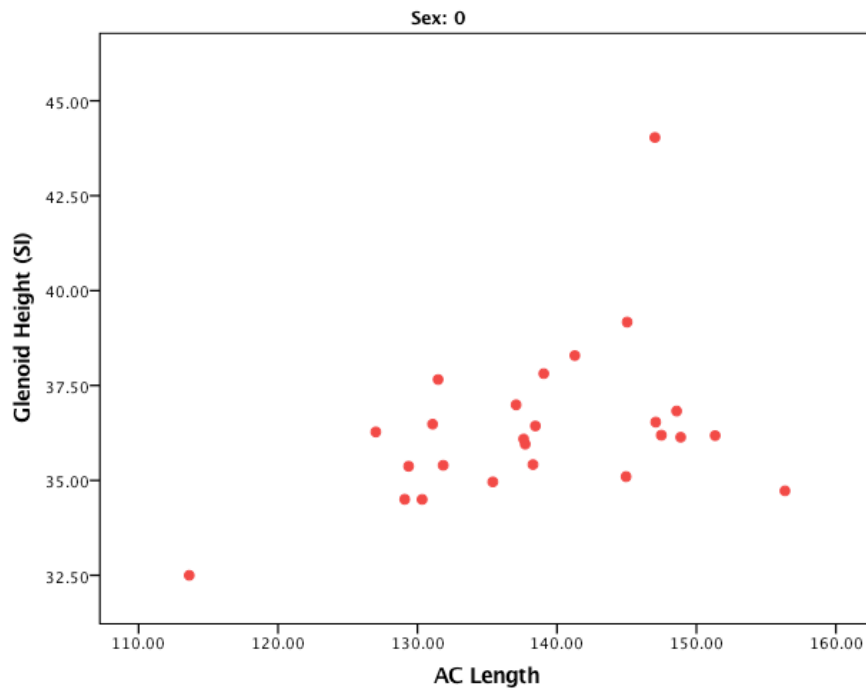


Figure B.7 Scatter Plot Demonstrating Poor Correlation Between Apparent Scapular Height (AC Length) and Glenoid Height in Females

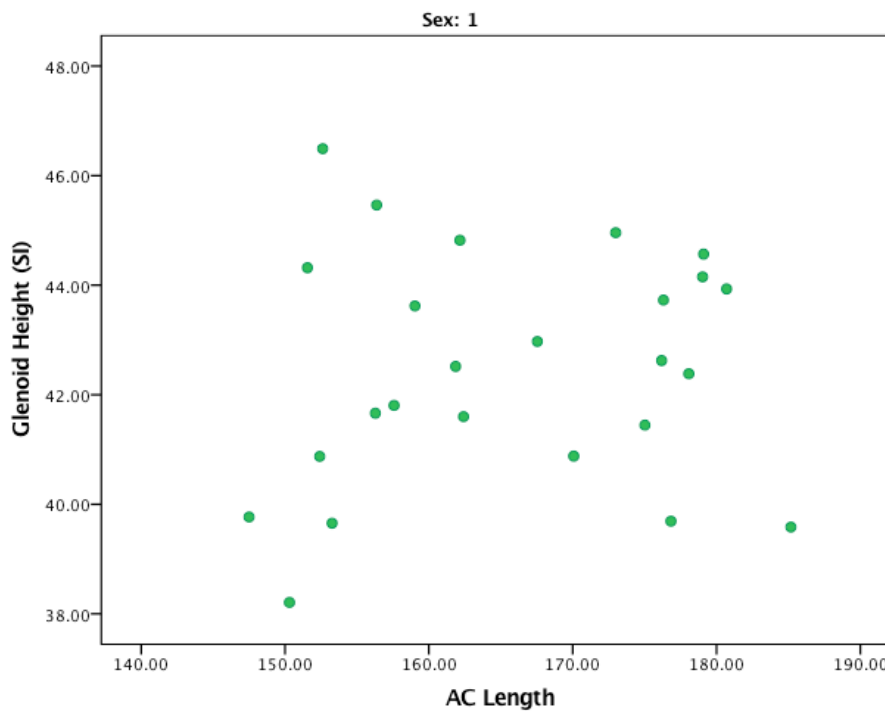


Figure B.8 Scatter Plot Demonstrating Poor Correlation Between Apparent Scapular Height (AC Length) and Glenoid Height in Males

Regression Analysis – Prediction of Glenoid Height by the Apparent Scapular Height(AC)

| Regression | | | | | | |
|--|------------------------|-----------------------------|-------------------|----------------------------|--------|-------------------|
| Variables Entered/Removed^a | | | | | | |
| Model | Variables Entered | Variables Removed | Method | | | |
| 1 | AC Length ^b | . | Enter | | | |
| a. Dependent Variable: Glenoid Height (SI) | | | | | | |
| b. All requested variables entered. | | | | | | |
| Model Summary | | | | | | |
| Model | R | R Square | Adjusted R Square | Std. Error of the Estimate | | |
| 1 | .737 ^a | .543 | .533 | 2.54423474 | | |
| a. Predictors: (Constant), AC Length | | | | | | |
| ANOVA^a | | | | | | |
| Model | | Sum of Squares | df | Mean Square | F | Sig. |
| 1 | Regression | 368.910 | 1 | 368.910 | 56.991 | .000 ^b |
| | Residual | 310.710 | 48 | 6.473 | | |
| | Total | 679.620 | 49 | | | |
| a. Dependent Variable: Glenoid Height (SI) | | | | | | |
| b. Predictors: (Constant), AC Length | | | | | | |
| Coefficients^a | | | | | | |
| Model | | Unstandardized Coefficients | | Standardized Coefficients | t | Sig. |
| | | B | Std. Error | Beta | | |
| 1 | (Constant) | 15.156 | 3.235 | | 4.685 | .000 |
| | AC Length | .160 | .021 | .737 | 7.549 | .000 |
| a. Dependent Variable: Glenoid Height (SI) | | | | | | |

Figure B.9 Regression Equation Glenoid Height = Constant + Slope x Value of Predictor is used to calculate (Glenoid Height = 15.156 + 0.160 X Apparent Scapular Height)

Regression Analysis – Prediction of Glenoid Height by the True Scapular Height (AB + BC)

| Regression | | | | | | |
|--|---------------------------|-------------------|--------|--|--|--|
| Variables Entered/Removed^a | | | | | | |
| Model | Variables Entered | Variables Removed | Method | | | |
| 1 | SUM (AB, BC) ^b | . | Enter | | | |

a. Dependent Variable: Glenoid Height (SI)
b. All requested variables entered.

| Model Summary | | | | |
|----------------------|-------------------|----------|-------------------|----------------------------|
| Model | R | R Square | Adjusted R Square | Std. Error of the Estimate |
| 1 | .722 ^a | .522 | .512 | 2.60217367 |

a. Predictors: (Constant), SUM (AB, BC)

| ANOVA^a | | | | | | |
|--------------------------|------------|----------------|----|-------------|--------|-------------------|
| Model | | Sum of Squares | df | Mean Square | F | Sig. |
| 1 | Regression | 354.597 | 1 | 354.597 | 52.368 | .000 ^b |
| | Residual | 325.023 | 48 | 6.771 | | |
| | Total | 679.620 | 49 | | | |

a. Dependent Variable: Glenoid Height (SI)
b. Predictors: (Constant), SUM (AB, BC)

| Coefficients^a | | | | | | |
|---------------------------------|--------------|-----------------------------|------------|---------------------------|-------|------|
| Model | | Unstandardized Coefficients | | Standardized Coefficients | t | Sig. |
| | | B | Std. Error | Beta | | |
| 1 | (Constant) | 15.642 | 3.307 | | 4.730 | .000 |
| | SUM (AB, BC) | .141 | .019 | .722 | 7.237 | .000 |

a. Dependent Variable: Glenoid Height (SI)

Figure B.10 Regression Equation $\text{Glenoid Height} = \text{Constant} + \text{Slope} \times \text{Value of Predictor}$ is used to calculate $(\text{Glenoid Height} = 15.642 + 0.141 \times \text{True Scapular Height})$

Regression Analysis – Prediction of Glenoid Width by the Apparent Scapular Height(AC)

| Regression | | | | | | |
|--|------------------------|-----------------------------|-------------------|----------------------------|--------|-------------------|
| Variables Entered/Removed^a | | | | | | |
| Model | Variables Entered | Variables Removed | Method | | | |
| 1 | AC Length ^b | . | Enter | | | |
| a. Dependent Variable: Glenoid Width (AP) | | | | | | |
| b. All requested variables entered. | | | | | | |
| Model Summary | | | | | | |
| Model | R | R Square | Adjusted R Square | Std. Error of the Estimate | | |
| 1 | .756 ^a | .571 | .563 | 2.45977428 | | |
| a. Predictors: (Constant), AC Length | | | | | | |
| ANOVA^a | | | | | | |
| Model | | Sum of Squares | df | Mean Square | F | Sig. |
| 1 | Regression | 387.321 | 1 | 387.321 | 64.015 | .000 ^b |
| | Residual | 290.423 | 48 | 6.050 | | |
| | Total | 677.745 | 49 | | | |
| a. Dependent Variable: Glenoid Width (AP) | | | | | | |
| b. Predictors: (Constant), AC Length | | | | | | |
| Coefficients^a | | | | | | |
| Model | | Unstandardized Coefficients | | Standardized Coefficients | t | Sig. |
| | | B | Std. Error | Beta | | |
| 1 | (Constant) | 3.201 | 3.127 | | 1.024 | .311 |
| | AC Length | .163 | .020 | .756 | 8.001 | .000 |
| a. Dependent Variable: Glenoid Width (AP) | | | | | | |

Figure B.11 Regression Equation Glenoid Width = Constant + Slope x Value of Predictor is used to calculate (Glenoid Width = 3.2 + 0.163 X Apparent Scapular Height)

Regression Analysis – Prediction of Glenoid Width by the True Scapular Height (AB+ BC)

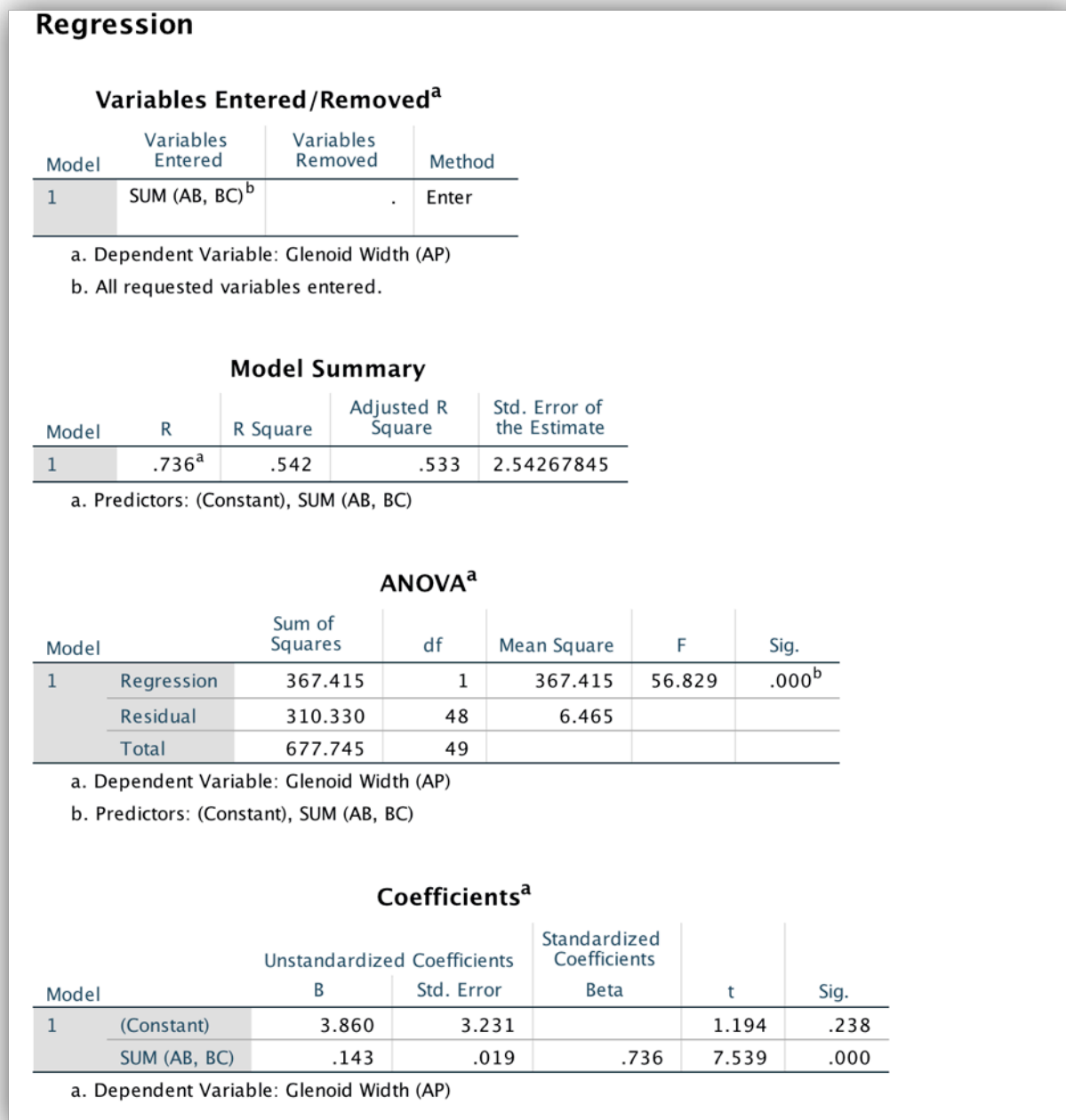


Figure B.12 Regression Equation Glenoid Width = Constant + Slope x Value of Predictor is used to calculate (Glenoid Width = 3.86 + 0.143 X True Scapular Height)

Regression Analysis – Prediction of Glenoid Height by Height of the Superior Border of the Scapula (AB)

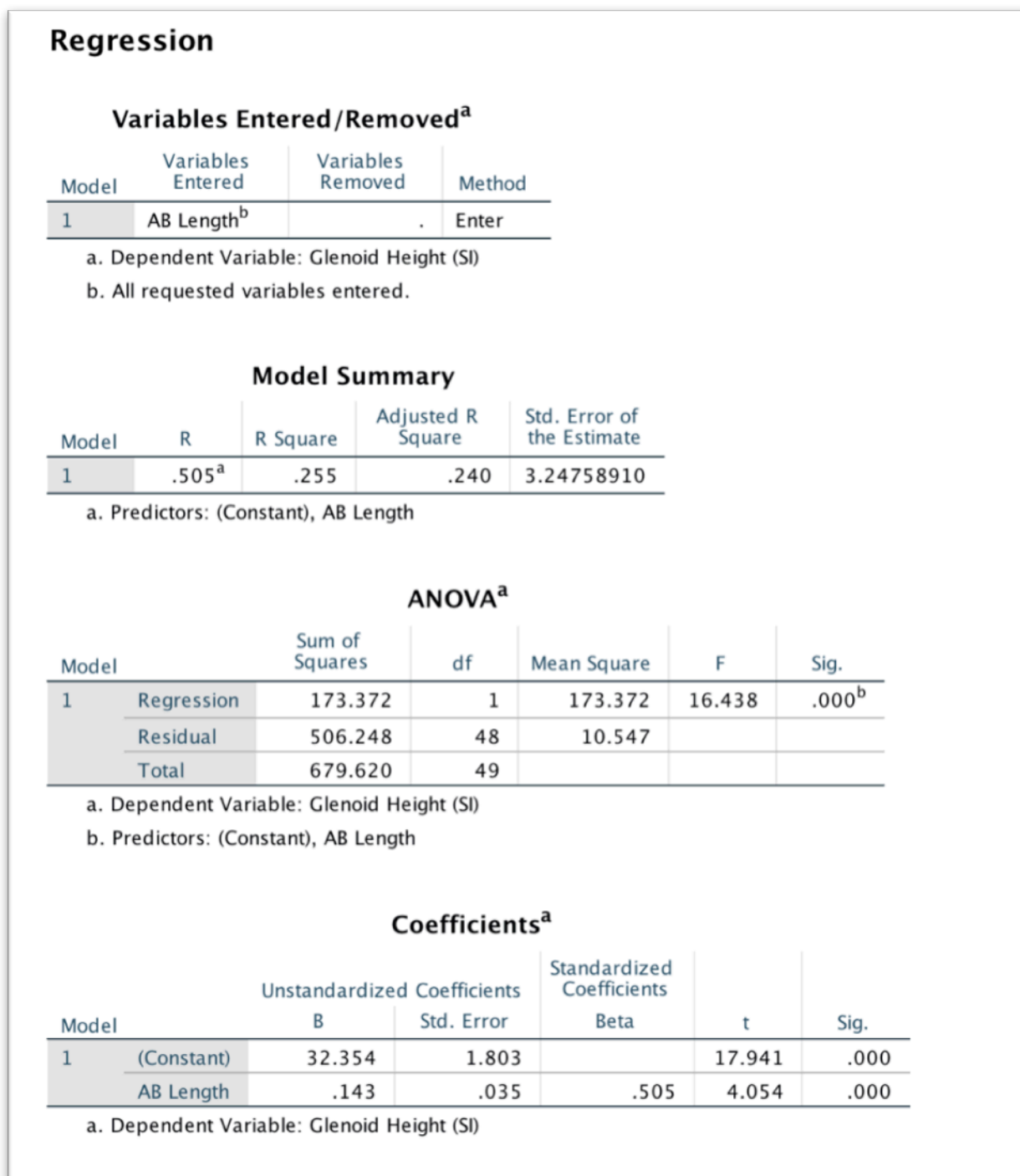


Figure B.13 Regression Equation Glenoid Height = Constant + Slope x Value of Predictor is used to calculate (Glenoid Height = 32.35 + 0.143 X Scapular Height of the Superior Border)

Appendix C – Scapular Co-Ordinate System Data Analysis

Independent Samples Test

| | | t-test for Equality of Means | | |
|---------------|-----------------------------|------------------------------|-----------------|-----------------------|
| | | Sig. (2-tailed) | Mean Difference | Std. Error Difference |
| ACR_COR Angle | Equal variances assumed | .291 | 3.84016000 | 3.59540751 |
| | Equal variances not assumed | .292 | 3.84016000 | 3.59540751 |
| COR_INF Angle | Equal variances assumed | .009 | -10.322800 | 3.78575978 |
| | Equal variances not assumed | .009 | -10.322800 | 3.78575978 |

Figure C.1 Demonstrating Results of t- Test For the Acromion – Coracoid Angle and the Coracoid- Inferior Pillar Angle between Males and Females

Independent Samples Test

| | | t-test for Equality of Means | | |
|---------------|-----------------------------|------------------------------|-----------------|-----------------------|
| | | Sig. (2-tailed) | Mean Difference | Std. Error Difference |
| ACR_COR Angle | Equal variances assumed | .291 | 3.84016000 | 3.59540751 |
| | Equal variances not assumed | .292 | 3.84016000 | 3.59540751 |
| ACR_INF Angle | Equal variances assumed | .030 | 6.48400000 | 2.89899458 |
| | Equal variances not assumed | .030 | 6.48400000 | 2.89899458 |

Figure C.2 Demonstrating Results of T Test For the Acromion Spine – Coracoid Angle and the Acromion Spine - Inferior Pillar Angle between Males and Females

Independent Samples Test

| | | t-test for Equality of Means | | |
|---------------|-----------------------------|------------------------------|-----------------|-----------------------|
| | | Sig. (2-tailed) | Mean Difference | Std. Error Difference |
| ACR_INF Angle | Equal variances assumed | .030 | 6.48400000 | 2.89899458 |
| | Equal variances not assumed | .030 | 6.48400000 | 2.89899458 |
| COR_INF Angle | Equal variances assumed | .009 | -10.322800 | 3.78575978 |
| | Equal variances not assumed | .009 | -10.322800 | 3.78575978 |

Figure C.3 Demonstrating Results of T Test For the Acromion Spine – Inferior Pillar Angle and the Coracoid- Inferior Pillar Angle between Males and Females

Group Statistics

| | Sex | N | Mean | Std. Deviation | Std. Error Mean |
|---------------|-----|----|------------|----------------|-----------------|
| ACR_COR Angle | .0 | 25 | 95.0485600 | 9.95115595 | 1.99023119 |
| | 1.0 | 25 | 91.2084000 | 14.9715856 | 2.99431711 |

Figure C.4 Demonstrates the Acromion Spine - Coracoid Angle Measurement for Females (0) and Males (1)

Group Statistics

| | Sex | N | Mean | Std. Deviation | Std. Error Mean |
|---------------|-----|----|------------|----------------|-----------------|
| COR_INF Angle | .0 | 25 | 130.551200 | 11.9047915 | 2.38095830 |
| | 1.0 | 25 | 140.874000 | 14.7164998 | 2.94329996 |

Figure C.5 Demonstrates the Coracoid – Inferior Pillar Angle Measurement for Females (0) and Males (1)

Group Statistics

| | Sex | N | Mean | Std. Deviation | Std. Error Mean |
|---------------|-----|----|------------|----------------|-----------------|
| ACR_INF Angle | .0 | 25 | 134.400800 | 9.53538407 | 1.90707681 |
| | 1.0 | 25 | 127.916800 | 10.9169909 | 2.18339817 |

Figure C.6 Demonstrates the Acromion Spine – Inferior Pillar Angle Measurement for Females (0) and Males (1)

**ELSEVIER LICENSE
TERMS AND CONDITIONS**

May 20, 2016

This is a License Agreement between ASHISH GUPTA ("You") and Elsevier ("Elsevier") provided by Copyright Clearance Center ("CCC"). The license consists of your order details, the terms and conditions provided by Elsevier, and the payment terms and conditions.

All payments must be made in full to CCC. For payment instructions, please see information listed at the bottom of this form.

| | |
|--|---|
| Supplier | Elsevier Limited The Boulevard, Langford Lane Kidlington, Oxford, OX5 1GB, UK |
| Registered Company Number | 1982084 |
| Customer name | ASHISH GUPTA |
| Customer address | 268 Grosvenor St London, ON N6A4V2 |
| License number | 3873270077444 |
| License date | May 20, 2016 |
| Licensed content publisher | Elsevier |
| Licensed content publication | Elsevier Books |
| Licensed content title | Developmental Juvenile Osteology |
| Licensed content author | Louise Scheuer, Sue Black |
| Licensed content date | 2000 |
| Number of pages | 28 |
| Start Page | 244 |
| End Page | 271 |
| Type of Use | reuse in a thesis/dissertation |
| I am an academic or government institution with a full-text subscription to this journal and the audience of the material consists of students and/or employees of this institute? | No |
| Portion | figures/tables/illustrations |
| Number of figures/tables/illustrations | 6 |
| Format | electronic |
| Are you the author of this Elsevier chapter? | No |
| Will you be translating? | No |
| Original figure numbers | Figure 8.8 (page 262), Figure 8.9 (page 263), Figure 8.11 (page 265), Figure 8.12 (page 266), FIGURE 8.14 (page 267) and Figure 8.17 (page 269) |

Title of your thesis/dissertation Role of Scapular Morphology in Reverse Shoulder Arthroplasty

Expected completion date Jun 2016

Estimated size (number of pages) 200

Elsevier VAT number GB 494 6272 12

Permissions price 0.00 CAD

VAT/Local Sales Tax 0.00 CAD / 0.00 GBP

Total 0.00 CAD

Terms and Conditions

INTRODUCTION

1. The publisher for this copyrighted material is Elsevier. By clicking "accept" in connection with completing this licensing transaction, you agree that the following terms and conditions apply to this transaction (along with the Billing and Payment terms and conditions established by Copyright Clearance Center, Inc. ("CCC"), at the time that you opened your Rightslink account and that are available at any time at <http://myaccount.copyright.com>).

GENERAL TERMS

2. Elsevier hereby grants you permission to reproduce the aforementioned material subject to

the terms and conditions indicated.

3. Acknowledgement: If any part of the material to be used (for example, figures) has appeared in our publication with credit or acknowledgement to another source, permission

must also be sought from that source. If such permission is not obtained then that material

may not be included in your publication/copies. Suitable acknowledgement to the source must be made, either as a footnote or in a reference list at the end of your publication, as follows:

"Reprinted from Publication title, Vol /edition number, Author(s), Title of article / title of

chapter, Pages No., Copyright (Year), with permission from Elsevier [OR APPLICABLE

SOCIETY COPYRIGHT OWNER]." Also Lancet special credit - "Reprinted from The Lancet, Vol. number, Author(s), Title of article, Pages No., Copyright (Year), with permission from Elsevier."

4. Reproduction of this material is confined to the purpose and/or media for which permission is hereby given.

5. Altering/Modifying Material: Not Permitted. However figures and illustrations may be

altered/adapted minimally to serve your work. Any other abbreviations, additions, deletions

and/or any other alterations shall be made only with prior written authorization of Elsevier

Ltd. (Please contact Elsevier at permissions@elsevier.com)

6. If the permission fee for the requested use of our material is waived in this instance, please be advised that your future requests for Elsevier materials may attract a fee.

7. Reservation of Rights: Publisher reserves all rights not specifically granted in the combination of (i) the license details provided by you and accepted in the course of this licensing transaction, (ii) these terms and conditions and (iii) CCC's Billing and Payment

terms and conditions.

8. License Contingent Upon Payment: While you may exercise the rights licensed immediately upon issuance of the license at the end of the licensing process for the transaction, provided that you have disclosed complete and accurate details of your proposed

use, no license is finally effective unless and until full payment is received from you (either

by publisher or by CCC) as provided in CCC's Billing and Payment terms and conditions. If

full payment is not received on a timely basis, then any license preliminarily granted shall be

deemed automatically revoked and shall be void as if never granted. Further, in the event that you breach any of these terms and conditions or any of CCC's Billing and Payment terms and conditions, the license is automatically revoked and shall be void as if never granted. Use of materials as described in a revoked license, as well as any use of the materials beyond the scope of an unrevoked license, may constitute copyright infringement

and publisher reserves the right to take any and all action to protect its copyright in the materials.

9. Warranties: Publisher makes no representations or warranties with respect to the licensed material.

10. Indemnity: You hereby indemnify and agree to hold harmless publisher and CCC, and

their respective officers, directors, employees and agents, from and against any and all claims arising out of your use of the licensed material other than as specifically authorized pursuant to this license.

11. No Transfer of License: This license is personal to you and may not be sublicensed, assigned, or transferred by you to any other person without publisher's written permission.

12. No Amendment Except in Writing: This license may not be amended except in a writing signed by both parties (or, in the case of publisher, by CCC on publisher's behalf).

13. Objection to Contrary Terms: Publisher hereby objects to any terms contained in any purchase order, acknowledgment, check endorsement or other writing prepared by you, which terms are inconsistent with these terms and conditions or CCC's Billing and Payment

terms and conditions. These terms and conditions, together with CCC's Billing and Payment

terms and conditions (which are incorporated herein), comprise the entire agreement between you and publisher (and CCC) concerning this licensing transaction. In the event of

any conflict between your obligations established by these terms and conditions and those

established by CCC's Billing and Payment terms and conditions, these terms and conditions shall control.

14. Revocation: Elsevier or Copyright Clearance Center may deny the permissions described

in this License at their sole discretion, for any reason or no reason, with a full refund payable

to you. Notice of such denial will be made using the contact information provided by you.

Failure to receive such notice will not alter or invalidate the denial. In no event will Elsevier

or Copyright Clearance Center be responsible or liable for any costs, expenses or damage

incurred by you as a result of a denial of your permission request, other than a refund of the

amount(s) paid by you to Elsevier and/or Copyright Clearance Center for denied permissions.

LIMITED LICENSE

The following terms and conditions apply only to specific license types:

15. Translation: This permission is granted for non-exclusive world English rights only unless your license was granted for translation rights. If you licensed translation rights you

may only translate this content into the languages you requested. A professional translator

must perform all translations and reproduce the content word for word preserving the integrity of the article.

16. Posting licensed content on any Website: The following terms and conditions apply as

follows: Licensing material from an Elsevier journal: All content posted to the web site must

maintain the copyright information line on the bottom of each image; A hyper-text must be

included to the Homepage of the journal from which you are licensing at

<http://www.sciencedirect.com/science/journal/xxxxx> or the Elsevier homepage for books at

<http://www.elsevier.com>; Central Storage: This license does not include permission for a scanned version of the material to be stored in a central repository such as that provided by

Heron/XanEdu.

Licensing material from an Elsevier book: A hyper-text link must be included to the Elsevier

homepage at <http://www.elsevier.com> . All content posted to the web site must maintain the

copyright information line on the bottom of each image.

Posting licensed content on Electronic reserve: In addition to the above the following clauses are applicable: The web site must be password-protected and made available only to

bona fide students registered on a relevant course. This permission is granted for 1 year only.

You may obtain a new license for future website posting.

17. For journal authors: the following clauses are applicable in addition to the above:

Preprints:

A preprint is an author's own write-up of research results and analysis, it has not been peerreviewed,

nor has it had any other value added to it by a publisher (such as formatting, copyright, technical enhancement etc.).

Authors can share their preprints anywhere at any time. Preprints should not be added to or

enhanced in any way in order to appear more like, or to substitute for, the final versions

of

articles however authors can update their preprints on arXiv or RePEc with their Accepted

Author Manuscript (see below).

If accepted for publication, we encourage authors to link from the preprint to their formal

publication via its DOI. Millions of researchers have access to the formal publications on

ScienceDirect, and so links will help users to find, access, cite and use the best available version. Please note that Cell Press, The Lancet and some society-owned have different preprint policies. Information on these policies is available on the journal homepage.

Accepted Author Manuscripts: An accepted author manuscript is the manuscript of an article that has been accepted for publication and which typically includes author incorporated

changes suggested during submission, peer review and editor-author communications.

Authors can share their accepted author manuscript:

- immediately

via their non-commercial person homepage or blog

by updating a preprint in arXiv or RePEc with the accepted manuscript

via their research institute or institutional repository for internal institutional

uses or as part of an invitation-only research collaboration work-group

directly by providing copies to their students or to research collaborators for their personal use

for private scholarly sharing as part of an invitation-only work group on

commercial sites with which Elsevier has an agreement

- after the embargo period

via non-commercial hosting platforms such as their institutional repository

via commercial sites with which Elsevier has an agreement

In all cases accepted manuscripts should:

- link to the formal publication via its DOI

- bear a CC-BY-NC-ND license - this is easy to do

- if aggregated with other manuscripts, for example in a repository or other site, be shared in alignment with our hosting policy not be added to or enhanced in any way to appear more like, or to substitute for, the published journal article.

Published journal article (JPA): A published journal article (PJA) is the definitive final record of published research that appears or will appear in the journal and embodies all value-adding publishing activities including peer review co-ordination, copy-editing, formatting, (if relevant) pagination and online enrichment.

Policies for sharing publishing journal articles differ for subscription and gold open access

articles:

Subscription Articles: If you are an author, please share a link to your article rather than the

full-text. Millions of researchers have access to the formal publications on ScienceDirect,

and so links will help your users to find, access, cite, and use the best available version.

Theses and dissertations which contain embedded PJAs as part of the formal submission can

be posted publicly by the awarding institution with DOI links back to the formal publications on ScienceDirect.

If you are affiliated with a library that subscribes to ScienceDirect you have additional

private sharing rights for others' research accessed under that agreement. This includes use

for classroom teaching and internal training at the institution (including use in course packs

and courseware programs), and inclusion of the article for grant funding purposes.

Gold Open Access Articles: May be shared according to the author-selected end-user license and should contain a CrossMark logo, the end user license, and a DOI link to the formal publication on ScienceDirect.

Please refer to Elsevier's posting policy for further information.

18. For book authors the following clauses are applicable in addition to the above:

Authors are permitted to place a brief summary of their work online only. You are not allowed to download and post the published electronic version of your chapter, nor may you

scan the printed edition to create an electronic version. Posting to a repository: Authors are

permitted to post a summary of their chapter only in their institution's repository.

19. Thesis/Dissertation: If your license is for use in a thesis/dissertation your thesis may be

submitted to your institution in either print or electronic form. Should your thesis be published commercially, please reapply for permission. These requirements include permission for the Library and Archives of Canada to supply single copies, on demand, of

the complete thesis and include permission for Proquest/UMI to supply single copies, on demand, of the complete thesis. Should your thesis be published commercially, please reapply for permission. Theses and dissertations which contain embedded PJAs as part of

the formal submission can be posted publicly by the awarding institution with DOI links back to the formal publications on ScienceDirect.

Elsevier Open Access Terms and Conditions

You can publish open access with Elsevier in hundreds of open access journals or in nearly

2000 established subscription journals that support open access publishing. Permitted third

party re-use of these open access articles is defined by the author's choice of Creative Commons user license. See our open access license policy for more information.

Terms & Conditions applicable to all Open Access articles published with Elsevier:

Any reuse of the article must not represent the author as endorsing the adaptation of the article nor should the article be modified in such a way as to damage the author's honour or

reputation. If any changes have been made, such changes must be clearly indicated.

The author(s) must be appropriately credited and we ask that you include the end user license and a DOI link to the formal publication on ScienceDirect.

If any part of the material to be used (for example, figures) has appeared in our publication

with credit or acknowledgement to another source it is the responsibility of the user to ensure their reuse complies with the terms and conditions determined by the rights holder.

Additional Terms & Conditions applicable to each Creative Commons user license:

CC BY: The CC-BY license allows users to copy, to create extracts, abstracts and new works from the Article, to alter and revise the Article and to make commercial use of the Article (including reuse and/or resale of the Article by commercial entities), provided the

user gives appropriate credit (with a link to the formal publication through the relevant DOI), provides a link to the license, indicates if changes were made and the licensor is not

represented as endorsing the use made of the work. The full details of the license are available at <http://creativecommons.org/licenses/by/4.0>.

CC BY NC SA: The CC BY-NC-SA license allows users to copy, to create extracts, abstracts and new works from the Article, to alter and revise the Article, provided this is not

done for commercial purposes, and that the user gives appropriate credit (with a link to the

formal publication through the relevant DOI), provides a link to the license, indicates if changes were made and the licensor is not represented as endorsing the use made of the work. Further, any new works must be made available on the same conditions. The full details of the license are available at <http://creativecommons.org/licenses/by-nc-sa/4.0>.

CC BY NC ND: The CC BY-NC-ND license allows users to copy and distribute the Article,

provided this is not done for commercial purposes and further does not permit distribution of

the Article if it is changed or edited in any way, and provided the user gives appropriate credit (with a link to the formal publication through the relevant DOI), provides a link to the

license, and that the licensor is not represented as endorsing the use made of the work. The

full details of the license are available at <http://creativecommons.org/licenses/by-nc-nd/4.0>.

Any commercial reuse of Open Access articles published with a CC BY NC SA or CC BY

NC ND license requires permission from Elsevier and will be subject to a fee.

Commercial reuse includes:

- Associating advertising with the full text of the Article
- Charging fees for document delivery or access
- Article aggregation
- Systematic distribution via e-mail lists or share buttons

Posting or linking by commercial companies for use by customers of those companies.

20. Other Conditions:

v1.8

CURRICULUM VITAE

| | |
|----------------------|-------------------------|
| NAME | Dr Ashish Gupta |
| DATE OF BIRTH | 31 December 1978 |

Professional Qualifications

| | | |
|--------------------|------|---|
| Masters in Surgery | 2016 | University of Western Ontario |
| FRACS (Orth) | 2013 | Australian Orthopedic Association Royal Australasian College of Surgeons |
| MBBS | 2002 | Kasturba Medical College Manipal, INDIA |

Fellowships

- Fowler Kennedy Institute Sports Fellowship and Hand and Upper Limb Clinic Fellowship, London, ON- Dr R Litchfield, Dr George Athwal July 2015- June 2016
- Shoulder Arthroplasty Fellowship Klinikum Bogenhausen, Munich Germany Dr L Seebauer; 1Feb2015 - 30 June 2015
- Alps Surgery Institute Advanced Shoulder Arthroscopy and Arthroplasty Fellowship, Annecy, France Dr L Lafosse; 25th Jan 2014-25th Jan 2015

Certification Exams Passed

- ABIME Certification Exam- Certified Independent Medical Examiner- 2015
- The Orthopaedic Basic Sciences Exam (OPBS) in 2009
- Basic Sciences Surgical Exam Part 1& 2 - (RACS) 2007
- Australian Medical Council Part 1 & Part 2 Exams

Completed in Feb 2006.

Achievements During MBBS - Passed with Distinction

| | |
|---------------------------------|--------------------------------|
| First Professional Exam | Passed with Distinction |
| Anatomy | Distinction |
| Physiology | Distinction |
| Biochemistry | First Class |
| Second Professional Exam | Passed with Distinction |
| Pathology | Distinction |
| Microbiology | Distinction |
| Pharmacology | Distinction |
| Forensic Science | Distinction |
| Third Professional Exam | Passed with Distinction |
| E N T | Distinction |
| Ophthalmology | Distinction |
| Community Medicine | First Class |
| Final Professional Exam | Passed in First Class |
| Medicine | Distinction |
| Surgery | Distinction |
| Pediatrics | First Class |
| Obstetrics & Gynecology | First Class |

Scholarships and Research Grants

1. Department of Surgery Scholarship University of Western Ontario Masters Program 2015-2016
2. Arthritis Australia Research Grant 2015
3. Arthritis Australia Research Grant 2014
4. Stryker Travelling/ Outreach Fellowship AOA Outreach 2012

Current Working Position

- Consultant Orthopaedic Surgeon Greenslopes Pvt Hospital and Mater Adults Hospital, Brisbane, QLD Australia

Last Working Position Held

- Fowler Kennedy Institute Sports Fellowship and Hand and Upper Limb Clinic Fellowship, London, ON- Dr R Litchfield, Dr G Athwal July 2015- June 2016
- Shoulder Arthroplasty Fellowship Klinikum Bogenhausen, Munich Germany Dr L Seebauer; 1Feb2015 - 30 June 2015
- Fellowship of Shoulder Advanced Arthroscopy and Arthroplasty with Dr Laurent Lafosse , Alps Shoulder Institute, Annecy France Jan 2014- Jan 2015
- Staff Specialist Orthopaedics

Department of Orthopaedics Townsville Hospital Townsville,
Australia 4810

Orthopaedic Surgery Training

- Orthopaedic Registrar (SET5) [Surgical Education Trainee of the Royal Australasian College of Surgeons]
 - Orthopaedic Registrar (SET5)
 - Greenslopes Hospital and Royal Brisbane Hospital (Feb 2012- Feb 2013)
 - Orthopaedic Registrar (SET4)

- Mater Children's Hospital, (Aug 2011- Feb 2012)
 - Orthopaedic Registrar (SET 4)
 - Princess Alexandra Hospital, Brisbane (Jan – Aug 2011)
 - Orthopaedic Registrar (SET3)
 - Ipswich General Hospital, 2010
 - Orthopaedic Registrar (SET2)
 - Townsville General Hospital, 2009
 - Orthopaedic Registrar (SET1)
 - The Prince Charles Hospital , Brisbane 2008
- Principal House Officer (Non Training Registrar) in Orthopaedics
 - Mater Children's and Adult Hospital Brisbane 2007
- Principal House Officer in Orthopedics
 - QEII Hospital Brisbane
 - From 17 Jan 2006- 15 Jan 2007
- Principal House Officer in Orthopedics
 - Bundaberg Base Hospital From 17 Jan 2005-16 Jan 2006
- Junior House Officer PGY-2
 - Bundaberg Base Hospital
 - From : 26th January 2004 – 17th January 2005
- Intern – PGY1
 - Colonial War Memorial Hospital

SUVA , FIJI Islands

From : 25th January, 2003 to 24th January, 2004 Rotations
through Medicine, Obs & Gynae, Surgery (Ortho, G. Surgery, ENT, Ophthalmology)
Elective Rotation at the National Center of Rehabilitation Medicine, Suva

Certificates and Courses

1. Completed ABIME AMA 5 Guideline course , Las Vegas October 2015.
2. Completed ABIME Return To Work Course, Las Vegas October 2015
3. Completed ABIME writing Medico legal reports Course, Las Vegas October 2015
4. Completed the EMST/ATLS course.
5. Completed the ASSET (Basic Surgical Skills)course by the RACS.
6. Completed the Care of the Critically Ill Surgical Patient course by the RACS
7. Completed the CLEAR course by the RACS
8. Completed the Pre Hospital Trauma Life Support (PHTLS) course.
9. Certificate of successful completion of Neonatal Resuscitation Course, held by the American Acad. Of Pediatrics.
10. Completed Mastering Your Risk – Risk Management Workshop.
11. Completed Human Error and Patient Safety Workshop.
12. Passed the IELTS exam with a Band Score of 8 in the Academic Module

Publications:

1. Complications of the Latarjet Procedure, Gupta A, Delaney R, Petkin K, Lafosse L. Complications of the Latarjet procedure. Current Reviews in Musculoskeletal Medicine. 2015 Mar; 8(1): 59-66.
2. Pain Levels after Local Anaesthetic with or without Hyaluronidase in Carpal Tunnel Release: A Randomized Controlled Trial. G. Yeo, A. Gupta, G. Ding, H. Skerman, M.Khatun and D.Melsom ; Advances in Orthopedics Volume 2015, Article ID 784329, <http://dx.doi.org/10.1155/2015/784329>

Book Chapters

1. Biceps Pathology in Sports : A Gupta, B Litchfield Shoulder and Elbow Injuries in Athletes: Prevention, Treatment, and Return to Sport.

2. Reverse Shoulder Arthroplasty for Massive Antero superior Rotator Cuff Failure - Current issues and emerging uses of Reverse Shoulder Arthroplasty: D Dines, J Dines, B Edwards; Thieme Inc. **Ashish Gupta**, David Haeni, Laurent Lafosse (In Press)
3. Open Rotator Cuff Repair- Rotator Cuff Injuries: Patrick J. McMahon; Springer Inc. **Ashish Gupta**, Robert Litchfield. (In Press)
4. Nerve Entrapment Syndromes in the Shoulder: Diagnosis, Principles and Different Techniques for Nerve Decompression - Nerve Entrapment Syndromes in the Shoulder: Diagnosis, Principles and Different Techniques for Nerve Decompression Laurent Lafosse, **Ashish Gupta**, Thibault Lafosse, Gonzalo Samitier, Kalojan Petkin
5. Nerve Entrapment Syndromes in the Shoulder. Brachial Plexus and Thoracic Outlet Syndrome in Athletes - Sports Injuries: Prevention, Diagnosis, Treatment and Rehabilitation. 2nd Edition. Laurent Lafosse, **Ashish Gupta**, Thibault Lafosse, Gonzalo Samitier, Kalojan Petkin
6. Arthroscopic Latarjet - The Shoulder: AANA Advanced Arthroscopic Surgical Techniques 2016 . **Ashish Gupta**, Laurent Lafosse,

Poster Presentations

1. Morphologic Analysis of the Three Columns of the Scapula: Surgical Implications in Reverse Shoulder Arthroplasty ORS San Diego 2017 **Ashish Gupta**, Nikolas K. Knowles, George S. Athwal, Louis M. Ferreira.
2. Relationships of Scapular Plane Definitions: Application to Glenoid Fixation in Total Shoulder Arthroplasty ORS San Diego 2017 **Ashish Gupta**, Nikolas K. Knowles, George S. Athwal, Louis M. Ferreira.
3. Y shaped biceps tenotomy with tenodesis effect. Kalojan Petkin, Ashish Gupta, Gaetan Opsomer, Gonzalo Samitier, David Hni, Stephen A.Parada, Laurent Lafosse ; 26th Congress of the European Society for Surgery of the Shoulder and the Elbow held in Milano, September 16-19, 2015
4. Hyaluronidase and its effect on pain while injecting Local Anesthetic During Carpal Tunnel Release a Randomized Control Trial- AOA NZOA international meeting Rotarua New Zealand 2011

Presentations

1. 3 Columns of the Scapula Role of Scapular Morphology in RSA : **A Gupta**, Nikolas Knowles, L Ferriera, G Athwal ISTA October 2016 Boston USA
2. Glenoid bone loss in shoulder arthroplasty: **A Gupta**, M Koch, C Thusbass , L Seebauer AOA NZOA combined Annual Meeting Cairns October 2016
3. Revision of Reverse Shoulder Replacement **A Gupta**, M Koch, J Lifka, L Seebauer AOA NZOA combined Annual Meeting Cairns October 2016
4. Management of glenoid bone loss: **A Gupta**, M Koch, C Thusbass , L Seebauer Shoulder and Elbow Society of Australia Darwin August 2016
5. Revision of Reverse Shoulder Arthroplasty: **A Gupta**, M Koch, J Lifka , L Seebauer Shoulder and Elbow Society of Australia Darwin August 2016
6. Revision of Reverse Shoulder Arthroplasty- M Koch, J Lifka, A Gupta, Ludwig Seebauer , March2, AAOS Orlando 2016.
7. Global Perspectives on Revision of Reverse Shoulder Arthroplasty - M Koch, J Lifka, A Gupta, Ludwig Seebauer , March1, AAOS Orlando 2016
8. Reverse Shoulder Arthroplasty Using Trans Deltoid Approach Technical Note and Results Video Theatre – G Samitier, A Gupta, K petkin L Lafosse – Video Theatre, AAOS Orlando 2016
9. Efficacy of Suprascapular nerve block compared with Subacromial injection: A randomized controlled trial in patients with rotator cuff tears. Dr J Coory, Dr M Wilkinson , Dr A Gupta, Australian Orthopaedic Association International Annual Meeting Brisbane October 2015.
10. Arthroscopic Latarjet – Video Theatre AAOS Annual Meeting Las Vegas 2015 G Samitier, A Gupta, K Petkin L Lafosse
11. Soft Tissue repair techniques –Shoulder Instability; Anney Arthroscopic Arthroplasty Shoulder Academy (AASA) September 2014
12. Bankart When and How - Anney Arthroscopic Arthroplasty Shoulder Academy (AASA) February 2014
13. Randomized Control trial of Dynamic Hip Screw vs Long Cephalomedullary nail for the Treatment of Intertrochanteric Fractures Prospective Randomized Control Trial – AOA NZOA international meeting Rotarua New Zealand 2011
14. Orthopaedic Outreach Lessons Learnt. – AOA NZOA International meeting Rotarua New Zealand 2011
15. Orthopedic Manifestations of Prader Willi Syndrome – Qld Branch of AOA meeting in Townsville 9-11 June 2007
16. High Flex Knee Design Solving the Problem or Bending the Rules. Qld Branch of AOA meeting in Noosa June 2008

Voluntary Work

1. Member of the Orthopaedic Outreach Society of AOA
2. Orthopaedic Outreach team to Latouka Hospital Fiji – Part of the Annual Outreach team to Latouka Hospital. Have been going to Fiji for 5 years now and can see an improvement our team has made in Registrar teaching, basic Orthopaedic knowledge of the local fraternity. The case load is very challenging and operating with the local infrastructure brings its own set of challenges.

Teaching

- Junior Lecturer for James Cook University Medical School 2009
- Jnr Lecturer for Univ of Qld Medical School
- Actively involved in departmental teaching of registrars.

Referees

- 1.** Dr George S Athwal
- 2.** Dr Desmond Soares
- 3.** Dr Matthew Wilkinson